

AD-A154 743

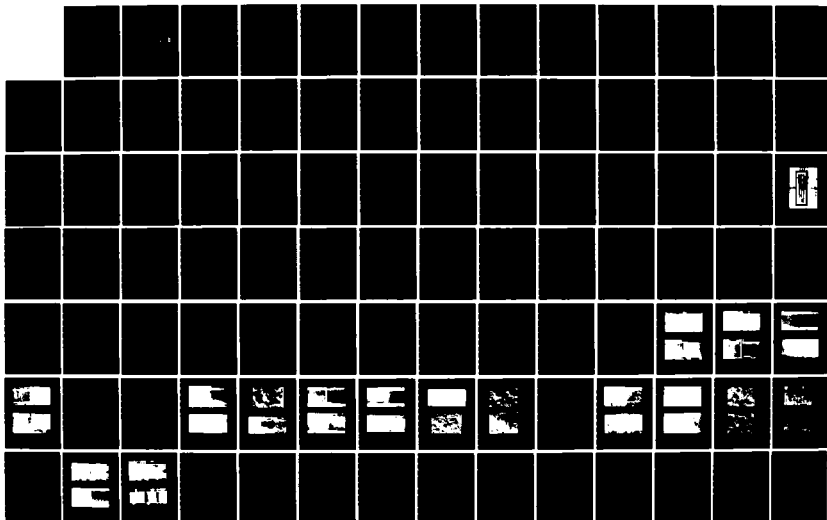
ENDURANCE AND HEAT-TRANSFER PERFORMANCE OF POLYMER
COATINGS FOR THE PROMO. (U) NAVAL POSTGRADUATE SCHOOL
MONTEREY CA D J LOONEY DEC 84 NPS-69-84-015

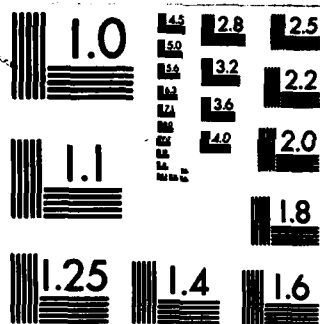
1/2

UNCLASSIFIED

F/G 11/3

NL





MICROCOPY RESOLUTION TEST CHART
NATIONAL BUREAU OF STANDARDS-1963-A

AD-A154 743

NAVAL POSTGRADUATE SCHOOL

Monterey, California



ENDURANCE AND HEAT-TRANSFER PERFORMANCE
OF POLYMER COATINGS FOR THE PROMOTION
OF DROPWISE CONDENSATION OF STEAM

by

Daniel J. Looney

December 1984

Thesis Advisor:

P. J. Marto

Approved for public release; Distribution unlimited.

Prepared for:
National Science Foundation
Division of Engineering
Washington, D. C. 20550

DTIC FILE COPY

85 5 15 004

NAVAL POSTGRADUATE SCHOOL
Monterey, California


Commodore Robert H. Shumaker
Superintendent

David A. Schrady
Provost

This thesis prepared in conjunction with research supported in part by National Science Foundation, Division of Engineering, Washington, DC under MEA82-03567.

Reproduction of all or part of this report is authorized.

Released as a
Technical Report by:


John N. Dyer
Dean of Science and
Engineering

Unclassified

SECURITY CLASSIFICATION OF THIS PAGE (When Data Entered)

REPORT DOCUMENTATION PAGE		READ INSTRUCTIONS BEFORE COMPLETING FORM										
1. REPORT NUMBER NPS-69-84-015	2. GOVT ACCESSION NO.	3. RECIPIENT'S CATALOG NUMBER										
4. TITLE (and Subtitle) Endurance and Heat-Transfer Performance of Polymer Coatings for the Promotion of Dropwise Condensation of Steam		5. TYPE OF REPORT & PERIOD COVERED Master of Science Thesis; December 1984										
7. AUTHOR(s) Daniel J. Looney		6. PERFORMING ORG. REPORT NUMBER										
9. PERFORMING ORGANIZATION NAME AND ADDRESS Naval Postgraduate School Monterey, California 93943		8. CONTRACT OR GRANT NUMBER(s)										
11. CONTROLLING OFFICE NAME AND ADDRESS Naval Postgraduate School Monterey, California 93943		10. PROGRAM ELEMENT, PROJECT, TASK AREA & WORK UNIT NUMBERS N6227182WE20114										
13. MONITORING AGENCY NAME & ADDRESS (if different from Controlling Office) National Science Foundation Washington, DC 20550 Division of Engineering		12. REPORT DATE December 1984										
		13. NUMBER OF PAGES 139										
		14. SECURITY CLASS. (of this report) Unclassified										
		15a. DECLASSIFICATION/DOWNGRADING SCHEDULE										
16. DISTRIBUTION STATEMENT (of this Report) Approved for public release; distribution unlimited.												
17. DISTRIBUTION STATEMENT (of the abstract entered in Block 20, if different from Report)		<table border="1"> <tr> <td colspan="2">Accession For</td> </tr> <tr> <td>NTIS GRANT</td> <td><input checked="" type="checkbox"/></td> </tr> <tr> <td>DTIC TAB</td> <td><input type="checkbox"/></td> </tr> <tr> <td>Unannounced</td> <td><input type="checkbox"/></td> </tr> <tr> <td>Justification</td> <td></td> </tr> </table>	Accession For		NTIS GRANT	<input checked="" type="checkbox"/>	DTIC TAB	<input type="checkbox"/>	Unannounced	<input type="checkbox"/>	Justification	
Accession For												
NTIS GRANT	<input checked="" type="checkbox"/>											
DTIC TAB	<input type="checkbox"/>											
Unannounced	<input type="checkbox"/>											
Justification												
18. SUPPLEMENTARY NOTES		<table border="1"> <tr> <td colspan="2">By</td> </tr> <tr> <td colspan="2">Distribution/</td> </tr> <tr> <td colspan="2">Availability Codes</td> </tr> <tr> <td>Dist</td> <td>Avail and/or Special</td> </tr> <tr> <td>A/</td> <td></td> </tr> </table>	By		Distribution/		Availability Codes		Dist	Avail and/or Special	A/	
By												
Distribution/												
Availability Codes												
Dist	Avail and/or Special											
A/												
19. KEY WORDS (Continue on reverse side if necessary and identify by block number) Dropwise Condensation, Fluoroacrylic, Polymer Coatings, Parylene, Heat-transfer Enhancement, Fluoroepoxy,												
20. ABSTRACT (Continue on reverse side if necessary and identify by block number) Ten polymer coatings were evaluated for the long term promotion of dropwise condensation of steam. Four of the coatings were experimental coatings developed by the Naval Research Laboratory and six were commercial coatings. Continuous dropwise condensation in excess of 10,000 hours was obtained for several of the coatings that were applied to rough surfaces.												

DD FORM 1 JAN 73 1473

EDITION OF 1 NOV 68 IS OBSOLETE
S/N 0102-LF-014-6601

Unclassified

SECURITY CLASSIFICATION OF THIS PAGE (When Data Entered)

Unclassified

SECURITY CLASSIFICATION OF THIS PAGE (When Data Entered)

Three commercial coatings, in addition to an NRL fluoro-acrylic coating, were evaluated for heat-transfer performance. The effects of roughness, substrate thermal conductivity, coating thickness, and vapor velocity on the heat-transfer coefficient were studied for dropwise condensation of steam on a horizontal tube. Dropwise heat-transfer coefficients were also determined for steam condensing on silver-electroplated tubes, in order to compare the results with those from the polymer-coated tubes. Heat-transfer coefficient enhancement factors of as much as 10-12 were obtained for dropwise condensation when compared to filmwise results. Originator

Supplied keywords include:

SEE DD14731 (Block 19)

S. N 0102- LF-014-6601

Unclassified

SECURITY CLASSIFICATION OF THIS PAGE (When Data Entered)

Approved for public release; distribution is unlimited.

Endurance and Heat-Transfer Performance of Polymer Coatings
for the Promotion of Dropwise Condensation of Steam

by

Daniel J. Looney
Lieutenant, United States Navy
B.N.E., Georgia Institute of Technology, 1978

Submitted in partial fulfillment of the
requirements for the degree of

MASTER OF SCIENCE IN MECHANICAL ENGINEERING

from the

NAVAL POSTGRADUATE SCHOOL
December 1984

Author:

Daniel J. Looney

Daniel J. Looney

Approved by:

P. J. Marto

P. J. Marto, Thesis Advisor

A. S. Wanniarachchi

A. S. Wanniarachchi, Co-Advisor

P. J. Marto

P. J. Marto, Chairman,
Department of Mechanical Engineering

John N. Dyer

John N. Dyer,
Dean of Science and Engineering

ABSTRACT

Ten polymer coatings were evaluated for the long term promotion of dropwise condensation of steam. Four of the coatings were experimental coatings developed by the Naval Research Laboratory and six were commercial coatings. Continuous dropwise condensation in excess of 10,000 hours was obtained for several of the coatings that were applied to rough surfaces.

Three commercial coatings, in addition to an NRL fluoroacrylic coating, were evaluated for heat-transfer performance. The effects of roughness, substrate thermal conductivity, coating thickness, and vapor velocity on the heat-transfer coefficient were studied for dropwise condensation of steam on a horizontal tube. Dropwise heat-transfer coefficients were also determined for steam condensing on silver-electroplated tubes, in order to compare the results with those from the polymer-coated tubes. Heat-transfer coefficient enhancement factors of as much as 10-12 were obtained for dropwise condensation when compared to filmwise results.

TABLE OF CCNTENTS

I.	INTRODUCTION	16
A.	BACKGROUND INFORMATCN	16
B.	DESCRIPTION OF THE DROPWISE CONDENSATION PROCESS	17
	1. Drop Nucleation and Growth	17
	2. Drop Contact Angle	18
C.	FACTORS INFLUENCING DROPWISE CONDENSATION HEAT TRANSFER	20
D.	PROMOTION CF DROPWISE CONDENSATION	26
	1. Chemical Promoters	26
	2. Noble Metals	27
	3. Polymer Coatings	28
E.	RESEARCH OBJECTIVE	33
II.	ENDURANCE TEST APPARATUS AND PROCEDURES	36
A.	TEST APPARATUS	36
B.	PROCEDURE	36
	1. Substrate Preparation	39
	2. Photographic and SEM Investigation	39
	3. Physical Property Tests	40
C.	POLYMER COATINGS EVALUATED	40
	1. NRL Fluoroepoxy	41
	2. NRL Fluoroacrylic	42
	3. Parylene	43
	4. No-Stik	45
	5. Emralcn-333	45
III.	HEAT-TRANSFER MEASUREMENTS	46
A.	APPARATUS	46

B.	TUBES TESTED	48
1.	Plain Tubes	48
2.	Polymer-Coated Tubes	52
3.	Silver-Electroplated Tubes	53
C.	EXPERIMENTAL PROCEDURE	54
1.	Non-Condensing Gas Problem	54
2.	Mixing Chamber Calibration	54
3.	Data Collection Procedures	55
D.	DATA REDUCTION	57
1.	Modified Wilson Plot Program (WILSON3)	57
2.	Dropwise Data Reduction Program	59
IV.	RESULTS AND DISCUSSION	61
A.	ENDURANCE TEST RESULTS	61
1.	NRL Fluoroepoxy	62
2.	NRL Fluoroacrylic	63
3.	Parylene	69
4.	No-Stik	77
5.	Emralon-333	81
B.	HEAT-TRANSFER RESULTS FOR PLAIN TUBES	82
1.	Sensitivity of Data Reduction on Substrate Thermal Conductivity	84
2.	Modified Wilson Method Results	86
C.	HEAT-TRANSFER RESULTS FOR POLYMER-COATED TUBES	88
1.	Fluoroacrylic Coated Tubes	88
2.	Parylene-D Coated Tubes	95
3.	No-Stik Coated Tubes	95
4.	Emralon-333 Coated Tube	101
5.	Silver-Electroplated Tubes	101
D.	EFFECT OF SUBSTRATE THERMAL CONDUCTIVITY ON THE DROPWISE HEAT-TRANSFER COEFFICIENT	107
E.	EFFECT OF VAPOR VELOCITY ON THE DROPWISE HEAT-TRANSFER COEFFICIENT	108

F.	AN ALTERNATIVE APPROACH TO THE MODIFIED WILSON METHOD	108
V.	CONCLUSIONS AND RECOMMENIATIONS	113
A.	CONCLUSIONS	113
B.	RECOMMENDATIONS	114
APPENDIX A:	UNCERTAINTY ANALYSIS	116
APPENDIX B:	COMPUTER PROGRAM USED FOR WILSON PLOT DATA REDUCTION	117
APPENDIX C:	COMPUTER PROGRAM USED FOR HEAT-TRANSFER DATA REDUCTION	124
LIST OF REFERENCES	135
INITIAL DISTRIBUTION LIST	139

LIST OF TABLES

I.	Critical Surface Tensions of Low Energy Surfaces	23
II.	Properties of Some Polymers	35
III.	Endurance Test Results	85
IV.	Substrate Thermal Conductivity used for Data Reduction	86
V.	Sieder-Tate Coefficients used in Data Reduction	87

LIST OF FIGURES

1.1	Comparison of Film and Dropwise Condensation Modes	21
1.2	Drop Contact Angle	22
1.3	Variation of Surface Tension with Amount of Fluorine and Chlorine Replacement of Hydrogen . . .	24
2.1	Endurance Test Apparatus	37
2.2	Steam Chamber in Operation	38
2.3	General Formula for NRL Fluoroepoxy	41
2.4	NRL Fluoroacrylic	43
2.5	Chemical Formula for Parylene-N	44
2.6	Chemical Formula for Parylene-D	44
3.1	Schematic of Heat-Transfer Apparatus	49
3.2	Details of Test Section (Insert not shown)	50
3.3	Schematic of Purge System and Sump Tank	51
3.4	Mixing Chamber Calibration	56
4.1	NRL C-6 CuNi/R 6,000 hrs. and Parylene-D on CuNi/R 2,800 hrs.	64
4.2	NRL C-6 Ti/R 9,650 hrs. and on Cu/R 7,670 hrs. . .	64
4.3	NRL Mixed Fluoroepoxy on CuNi/220 grit/wp/0 hrs. and on CuNi/220 grit/0 hrs.	65
4.4	NRL Mixed Fluoroepoxy on CuNi/40 grit/wp/0 hrs. and on CuNi/40 grit/0 hrs.	65
4.5	NRL Mixed Fluoroepoxy on Cu/glassbead/wp/0 hrs. and on Cu/220 grit/0 hrs.	66
4.6	NRL Mixed Fluoroepoxy on Ti/40 grit/1,120 hrs. and on Ti/glassbead/wp/1,120 hrs.	66
4.7	NRL Mixed Fluoroepoxy on CuNi/220 grit/wp/1,120 hrs and on CuNi/220 grit/1,120 hrs.	67

4.8	NRL Mixed Fluoroepoxy on CuNi/40 grit/wp/350 hrs. and on CuNi/40 grit/350 hrs.	67
4.9	NRL Fluoroacrylic on Cu/R/6,400 hrs. and on Ti/R/6,400 hrs.	70
4.10	NRL Fluoroacrylic on Cu/R/7,690 hrs. and on Ti/R/7,670 hrs.	70
4.11	NRL Fluoroacrylic on CuNi/R/6,500 hrs. (SEM x1000)	71
4.12	NRL Fluoroacrylic on Au-Cu/R, Au-Ti/R, and Au-Cu/S 2,500 hrs.	71
4.13	NRL Fluoroacrylic on Au-Cu/R and Au-Ti/R 6,540 hrs.	72
4.14	NRL Crosslinked Fluoroacrylic on Ti/40 grit CuNi/220 grit/wp/0 hrs.	72
4.15	NRL Crosslinked Fluoroacrylic on Cu/40 grit and Cu/40 grit/wp/0 hrs.	73
4.16	NRL Crosslinked Fluoroacrylic on CuNi/40 grit, CuNi/40 grit/wp, and CuNi/glassbead/0 hrs.	73
4.17	NRL Crosslinked Fluoroacrylic on Cu/220 grit/wp, Cu/glassbead/wp, and Ti/40 grit/wp/0 hrs.	74
4.18	NRL Crosslinked Fluoroacrylic on Cu/40 grit SEM (x200)	74
4.19	NRL Crosslinked Fluoroacrylic on Cu/glb'd SEM (x200)	75
4.20	NRL Crosslinked Fluoroacrylic on CuNi/glb'd/wp SEM (x1000)	75
4.21	Parylene-D: Cu/R/0.5 μ m/2,800 hrs and Cu/S/1.0 μ m/1,600 hrs	77
4.22	Parylene-D: Cu/S/0.5 μ m and Cu/R/0.5 μ m 4080 hrs.	77
4.23	Parylene-D: Ti/S/0.5 μ m and Ti/R/0.5 μ m 3275 hrs.	78
4.24	Parylene-D CuNi/R/0.5 μ m/4,050 hrs. and Gold on Ti/R/6,540 hrs.	78

4.25	Parylene-D on Ti/R/0.5 μm /0 hrs. SEM (x1000)	79
4.26	Parylene-D on Cu/R/0.5 μm /0 hrs. SEM (x200)	79
4.27	Parylene-D on Ti/S/0.5 μm /0 hrs. SEM (x200)	80
4.28	Parylene-D on CuNi/S/1.0 μm /0 hrs. SEM (x200)	80
4.29	No-Stik(Cu) on Ti/7,670 hrs. and Ti/9,650 hrs.	82
4.30	No-Stik(NiCr) and No-Stik(Al) on CuNi at 780 hrs.	82
4.31	Emralon-333 on Ti/6,400 hrs. and Brass/6,400 hrs.	83
4.32	Emralon-333 on Ti/7670 hrs, Brass and Ti 9,650 hrs.	83
4.33	Wilson Plot Obtained from Data Taken During Filmwise Condensation on a Horizontal Copper Tube	89
4.34	Heat-Transfer Results for Filmwise Condensation on a Horizontal Thin-Walled Copper Tube.	90
4.35	Comparison of Filmwise Condensation Data with the Fujii-Honda Correlation and the Nusselt Equation	91
4.36	Heat-Transfer Results Obtained from Dropwise Condensation on Horizontal, Polymer-Coated, Thick-Walled, Copper Tubes	92
4.37	Heat-Transfer Results for NRL Fluoroacrylic-Coated, Thick-Walled Copper, Aluminum, and Stainless-Steel Tubes	96
4.38	Dropwise Heat-Transfer Coefficients for Thick-Walled, NRL Fluoroacrylic-Coated Tubes at Atmospheric Pressure	97
4.39	Dropwise Condensation Results for NRL Fluoroacrylic-Coated, Thin-Walled Tubes with Wash Primer	98
4.40	Comparison of NRL Fluoroacrylic-Coated, Smooth Tubes with Primer. Tube (clockwise from upper left): Cu, Al, CuNi, SS	99

4.41	Comparison of NRL Fluoroacrylic-Coated Copper Tubes with and without Wash Primer and for Roughness Effects	100
4.42	Dropwise Condensation on No-Stik(Al) Coated Copper Tube	103
4.43	Dropwise Condensation on Emralon-333 Coated Copper Tube	103
4.44	Comparison of Dropwise Quality on Silver-Electroplated Cu (top) and CuNi (bottom) Tubes. P = 85 mmHg, Vv = 2.0 m/s	104
4.45	Dropwise Heat-Transfer Coefficients for Silver-Electroplated, Thin-Walled Copper and CuNi Tubes	105
4.46	Dropwise Heat-Transfer Coefficients for Silver-Electroplated Tubes at Atmospheric Pressure . . .	106
4.47	Effect of Vapor Velocity on the Dropwise Heat-Transfer Coefficient (NRL Fluoroacrylic with Wash Primer)	109
4.48	Dropwise Heat-Transfer Coefficient Versus Vapor Velocity. NRL Fluoroacrylic with Primer on Copper Tube	110

NOMENCLATURE

A_i	Inside surface area of tube
A_o	Outside surface area of tube
C_i	Sieder-Tate coefficient
D_o	Outside diameter of tube
F	$g D_o \mu_f h_{fg} / V_v^2 k_f \Delta T$
g	Local gravitational acceleration
h_{fg}	Specific enthalpy of vaporization
h_i	Water-side heat-transfer coefficient
h_{Nu}	Steam-side heat-transfer coefficient based on Nusselt equation
h_o	Steam-side heat-transfer coefficient based on Fujii-Honda equation
k_f	Thermal conductivity of fluid
k	Substrate thermal conductivity
LMTD	Log-mean-temperature difference
Nu	Steam-side Nusselt number
Pr	Cooling water Prandtl number
q	Heat flux based on the outside area
Q	Heat-transfer rate
Re	Cooling water Reynolds number
\tilde{Re}	Steam-side, two-phase Reynolds number $(\rho_f V_v D_o / \mu_f)$
R_w	Wall thermal resistance based on outside area
ΔT	Local temperature drop across condensate film
U_o	Overall heat-transfer coefficient
V_v	Steam velocity

X Wilson plot parameter defined by equation (3.7)

Y Wilson plot parameter defined by equation (3.8)

Greek Symbols

α_F Leading coefficient for Fujii-Honda equation

α_{Nu} Leading coefficient for Nusselt equation

Γ Wilson plot parameter defined by equation (3.3)

θ Drop contact angle

μ Viscosity of cooling water at bulk temperature

μ_f Viscosity of condensate at film temperature

μ_w Viscosity of cooling water at inner wall temperature

Ω Wilson plot parameter defined by equation (3.4)

ACKNOWLEDGEMENT

The author wishes to express his sincere thanks to Dr. James R. Griffith of the Naval Research Laboratory for his cooperation and assistance in providing many of the coatings which were vital to the success of this thesis. In addition, his professional support helped answer many questions which arose during the investigation.

The author also wishes to thank Dr. P. J. Marto, Dr. A.S. Wanniarachchi, Dr. D. H. Boone, and Dr. J.W. Rose for their recommendations and guidance throughout the course of this thesis.

I. INTRODUCTION

A. BACKGROUND INFORMATION

Despite remarkable technological advancements that have been achieved in almost every engineering field, very few improvements have been made in marine condenser designs. With increased operations in warm water areas, improved condenser performance is very important for the U. S. Navy to maintain efficient operation of both marine propulsion and distilling plants. Significant reductions in size and weight of condensers are also in the Navy's interest to accommodate modern weapon systems without loss of ship stability or speed.

All condensers, on board ships as well as in commercial power plants, currently utilize the filmwise mode of condensation. During film condensation, a sizable resistance to heat transfer occurs on the vapor side because of the continuous layer of liquid that forms on the condensing surface. Many investigators have shown that the filmwise heat-transfer coefficient can be improved by a factor of twenty or more using dropwise condensation. This can give up to fifty-percent improvement in the overall heat-transfer coefficient. An analysis by Search [Ref. 1] showed that a twenty percent reduction in weight, and a twenty five percent reduction in volume could be obtained by promoting dropwise condensation on plain copper-nickel tubes in marine condensers operating at low pressures.

The majority of previous research has been directed toward the understanding of the microscopic mechanisms of dropwise condensation, along with experimental heat-transfer measurements. Many promoters have been identified; however,

only a few are able to endure greater than 3000 hours of continuous dropwise condensation. Before the benefits of dropwise condensation can be fully utilized for industrial and marine condensers, methods for applying permanent hydrophobic coatings must be found. Although a permanent coating would be ideal, coatings promoting continuous dropwise condensation in excess of four years would be satisfactory for most applications. Coatings could then be refurbished during major maintenance periods.

B. DESCRIPTION OF THE DROPWISE CONDENSATION PROCESS

Dropwise condensation is a non-steady, non-uniform process where semi-spherical liquid droplets form when a vapor comes in contact with a colder, non-wetting (i. e., hydrophobic) surface. The combination of small drop size and rapid drop removal greatly reduces the dropwise heat-transfer resistance compared to that of a continuous liquid film. Figure 1.1 compares the two condensation modes for horizontal tubes.

1. Drop Nucleation and Growth

The theory that drops are formed by direct condensation on nucleation sites is well supported by the works of Umur and Griffith [Ref. 2], McCormick and Westwater [Ref. 3], and Reisbig [Ref. 4]. Nucleation sites consist of pits, scratches, and irregularities due to the inherent roughness of the condensing surface. Graham [Ref. 5] suggests that droplet growth is through a series of transition stages. Initially, a nucleated drop grows rapidly by direct condensation. Once drops grow big enough, perhaps covering half the distance between two nucleation sites, the drops begin to grow both by condensation and coalescence. These drops are in the "active" growth stage. As the drops

get larger, vapor condensation decreases and drop coalescence becomes the primary growth mechanism. These drops are in the "inactive" growth stage. Once a critical drop size is reached, where gravity and vapor-shear forces overcome surface-tension and frictional forces, the drop departs. The departing drop sweeps the surface clean of all drops in its path. Both drop coalescence and drop-sweeping effects expose bare surface to further nucleation.

Throughout the drop growth cycle, heat transfer is undergoing a transient process. Experimental results of Graham and Griffith [Ref. 6] show that about 90 % of the heat transfer occurs through active drop areas covering only 30 % of the condensing surface. Tanasawa and Ochiai [Ref. 7], and Tanaka [Ref. 8] found similar results. Almost 60 % of the condensing surface is covered by inactive drops. The remaining 10 % of the surface is bare with no condensation taking place. Active drop diameters range from 0.01-150 micrometers. Once drops grow greater than 150 micrometers in diameter, very little heat transfer occurs across the drop. A large conduction resistance exists and condensation on the inactive drop surface nearly stops.

2. Drop Contact Angle

The quality of dropwise condensation is best defined in terms of the contact angle between the liquid drop and the solid condensing surface. Zisman [Ref. 9] gives a detailed summary of previous works related to contact angle. Contact angle is defined in terms of three interfacial surface tension forces acting between the vapor, liquid, and solid phase boundaries. The orientation of surface-tension forces with contact angle θ , is shown in Figure 1.2 [Ref. 9].

For equilibrium,

$$\gamma_{sv} - \gamma_{sl} = \gamma_{lv} \cdot \cos(\theta) \quad (\text{eqn 1.1})$$

where, γ_{sv} , γ_{sl} , and γ_{lv} are the surface tensions at the solid-vapor, solid-liquid, and liquid-vapor interfaces. When the contact angle θ equals zero degrees, the surface will be completely wetted by the liquid. Surfaces which give contact angles with water of ninety degrees or greater are ideal for dropwise condensation. These surfaces are classified as non-wetting or hydrophobic. Zisman and his co-workers found that a linear relationship exists between the cosine of the contact angle and the surface tension at the liquid-vapor interface. They defined the critical surface tension, γ_c , as the extrapolated value at which $\cos \theta = 1$, where the solid surface is completely wetted by the liquid. The surface tension of a solid is more commonly known as the surface free energy.

The lower the surface free energy of a solid, compared to the critical surface tension of a liquid, the more hydrophobic the surface will be towards that liquid. Water has a liquid-vapor surface tension of 72 dynes/cm, at 25 degrees C.

Since metals have high surface energies, they are naturally wetted by water. In order to produce dropwise condensation, promoters having low surface energies such as polymers and organic compounds must be used. Table I, from Zisman [Ref. 9], gives critical surface tensions for low energy surfaces. The surface constituents listed form the repeating groups for polymers or the most remote groups in organic monomer layers. Associated polymers are also listed.

Zisman gave several significant conclusions based on experimental results. An understanding of these ideas is

essential in obtaining a permanent hydrophobic coating. First, the close-packing of monomer groups on a surface determines the hydrophobicity of a surface. The more close-packed the groups are, the greater the hydrophobicity of the surface. Second, groups containing fluorine atoms are the most hydrophobic. Hydrophobicity can be improved by packing more fluorine in the surface groups. Surfaces with perfluoromethyl groups ($-CF_3-$) have the lowest surface energies known. Figure 1.3, from [Ref. 9], shows how replacement of hydrogen atoms with fluorine and chlorine atoms changes the critical surface tension.

One other important note is how surface roughness affects contact angle. "True" surface contact angles are determined using clean polished metal surfaces. If the "true" contact angle is less than ninety degrees, then the observed contact angle on a roughened surface will be less than the "true" contact angle. Surfaces with "true" contact angles greater than ninety degrees will have greater angles on rough surfaces.

C. FACTORS INFLUENCING DROPWISE CONDENSATION HEAT TRANSFER

Some of the most important factors that affect the dropwise heat-transfer coefficient of steam include: 1) thermal conductivity of condensing surface, 2) non-condensing gases, 3) steam saturation pressure and vapor velocity, and 4) properties of the promoter. Promoter properties will be discussed later.

The effect of condensing surface thermal conductivity has still not been completely resolved. Hanneman and Mikic [Ref. 10] proposed the theory that a thermal constriction resistance exists in the solid surface due to the non-uniformity of drop size and spacing.

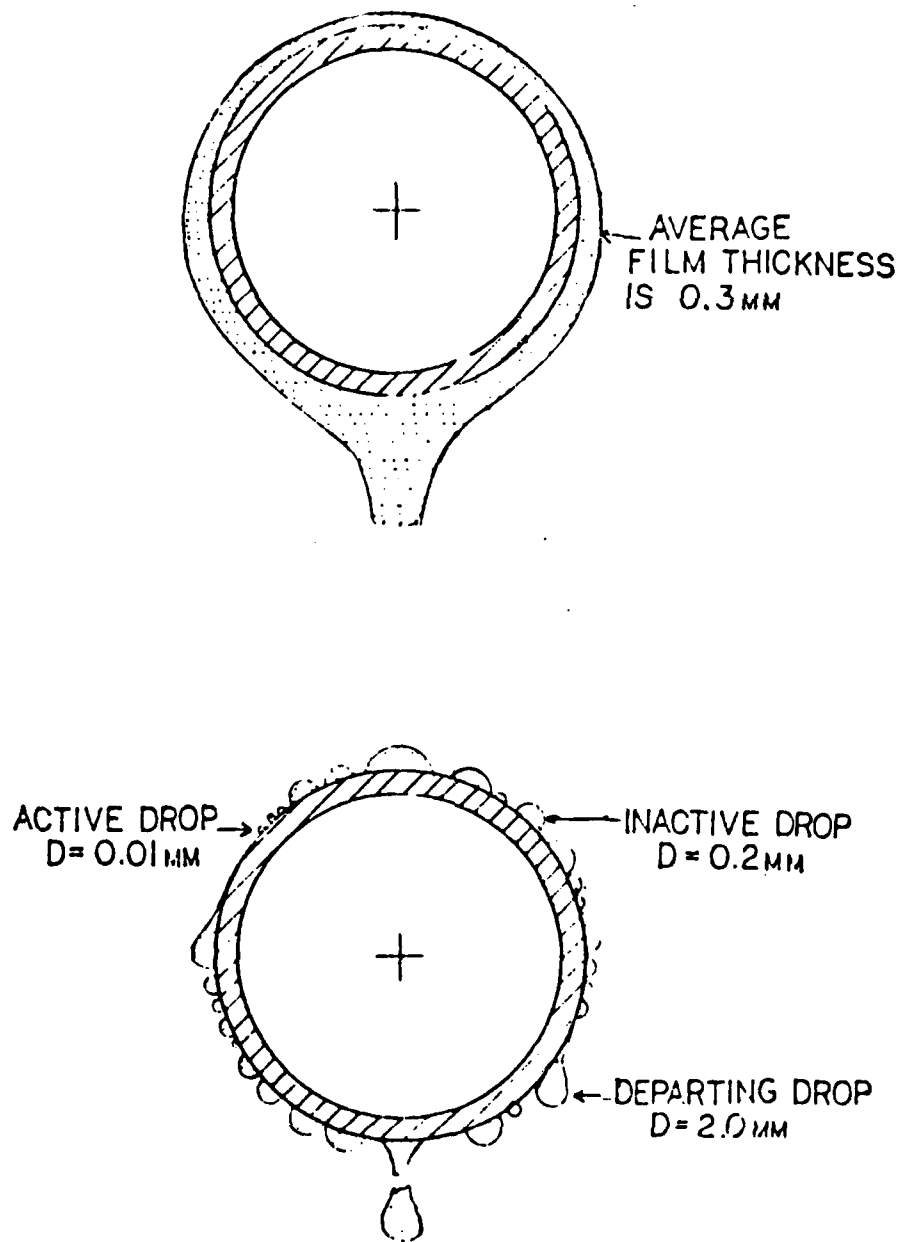


Figure 1.1 Comparison of Film and Dropwise Condensation Modes.

VAPOR

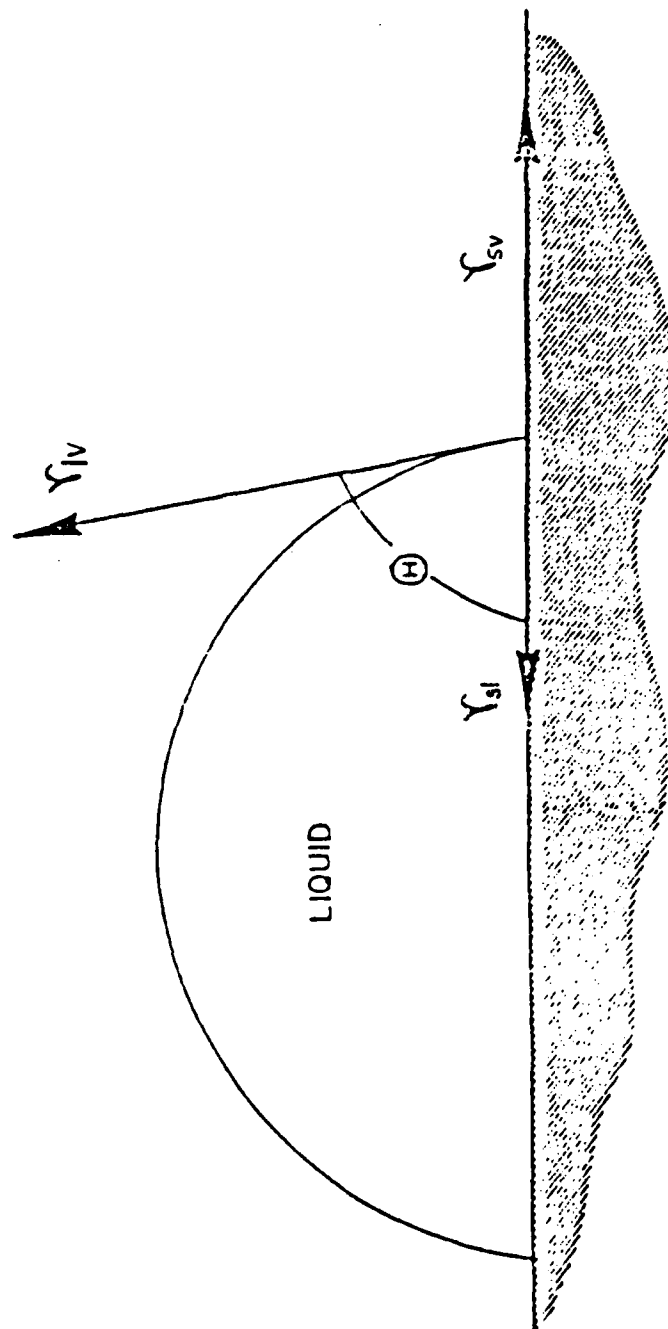


Figure 1.2 Drop Contact Angle.

TABLE I
Critical Surface Tensions of Low Energy Surfaces

Surface Constitution	dynes/cm at 20 C
A. Fluorocarbon Surfaces	
-CF ₃	6
-CF ₂ H	15
-CF ₃ and -CF ₂ -	17
-CF ₂ -	18
-CH ₂ -CF ₃	20
-CF ₂ -CFH-	22
-CF ₂ -CH ₂ -	25
-CFH-CH ₂ -	28
B. Hydrocarbon Surfaces	
-CH ₃ (crystal)	22
-CH ₃ (monolayer)	24
-CH ₂ -	31
-CH ₂ - and $\nabla\nabla\text{CH}\nabla\nabla$	33
$\nabla\nabla\text{CH}\nabla\nabla$ (phenyl ring edge)	35
C. Chlorocarbon Surfaces	
-CClH-CH ₂ -	39
-CCl ₂ -CH ₂ -	40
=CCl ₂	43
D. Nitrated Hydrocarbon Surfaces	
-CH ₂ ONO ₂ (crystal)	40
-C(NO ₂) ₃ (monolayer)	42
-CH ₂ NHNO ₂ (crystal)	44
-CH ₂ ONO ₂ (crystal)	45

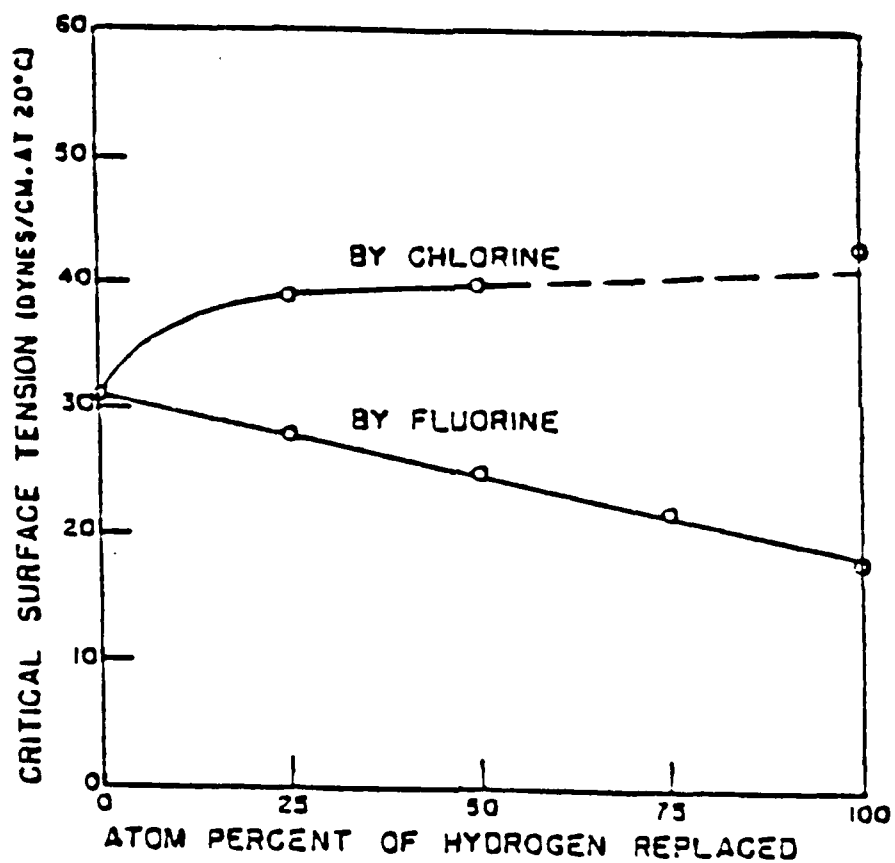


Figure 1.3 Variation of Surface Tension with Amount of Fluorine and Chlorine Replacement of Hydrogen.

Aksan and Rose [Ref. 11] suggested that rapid coalescence between drops could lead to a uniform surface temperature. Therefore, the constriction resistance would be small. Data are available to support both of these proposed models. Inconsistencies were believed to be due to temperature measurement errors, the presence of non-condensing gases, or promoter effectiveness.

Later, work by Rose [Ref. 12] and Stylianou and Rose [Ref. 13], showed little dependence of the dropwise heat-transfer coefficient on substrate thermal conductivity. Rose's work showed that the promoter effectiveness varied significantly with condenser material. The chemical promoter which he used gave excellent dropwise condensation on copper and brass tubes, but mixed condensation on aluminum and stainless steel tubes. When the aluminum and stainless-steel tubes were copper plated, they had the same dropwise quality as the plain copper tube. This agrees with Zisman's theories on the relation between surface properties and wettability, discussed earlier. Copper is one of the most reactive metals and would tend to adsorb a hydrophobic monolayer better than stainless-steel or aluminum.

Hanneman [Ref. 14] presented a model for constriction resistance and noted that it could be significant for very thin, low thermal conductivity surfaces. Recently, Waas et al. [Ref. 15] reported results for steam condensing on gold-plated copper, aluminum, brass, bronze, and stainless-steel surfaces. A definite decrease in dropwise heat-transfer coefficient was shown with decreasing thermal conductivity. It was also noted that surface thermal conductivity was controlling the constriction resistance and not thermal diffusivity.

Non-condensing gas problems have practically been eliminated in recent experiments. This is a very important step in obtaining accurate data since even small amounts of non-condensing gases can cause a drastic reduction in heat transfer.

Graham [Ref. 5] showed an increase in dropwise heat-transfer coefficient with increasing pressure for pressures above atmospheric. Brown and Thomas [Ref. 16] showed similar results for pressures below atmospheric.

Increasing vapor velocity causes an increase in the dropwise heat-transfer coefficient. Increased vapor-shear forces remove the drops at a smaller critical diameter which reduces the drop conduction resistance. Graham [Ref. 5] showed that an upper limit of 1.66 m/s exists, above which there is little effect.

D. PROMOTION OF DROPWISE CONDENSATION

Dropwise condensation can be promoted on high energy metal surfaces by coating them with an organic substance that has a low critical surface tension, preferably less than 35 dynes/cm. This surface can be produced with organic chemical promoters, noble metals or polymer coatings.

1. Chemical Promoters

Hydrophobic monolayers of organic compounds can be applied to condenser surfaces directly or by continuous injection into the steam. Blackman, Dewar, and Hampson [Ref. 17] tested many hydrocarbon compounds, using both methods of application.

In order for an organic compound to be a suitable promoter, anchoring groups containing sulphur (SO_2 , SH), selenium (Se), amines (NH_3), hydroxyl ($-\text{OH}$), or carboxyl (COOH) molecules were required. Anchoring groups adsorb onto

the metal surface, leaving the hydrophobic groups (see Table I) on the exposed surface. Ideal dropwise condensation was obtained by many investigators, but with only limited endurance. Coatings applied by the direct method generally lasted only a few hundred hours. However, some researchers promoted good dropwise condensation that lasted up to 3000 hours. By using continuous injections, continuous dropwise conditions have been obtained in excess of one year. However in this situation, the effect of promoter accumulation on plant chemistry is a serious problem.

Practically, all chemical promoters used previously were hydrocarbons. Since fluorocarbons are more hydrophobic than hydrocarbons, perhaps more research using fluorinated chemical promoters is warranted. In fact, Zisman [Ref. 9] showed that the most hydrophobic monolayer known was obtained using perfluorolauric acid, which has a critical surface tension of only 6 dynes/cm.

2. Noble Metals

In 1969, Bernett and Zisman [Ref. 18] showed that pure water spontaneously wets noble metals which are completely free of organic or oxide contaminants. However, noble metals are known to be excellent dropwise promoters because they readily adsorb organic impurities from the environment. Erb and Thelen [Ref. 19] obtained excellent dropwise condensation on electroplated gold, silver, rhodium, palladium, and platinum surfaces. Almost 11,000 hours of continuous dropwise condensation were obtained on the gold, rhodium, and palladium surfaces.

Woodruff and Westwater [Ref. 20] showed that, using gold, a minimum thickness of 0.1-0.2 micrometers was required to obtain ideal dropwise condensation of steam on electroplated surfaces. Recently, O'Neill and Westwater [Ref. 21] reported that, using electroplated silver, a

0.3 micrometer thickness gave the longest lifetime for continuous dropwise condensation of steam. An auger electron spectroscopy method was used to analyze the surface chemistry, and they found high concentrations of carbon atoms present. Special precautions were taken to prevent organic contamination; however, it was reported that unknown trace organics were present based on the carbon concentrations. No conclusions as to where the organics came from was given, except that the condensing water and gases, such as carbon dioxide or carbon monoxide, were eliminated as sources. One possible source could have been the electroplating baths. Most baths contain cyanide, a carbon-nitrogen ion, and other organic complexing additions [Ref. 22], such as salts of organic hydroxy acids or amines. These are used primarily as "brighteners".

Since noble metals offer very little heat-transfer resistance and are durable, they might make good permanent promoters. Palladium would seem to be the best since 11,000 hours of continuous dropwise condensation was reported [Ref. 19], and it is the least costly of the noble metals with the exception of silver.

3. Polymer Coatings

With continued advancements in thin-film technology, polymer coatings are improving as permanent dropwise promoters. Although there are numerous polymers available, only a few can be applied as hydrophobic ultra-thin coatings.

There are several important factors that must be considered in choosing an appropriate polymer coating for dropwise condensation. First, these coatings must be very thin. In order to obtain significant heat-transfer improvements, coating thickness must be 5 μm or less. This is because of the very low thermal conductivity of polymers.

Coatings must also be able to withstand temperatures in excess of 100 °C for prolonged periods of time. Brydson [Ref. 24] classified the following as heat-resistant polymers: 1) fluoropolymers, 2) inorganic polymers, primarily ones containing main-chain silicon atoms, 3) cross-linked organic polymers, 4) polymers containing p-phenylene groups and other ring structures such as Union Carbide's parylene series, 5) ladder and spiral polymers, and 6) co-ordination polymers. Brydson noted that there has been little success in producing adequate inorganic, ladder, spiral, and co-ordination polymers.

Moisture resistance is essential for effective polymer coating adhesion. Both Fish [Ref. 25] and Schuessler [Ref. 26] stress that no polymer coating is completely moisture resistant. This is owing to the "spaghetti" like nature of polymer carbon chains. Water molecules can diffuse through polymer coatings causing oxidation of metal substrates. In addition, all polymers absorb water which causes them to swell. The combination of substrate oxidation and coating swell is the primary breakdown mechanism for coating adhesion. Coatings can be compared for their ability to resist moisture, by their water transmission rate (WVTR or MTR) and by their absorptivity. Sometimes, permeability is used instead of WVTR. Fluoropolymers have the lowest values of WVTR and moisture absorptivity. Fish [Ref. 25] lists polytetrafluoroethylene and vinylidene chloride as having the best water resistance with a WVTR of 0.005 weight percent per hour.

Another important coating property is its thermal expansion coefficient. Polymers can be divided into two classes: thermoplastics and thermosetting polymers. Thermoplastics can soften or melt at elevated temperatures and have relatively high thermal expansion coefficients. Although they are not soluble in water, thermoplastics can

be dissolved with other compounds such as freon. Thermosetting polymers are completely insoluble because of cross-linking between the carbon chains. They are stronger than thermoplastics, but also tend to be brittle, having much lower thermal expansion coefficients.

Coating adhesion is the most difficult problem to overcome in developing a good dropwise coating. Gaynes [Ref. 27] discusses many aspects of organic coating adhesion and compares different testing methods. All of the factors discussed above contribute to a coating's adhesive durability. Gaynes points out that both molecular and mechanical forces are involved. Molecular forces include van der Waals and London forces, metallic bonding, hydrogen bonding, and electrostatic effects such as polarity. Increased polarity can improve adhesion but can decrease durability of the coating. Mechanical forces include internal stresses in the coating, thermal stresses at the coating-metal interface, and mechanical interlocking between coating and metal at the interface. Internal stresses are developed from either shrinkage or swelling, owing to moisture absorption, during and after coating application. Mechanical interlocking depends on the wettability and roughness of the substrate surface. During application, a coating that wets the surface will tend to fill cracks, pits, and valleys creating less voids. Holden et al. [Ref. 28], after testing fourteen polymer coatings exposed to steam at atmospheric pressure, concluded that roughness was essential for coating durability.

Refined application techniques are required to improve coating adhesion. Fish [Ref. 25] summarized different coating techniques available. The easiest and least-expensive method for applying thermoplastics is by dissolving the polymer into a solution and applying it by brushing, dipping, spinning, or spraying. The thickness of

the coating will depend on how thin the solution is and how well it wets the substrate. The solvent is then evaporated, leaving a polymer coating on the surface. The temperature used for evaporation of the solvent can be important.

Thermoplastics that cannot be dissolved into a solution have to be heated to the molten state, and then applied under pressure. A fluidized-bed coating is a similar method, where a hot substrate is immersed into a chamber of powdered polymer that is circulated with air. Coatings applied using these melt processes tend to be thicker and develop voids at the polymer-metal interface, making them inadequate for steam condensation.

Thermosetting polymers have to be applied as a resin with a curing agent. Polymerization and crosslinking occur after application. Curing rate and temperature must be controlled.

Several new techniques have been developed which are complex and expensive. The most successful are the glow discharge (plasma) polymerization and sputtering processes. An ion-beam sputtering process was developed by NASA Lewis Research Center [Ref. 29] for deposition of fluoropolymers, such as PTFE, FEP, CTFE, and PFA. A fluoropolymer target is placed in a vacuum chamber with an inert gas. The target is excited using an RF power supply, becoming a cathode electron emitter. The inert gas gets ionized and the ions bombard the target with sufficient force to dislodge polymer molecules. These molecules then embed themselves into the substrate. The process can only be used for line-of-sight coating, which is not suitable for condenser tubes unless the tubes were rotated during the application process.

The glow discharge process can produce coatings with most of the desired characteristics needed for dropwise condensation. This process uses a gaseous electric discharge, called a glow discharge, to produce a plasma or

ionized gas from an inert gas such as argon. Organic compounds used to produce the polymer are injected into the glow discharge in a gaseous, liquid, or solution form. The injected organics polymerize on the substrate surface. This technique can be used to polymerize uniformly thin films of most polymers. Sharma and Yasuda [Ref. 30] compared glow discharge effects for parylene coatings. Recently, Sadhir and Saunders [Ref. 31] produced coatings of hexamethyldisiloxane and hexafluorobenzene with this method. Table II lists properties of polymers that might be suitable for dropwise promoters. Fluorocarbons make the most durable and hydrophobic coatings. Until recently, PTFE (Teflon) coatings were primarily evaluated. Fox [Ref. 32], Marvel [Ref. 33], and Perkins [Ref. 34] using PTFE coatings, reported only minor improvements in dropwise heat-transfer coefficients and early coating deterioration. Brown and Thomas [Ref. 16] and Graham [Ref. 5] reported dropwise heat-transfer coefficients three times that of filmwise condensation with coating thicknesses of 2.5 and 1.5 micrometers. Holden [Ref. 23] reported very poor endurances for thin sputtered PTFE coatings. Holden also tested three coatings which used PTFE with either metal or resin binders. These were commercially-applied coatings called No-Stik, Nedox, and Emralon-333.

No-Stik is a copper-based coating impregnated with PTFE. It is developed by Plasma Coatings, Inc.. Results showed excellent durability and drop contact angles. However, the coating was too thick (50 μm) and reduced the dropwise heat-transfer coefficient, which included the resistance of the coating.

Nedox is a chrome-nickel, electro-deposited coating infused with PTFE. It is produced by General Magnaplate Corporation. Although, this coating was thin (5 μm), and enhanced the dropwise heat-transfer coefficient by a factor of ten, endurance was limited to 2000 hours.

Emralon-333, a trademark of Acheson Colloids Company, uses an organic resin binder with fluoropolymers to form the coating. Endurance tests showed continuous dropwise condensation for over 4,000 hours. Since the resin binder appeared to be eroding away, heat-transfer tests were not conducted.

Holden also reported some favorable results for a series of fluoroepoxies developed by Griffith et al. [Ref. 35] at the Naval Research Laboratory, in Washington, D.C.. These fluoroepoxies can be applied easily in a liquid state and cured as thin polymer films. Based on the surface properties of these epoxies, Hamston, Griffith, and Bowers [Ref. 10] indicated that they might make ideal dropwise coatings. Holden reported that these coatings produced 200 % to 240 % improvements in dropwise heat-transfer coefficients, with good durability. The coatings applied were 10-20 micrometers thick. Holden also reported a 5 to 6 times enhancement in the dropwise heat-transfer coefficient using an NRL fluoroacrylic and a Union Carbide parylene-N coating. Recent improvements of these and other coatings have been made and these require further testing.

E. RESEARCH OBJECTIVE

The primary purpose of this study was to evaluate the performance of organic polymers as promoters for dropwise condensation of steam. In addition, noble metal coatings were to be evaluated for comparison and as possible corrosion inhibitors for polymer coatings.

Endurance testing was continued for five coatings initiated by Holden [Ref. 23]. In addition, five new coatings were evaluated which were modifications of the previous coatings: 1) NRL crosslinked fluoroacrylic, 2) NRL mixed fluoroepoxy, 3) No-Stik (Al), 4) No-Stik (NiCr), and 5) parylene-D. A wash primer as well as a vacuum-deposited gold coating were evaluated as corrosion inhibitors.

Heat-transfer evaluations of No-Stik, parylene-D, and NRL fluoroacrylic were conducted. Effects of coating thickness, roughness, substrate thermal conductivity, and vapor velocity were considered.

TABLE II
Properties of Some Polymers

Polymer ^a Coating	Maximum Continuous Service Temperature C	Water Absorption Rate %/24 hr	Moisture Vapor Transmission Rate gm-mil/100 ² in ² -24hr	Thermoplastic (TP) or Thermosetting (TS)
Polyethylene	92 - 200	0.01	-	TP
Polyvinyl- chloride	70 - 105	0.1	-	TP
Epoxy	80 - 150	0.04-0.27	1.8 - 2.4	TS
Silicones	288	0.13	4.4 - 8.0	TS
Polytetra- fluoroethylene	260	0.005	-	TP
Parylene-N ^b	120 - 220	0.06	1.6	TP
Parylene-D ^b	120 - 220	-	0.25	TP
Parylene-C ^b	120 - 220	0.01	0.5	TP

a CRC Handbook of Tables for Applied Engineering
Science, 2nd edition

b Union Carbide, Parylene Environmentally Compatible
Conformal Coatings, Sales Brochure

Note: All values are typical

II. ENDURANCE TEST APPARATUS AND PROCEDURES

A. TEST APPARATUS

A detailed description of the construction of the endurance test apparatus was given by Holden [Ref. 23]. A schematic of the system is given in Figure 2.1. The system was made of three major components: 1) a steam chamber, 2) a heat sink, and 3) a de-superheater.

The steam chamber consisted of a stainless-steel rectangular box with glass windows. Steam entered at the top and was distributed uniformly along the length of the condensing block through a perforated stainless-steel manifold. A branch line, off the steam-condensate return line, kept the steam chamber open to the atmosphere. House steam from a central boiler was fed through a de-superheater prior to entering the steam chamber. This ensured that saturated steam, at atmospheric pressure, was condensed in the steam chamber. The de-superheater also helped to remove rust and scale carryover from the steam supply. Steam pressure was throttled until a steady wisp of steam was visible from the branch line.

The heat sink was made from two flat water-cooled copper plates separated by baffles for improved cooling water distribution. The heat sink held eighty four, 25.4 mm (1 in) square specimens. The specimens were bolted flush against the condensing block with clamps. Figure 2.2 shows the steam chamber in operation.

B. PROCEDURE

The following specimen preparation techniques refer only to the new coatings evaluated. For detailed procedures used to prepare specimens initiated by Holden, see [Ref. 23].

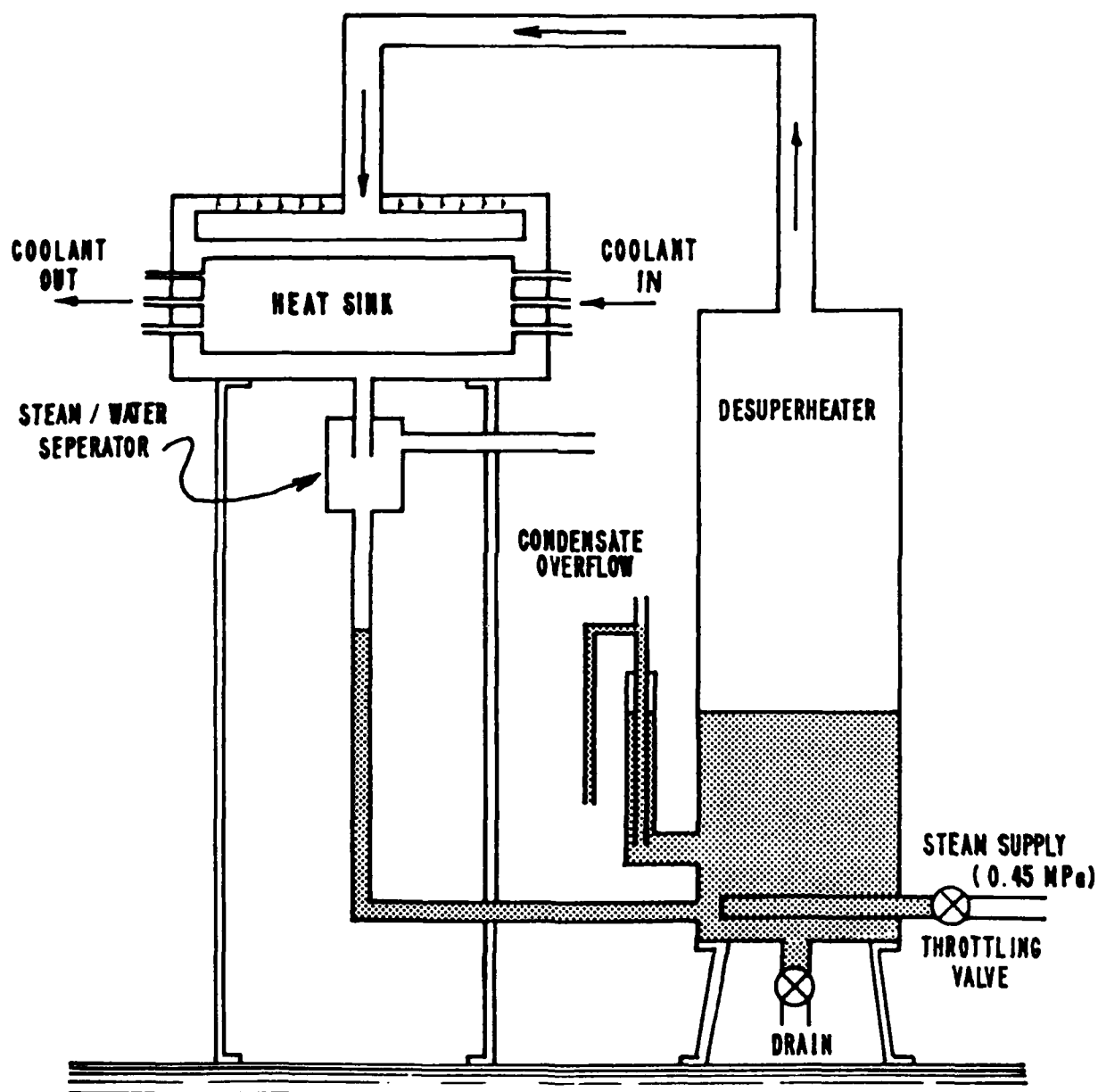


Figure 2.1 Endurance Test Apparatus.

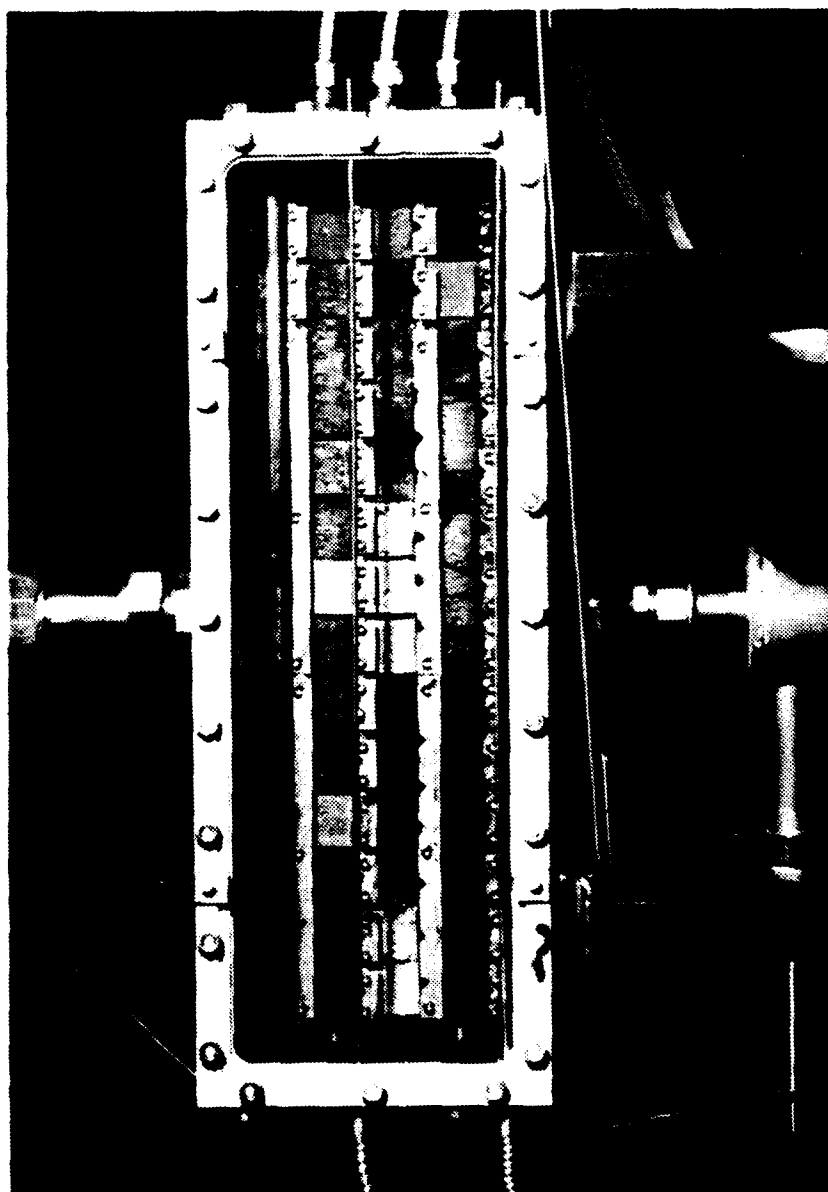


Figure 2.2.2 Steam Chamber in Operation.

1. Substrate Preparation

The following metals were used for specimen substrates: 1) Oxygen-free high-conductivity (OFHC) copper, 2) 90-10 copper-nickel, and 3) titanium. The copper and titanium specimens were 0.76 mm (0.03 in) thick. The 90-10 CuNi specimens were 1.52 mm (0.06 in) thick. All specimens were sheared into 25.4 mm (1.0 in) squares with edges sanded smooth.

Three surface roughnesses were evaluated for their effect on coating adhesion. These included: 1) number 40 glass-grit blast at a gage pressure of 20 psi, 2) number 220 AlO₂-grit blast at a gage pressure of 40 psi, and 3) industrial-size glass-bead blast at a gage pressure of 100 psi. The average RMS height for each surface roughness was determined by means of a surface profilometer.

All specimens were cleaned for ten minutes in an ultrasonic bath of ethanol. The specimens were handled with tongs and remained untouched by human hands thereafter. Specimens were sent to NRL, Washington, D. C., and coatings were applied directly with no further substrate preparation. Specimens sent out for commercial coatings had variations in roughness and handling procedures dictated by the manufacturer. These were considered proprietary by the manufacturer. Most industries use a grit blast followed by a degreasing procedure for substrate preparation.

2. Photographic and SEM Investigation

Visual observations of dropwise condensation on the specimens were conducted daily and photographs were taken every 500 hours. Micrographs were taken of selected specimens with a scanning electron microscope (SEM). Since the polymer coatings were not electrically conductive, a shadowing technique was used to obtain the SEM micrographs. A

thin layer of 100% pure gold was vacuum deposited for this purpose using an Ernest Fullam Vacuum Evaporator. Based on the volume of 203 μm (0.008 in) diameter gold wire used, and the vacuum chamber surface area, the thickness of the deposited gold layer was approximately 15 Angstroms.

3. Physical Property Tests

Two standard tests were performed which provided a relative indication of a coating's adhesive and hardness properties. A tape test for adhesion and a pencil test for hardness were used following ASTM specifications [Refs. 37,38]. Hardness testing was limited because of surface roughness. The standard test calls for mirror-smooth substrate surfaces; however, 220 grit blasted specimens were used for some coatings. Because of the limited availability of specimens, test results were assumed to be representative of the specimens. A large number of tests would be required to obtain statistically valid results.

Coating thickness was determined using several methods. Coatings with thicknesses greater than 10 μm were measured with a micrometer. The thickness of the NRL fluoroepoxies and fluoroacrylics were determined by weighing the specimens before and after coating application. A specific gravity of 1.6, determined experimentally by Dr. James Griffith at NRL, was used in the calculation of the thickness. A knife-edge scale was used with an accuracy of ± 0.0001 g. Verification of coating thicknesses from SEM photos was conducted whenever possible.

C. POLYMER COATINGS EVALUATED

Ten polymer coatings were evaluated for their ability to promote and sustain dropwise condensation of steam at atmospheric pressure. Five of the coatings were on specimens

initiated by Holden [Ref. 23]. The remaining five were modified versions of the coatings tested by Holden. The intent of the modifications was to improve coating durability.

Since the endurance test was designed to be harsh, it is important to note that none of the coatings were designed specifically for this purpose. Therefore, none of the results or qualitative assessments should be construed as critical statements of a particular coating's ability to perform in its intended environment. The following coatings were evaluated:

1. NRL Fluoroepoxy

Two variations of the NRL fluoroepoxy series were evaluated. These included the C-6 and "Mixed" fluoroepoxies. Both coatings were developed and applied by Dr. James Griffith at the Naval Research Laboratory. Fluoroepoxy is composed of two parts, a resin and a curing agent, mixed in a four-to-one weight ratio. The general formula for the resin is given in Figure 2.3.

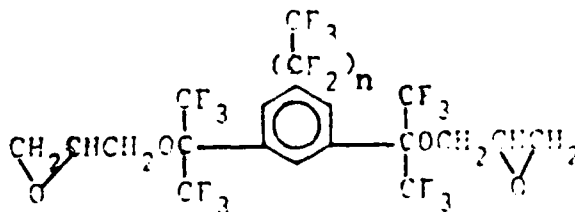


Figure 2.3 General Formula for NRL Fluoroepoxy.

Fluoroepoxies are named in terms of the value of "n", the number of carbon atoms in the perfluorinated, straight-chained, "dangling" group present on the number five position of the central benzene ring. For the C-6 fluoroepoxy, "n" equals six. Mixed fluoroepoxy is made of a combination of chains with "n" varying from five to eleven.

Longer dangling groups should make the polymer more hydrophobic. The curing agent was "c-o" ethylene diamine. The system was made compatible by dissolving both parts in methyl-ethyl ketone. The coatings were applied to the specimens with an artist brush. Polymerization occurs after application, producing a thermosetting polymer.

Four specimens coated with NRL C-6 fluoroepoxy on titanium, copper, and 90-10 CuNi substrates were evaluated. Holden [Ref. 23] obtained greater than 4000 hours of dropwise condensation on the specimens. All four substrates were prepared using a size 40 glass-head grit blast. The dropwise quality was classified as fair to good by Holden. He also noted that the copper and CuNi substrates were darkened from sub-coating corrosion.

In this thesis, fourteen specimens coated with NRL Mixed fluoroepoxy were evaluated. This coating was clear and glassy in appearance. All three surface roughnesses and substrate materials were used. Half of the specimens were coated with an ultra-thin "wash" primer (MIL-P-15328D) before the fluoroepoxy was applied. The wash primer was applied in an attempt to prevent subcoating corrosion.

2. NRL Fluoroacrylic

NRL fluoroacrylic was also developed and applied at the Naval Research Laboratory. NRL's "umbrella" fluoroacrylic is a thermoplastic, which is polymerized prior to application. The coating was dissolved in Freon and applied with an artist brush. Once applied, the Freon is evaporated leaving a very thin fluoroacrylic coating. The coating can be applied at room temperature making it one of the most practical thin-film-deposition techniques. The chemical structure of the fluoroacrylic is shown in Figure 2.4.

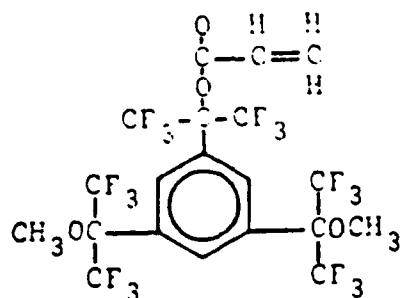


Figure 2.4 NRL Fluoroacrylic.

Six specimens coated with the umbrella fluoroacrylic were evaluated. Three of the specimens, which had rough copper, CuNi, and titanium substrates, were continued from Holden's work. Approximately 2,500 hours were previously obtained with good quality dropwise condensation. The copper specimen had a dark oxide layer. The remaining three specimens had a vacuum-deposited gold layer beneath the coating. Glass-bead roughened titanium and copper substrates were used in addition to a mirror-smooth copper substrate. The gold "flash" was used as a corrosion inhibitor. Three additional gold-flashed specimens were evaluated without polymer coatings for comparison. A crosslinked version of the fluoroacrylic was also evaluated. This was developed and applied by the same methods used for the umbrella fluoroacrylic with the addition of a crosslinking agent. Fourteen specimens were tested in the endurance rig. Several specimens were used for physical property tests. Half of the specimens had the wash primer subcoating which was used with the fluoroepoxies.

3. Parylene

Parylene is the generic name for a thermoplastic polymer series developed by Union Carbide Corporation. The two coatings tested from this series were Parylene-N and Parylene-D. Parylene-N is the basic member of the series, chemically known as poly-para-xylylene, shown in Figure 2.5.

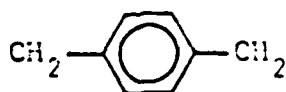


Figure 2.5 Chemical Formula for Parylene-N.

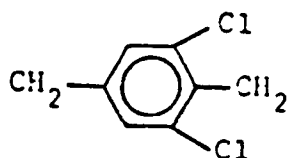


Figure 2.6 Chemical Formula for Parylene-D.

Parylene-D contains two chlorine atoms on the central benzene ring as shown in Figure 2.6. The coating is applied by condensing the vaporized constituents on the substrate in a vacuum. A glow-discharge process is sometimes used to activate the substrate for improved coating adhesion. Polymerization takes place on the surface providing an ultra-thin, uniform film.

The parylene coatings were applied by Lawrence Livermore National Laboratory which is licensed by Union Carbide. Parylene-N specimens, as tested by Holden [Ref. 23], gave disappointing results. This was primarily because of the lack of substrate preparation prior to coating. Coating thicknesses of 0.5 micrometers and 1.0 micrometer were evaluated. In this thesis, four Parylene-N coated specimens were evaluated to verify Holden's results. These specimens were from the same batch as Holden's.

Sixteen specimens coated with Parylene-D were also evaluated. Coatings were applied on smooth (600 grit) and rough (glass bead) substrates prepared by Holden. Both 0.5 and 1.0 micrometer thick coatings were tested.

4. No-Stik

No-Stik is a thermally-conductive coating developed by Plasma Coatings Incorporated. The coating process is proprietary information. The coating is applied by a thermal or plasma spray technique. Basically, No-Stik is a fluoropolymer coating loaded with metal during the application process.

The No-Stik(Cu) coating tested by Holden [Ref. 23] had copper as the base metal. Endurance testing was continued for these specimens, which had previously obtained 4,000 hours of good to excellent dropwise condensation. Holden's heat transfer results showed that the coating was too thick (80 μm) to give any heat-transfer enhancement. Two additional No-Stik coatings were therefore evaluated which had aluminum and nickel-chromium base metals. Attempts were also made to have the coating applied thinner.

5. Emralon-333

Emralon-333 is a one-component blend of fluorocarbon lubricants in an organic resin binder, produced by Acheson Colloids Company. The Emralon-333 was sprayed on using an external atomizing gun. Three specimens were evaluated in continuation of Holden's work. Greater than 4,000 hours were obtained previously with fair to good dropwise quality. Holden [Ref. 23] noted that the resin binder was slowly eroding away.

III. HEAT-TRANSFER MEASUREMENTS

A. APPARATUS

A detailed description of the apparatus used for heat-transfer measurements was given by Poole [Ref. 39] and Georgiadis [Ref. 41]. A schematic of the system is shown in Figure 3.1. Only a brief description of the apparatus is presented in this thesis.

A 0.305 m (12 in) diameter glass boiler, using ten 4000-watt immersion heaters, generated steam from distilled water. The steam then flowed through a reducer into an insulated vertical section 2.44 m (8 ft) long. After passing through a 180 degree bend, the steam flowed downward through a 1.52 m (5 ft) vertical section and entered a stainless-steel test section. Figure 3.2 shows a schematic of the test section with the tube mounted horizontally. A glass view port was installed to allow observation of the condensation process. A secondary coil condenser was used to condense any remaining steam. All condensate was returned to the boiler by gravity flow. Vapor velocities past the test tube of up to 8.0 m/s (26.2 ft/s) could be obtained when condensing at a pressure of 0.012 MPa (1.62 psia).

Two centrifugal pumps in series provided the cooling water flow for the tubes. A throttle valve was used to vary the flow from zero to a maximum of 0.55 liters/s (8.8 gal/min). The condensing pressure was controlled by throttling the flow of tap water through the secondary condenser.

A vacuum pump was operated continuously during the experiment to ensure that the non-condensing gas concentration was virtually zero. A 400 liter (106 gal) tank, used

to provide a positive suction head for the cooling-water pumps, was also used to condense any steam withdrawn by the vacuum suction line in order to prevent moisture buildup in the vacuum pump. This system is shown in Figure 3.3.

A silicon-controlled rectifier was used to regulate power to the heaters. This provided an accurate measure of the power being consumed. A mercury-in-glass manometer was used to measure the test section condensing pressure.

Since the coolant temperature rise (which was from 0.5 to 9 K) was the most important measurement in this experiment, two independent means to measure it were used: two quartz-crystal thermometers and a ten-junction, series-connected, copper-constantan thermopile. Proper insulation and adequate immersion depths were provided for all probes. The quartz thermometers had a resolution of 0.0001 K, but, calibrating against a platinum-resistance thermometer, the measurements were found to be accurate to within ± 0.03 K. The thermopile had a resolution of 0.003 K. During all data runs, the coolant temperature rise measured by the quartz thermometers and the thermopile agreed to within ± 0.03 K.

Two type-T thermocouples were used to measure the steam temperature for the test section. A calibrated rotameter was used to measure the cooling-water flow rate.

Raw data were recorded on disk by a Hewlett Packard 9826A computer interfaced with a Hewlett Packard 3497A Data Acquisition System. The rotameter and manometer readings were the only ones which had to be entered manually at the keyboard.

Spiral inserts were used to enhance the inside heat-transfer coefficient for the tubes tested. This was necessary because the inside heat-transfer resistance can become the governing thermal resistance during dropwise condensation.

A small error in determining the inside heat-transfer coefficient can give large errors when inferring the outside heat-transfer coefficient from the overall heat-transfer coefficient.

The spiral insert consisted of a 6.4 mm diameter stainless-steel rod with a copper wire wrapped and soldered around it. The diameter and pitch of the wrapped wire was 3.2 mm and 34 mm, respectively. The wire was machined to give a clearance of 0.5 mm between the outer wire diameter and the tube inside wall. Although ASTM standard sized tubes were used, the inside diameters varied for different tube materials. Therefore, three different inserts were required which had minor variations in pitch (± 3 mm) and outside diameter (± 0.7 mm).

B. TUBES TESTED

1. Plain Tubes

Prior to testing dropwise-coated tubes, data for plain tubes with filmwise condensation were obtained. These data were taken for two reasons. First, the data provided a basis for determining the enhancement obtained from tubes promoting dropwise condensation. The enhancement ratio was defined as the ratio of the dropwise heat-transfer coefficient to the filmwise heat-transfer coefficient. The values of the heat-transfer coefficients determined at a heat flux of 0.35 MW/m^2 were chosen for comparison purposes. Second, the filmwise data were used in a Modified Wilson Plot data-reduction program to obtain the inside heat-transfer coefficient.

Four tubes were used for filmwise data. These were machined from OFHC copper, 6061-T6 aluminum, 90-10 CuNi, and ASTM type 304 stainless steel. All of the tubes were 228.6 mm (9 in) long with a 133.4 mm (5.25 in) condensing length.

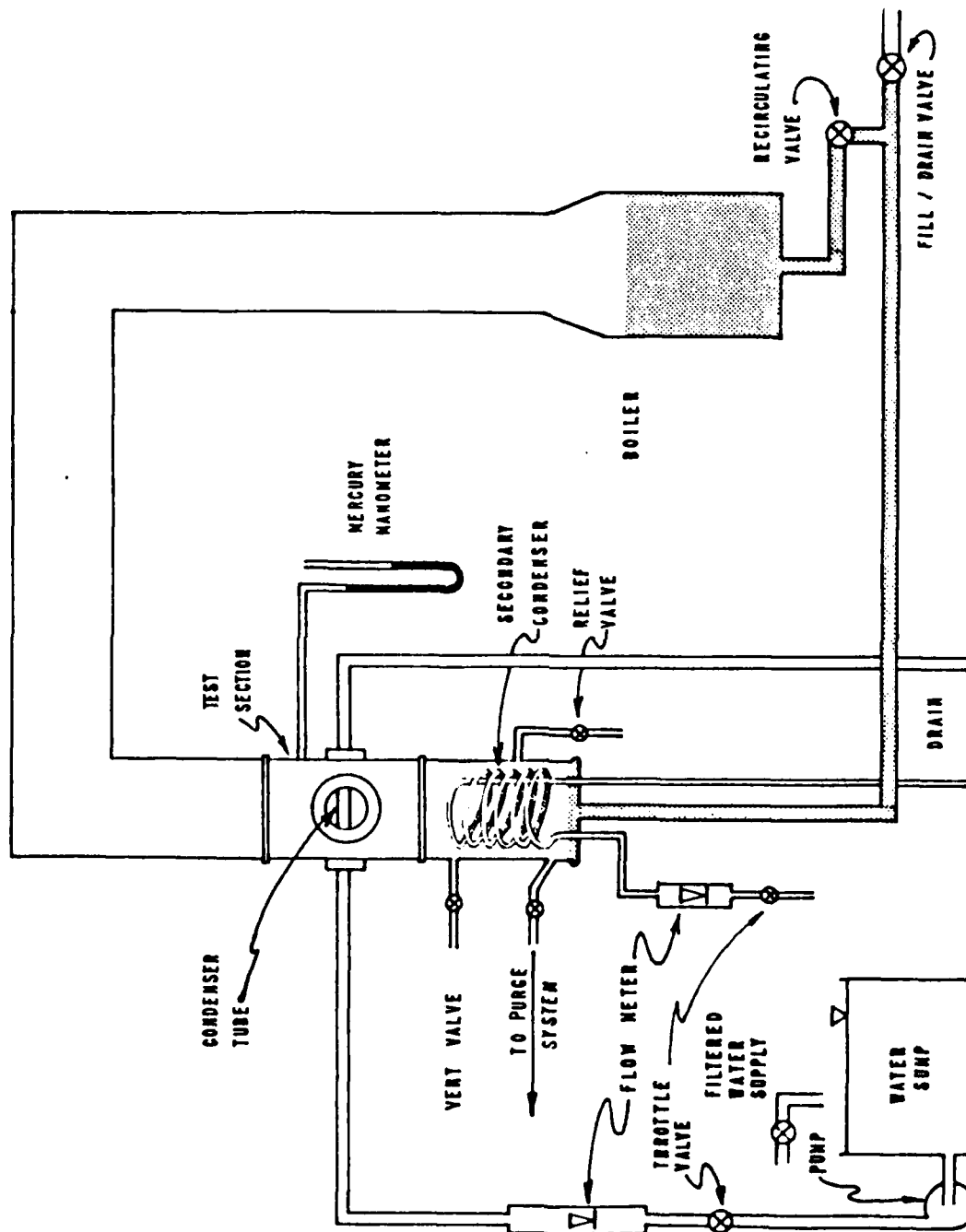


Figure 3.1 Schematic of Heat-Transfer Apparatus.

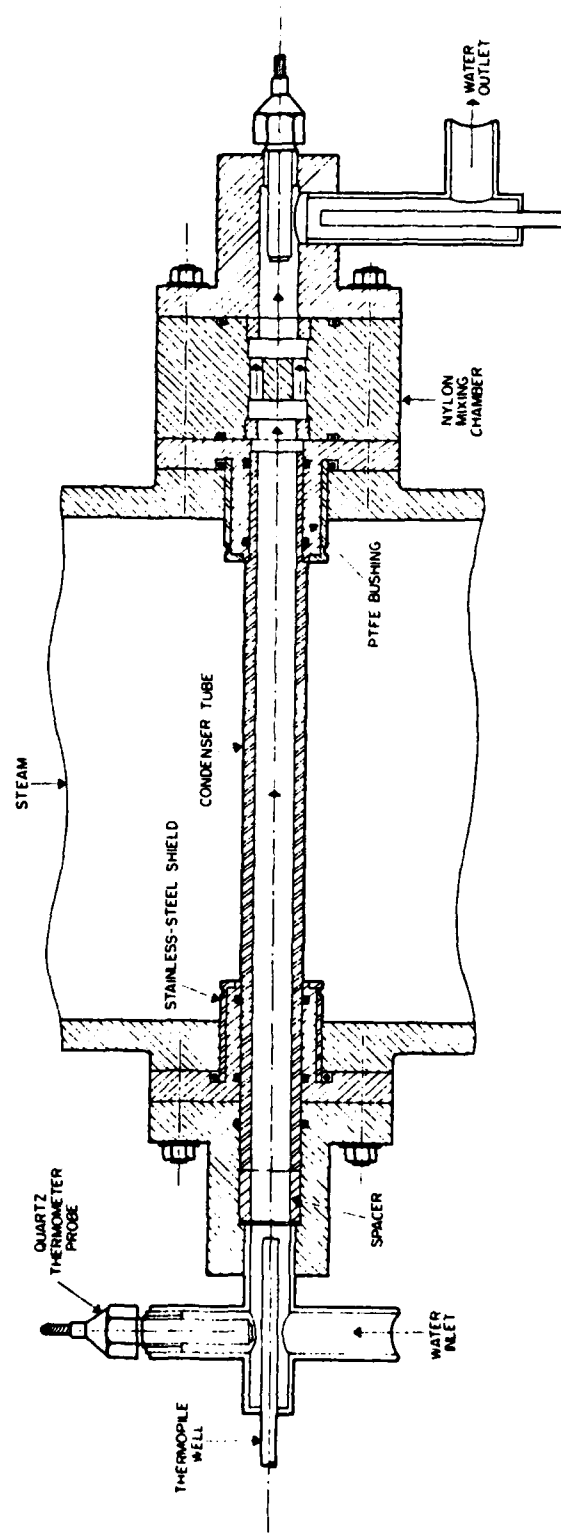


Figure 3.2 Details of Test Section (Insert not shown).

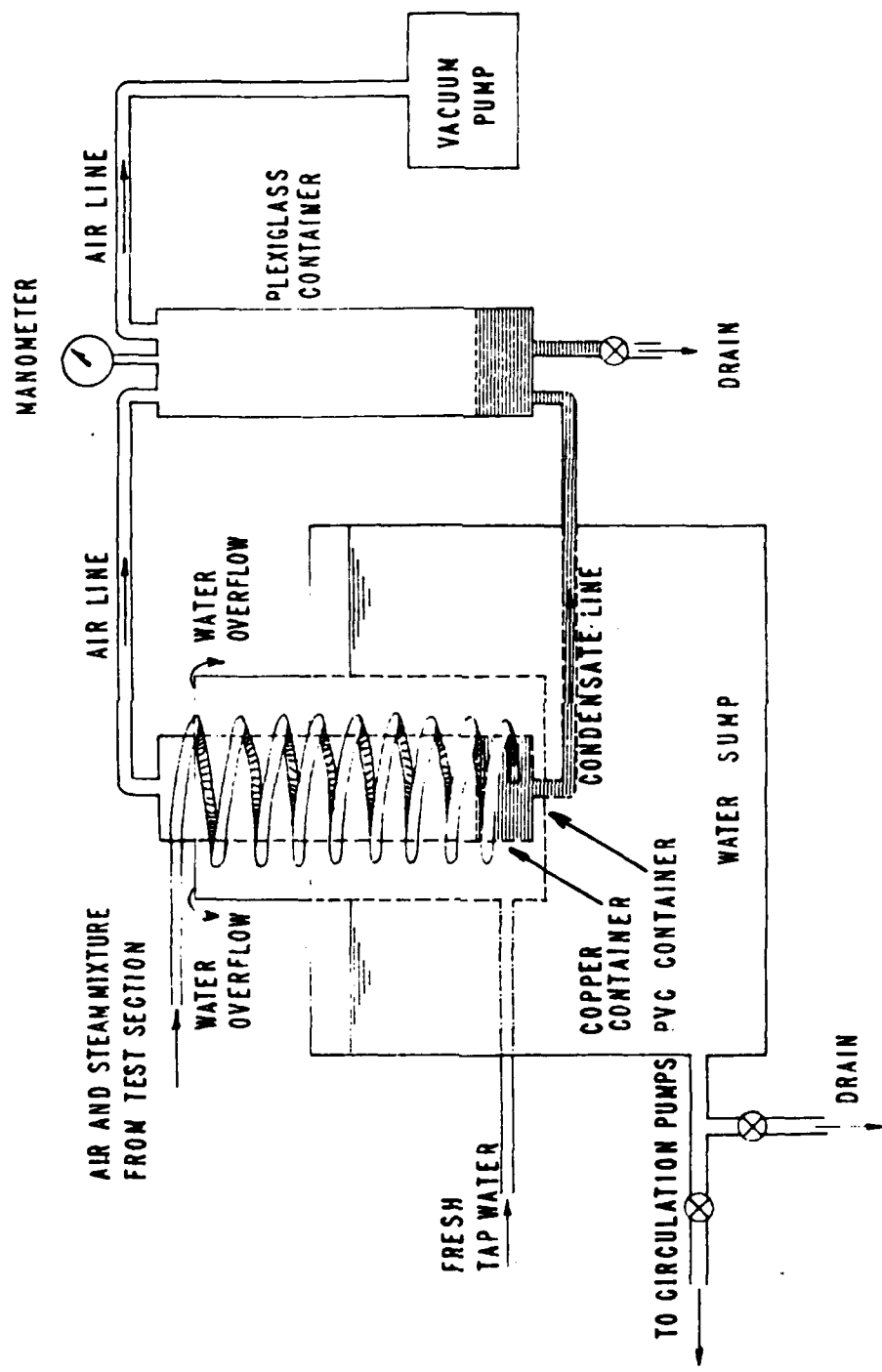


Figure 3.3 Schematic of Purge System and Sump Tank.

The outside diameter for the tube condensing section was 14.22 mm (0.560 in). The tube inlet end length was 60.33 mm (2.375 in) with a 19.05 mm (0.750 in) outside diameter. The tube outlet end length was 34.93 mm (1.375 in) with a 15.88 mm (0.625 in) outside diameter. Although standard size tubes were used, the inside diameters for the 90-10 CuNi and 304 stainless-steel tubes were found to be slightly larger than the copper and aluminum tubes. The inside diameter for the copper and aluminum tubes were measured to be 12.70 mm (0.500 in). Inside diameters of 13.21 mm (0.520 in) for the 90-10 CuNi tube and 13.36 mm (0.526 in) for the stainless-steel tube were measured.

2. Polymer-Coated Tubes

A second set of tubes was machined to the same specifications used for the plain tubes. These tubes were then cleaned with a solution of sodium hydroxide and ethanol. The tubes were rinsed with tap water and dried, and were then coated with a wash primer and with NRL fluoroacrylic. The NRL fluoroacrylic coating was applied by dipping the tubes in a solution of fluoroacrylic dissolved in Freon. The Freon was evaporated, leaving a thin fluoroacrylic coating. The surface roughness of the tubes was considered "smooth" because the coatings were applied on "as machined" surfaces. These tubes are also referred to as "thin-walled" tubes with measured wall thicknesses of 0.762 mm (0.03 in).

Five "thick-walled" tubes were machined and coated with NRL fluoroacrylic. All tube dimensions were the same as for the thin-walled tubes, with the exception of the condensing section outside diameter, which was 19.05 mm (0.750 in). Three of these tubes, one copper, one aluminum, and one stainless steel, were grit blasted with size forty glass grit at a gage pressure of 20 psi. Cleaning and coating procedures were the same as for the thin-walled tubes with the wash primer omitted.

The remaining two thick-walled tubes were coated with wash primer and NRL fluoroacrylic. One of the tubes was grit blasted with a number 220 grit at a gage pressure of 80 psi, and the other had a knurled roughness which was machined using a standard-fine-pitch knurling tool on a lathe.

Two as-machined, thick-walled copper tubes were coated with Parylene-D at Lawrence Livermore National Laboratory. The coatings were vacuum deposited in the same manner as the endurance specimens were coated. One tube was coated with a 1.0 μm thickness and the other with a 0.5 μm thickness.

A thick-walled copper tube was coated with Emralon-333 by Acheson Colloids Company. Surface preparation was determined by the manufacturer. Two additional thick-walled copper tubes were coated with No-Stik coatings by Plasma Coatings, Inc.. One was coated with an aluminum based fluoropolymer (No-Stik (Al)) and the other with a nickel-chromium based fluoropolymer (No-Stik (NiCr)). Surface preparation was determined by the manufacturer. When the coated tubes were received, they were slightly warped and discolored on the inside, indicating that they were exposed to high temperatures during the coating procedure.

3. Silver-Electroplated Tubes

Two thin-walled tubes were electroplated with silver by a local merchant. One OFHC-copper tube and one 90-10 CuNi tube were plated, both of which had smooth polished surfaces. The tubes were plated for one hour in a silver-cyanide electroplating bath.

C. EXPERIMENTAL PROCEDURE

1. Non-Condensing Gas Problem

Since the presence of non-condensing gases can result in significant errors in the condensing coefficient, considerable attention was given to avoid this problem. As also stated by Georgiadis [Ref. 41], the test apparatus was extremely leak-tight. While he reported a leak rate less than 2 mmHg in a 24-hr period, a leak test performed (at a pressure of 85 mmHg) during this work revealed a leak rate less than 1 mmHg in six days. In addition to this remarkably leak-tight test apparatus, the use of continuous purging (as discussed earlier) resulted in virtually no non-condensing gases being present. The computed non-condensing gas concentrations were less than $\pm 0.5\%$ (i.e., zero to within the accuracy of temperature and pressure measurements).

2. Mixing Chamber Calibration

A mixing chamber (see Figure 3.2) was used to obtain a meaningful mixing-cup temperature at the coolant outlet. Insulation was used to reduce errors in the calibration from heat transfer with the surroundings. A calibration was required to account for the temperature rise resulting from viscous dissipation during the mixing process. The coolant temperature rise was measured for various water velocities with the system at room temperature and pressure. A calibration line was plotted for each tube type and insert combination. During condensation data runs, the coolant temperature rise was corrected by subtracting the temperature rise determined from the mixing chamber calibration. Mixing chamber calibration results are plotted in Figure 3.4 for the copper, aluminum, stainless steel, and 90-10 CuNi tubes.

3. Data Collection Procedures

Perfect filmwise condensation was required when taking data for the plain tubes. The slightest amount of contamination caused scattered patches of dropwise condensation. These dropwise patches gave significant increases in the coolant temperature rise which would give erroneous results in data reduction. The tubes had to be thoroughly degreased to ensure good wettability. A solution of 50 % sodium hydroxide and ethanol was used, in equal weight proportions, for tube cleaning. A black oxide layer was formed on the copper and CuNi tubes by brushing the surface with the solution and steaming the tubes over a pot of boiling water. This oxide layer was necessary because copper is very reactive with the environment and readily adsorbs contaminants which tend to promote dropwise condensation. The oxide layer was extremely thin with negligible heat-transfer resistance, see Georgiadis [Ref. 41].

Four complete data runs were made for each of the plain tubes. Runs were made on different days after tube removal and reinstallation to ensure repeatability of the data. Each data run consisted of eighteen data sets. Data sets were taken using the following sequence of flowmeter readings (percent full-scale): 60-50-45-35-30-25-20-40-60. Two sets of readings were taken for each flowrate. Perfect filmwise condensation was observed throughout each data run. Test section condensing pressure was maintained at 85 mmHg (1.64 psia). Vapor velocity was maintained at 1.0 m/s.

The following flowmeter sequence (percent full-scale) was used for tubes promoting dropwise condensation: 80-70-60-45-35-26-20-55-80. All dropwise data runs were conducted at a condensing pressure of 85 mmHg with a 2.0 m/s vapor velocity.

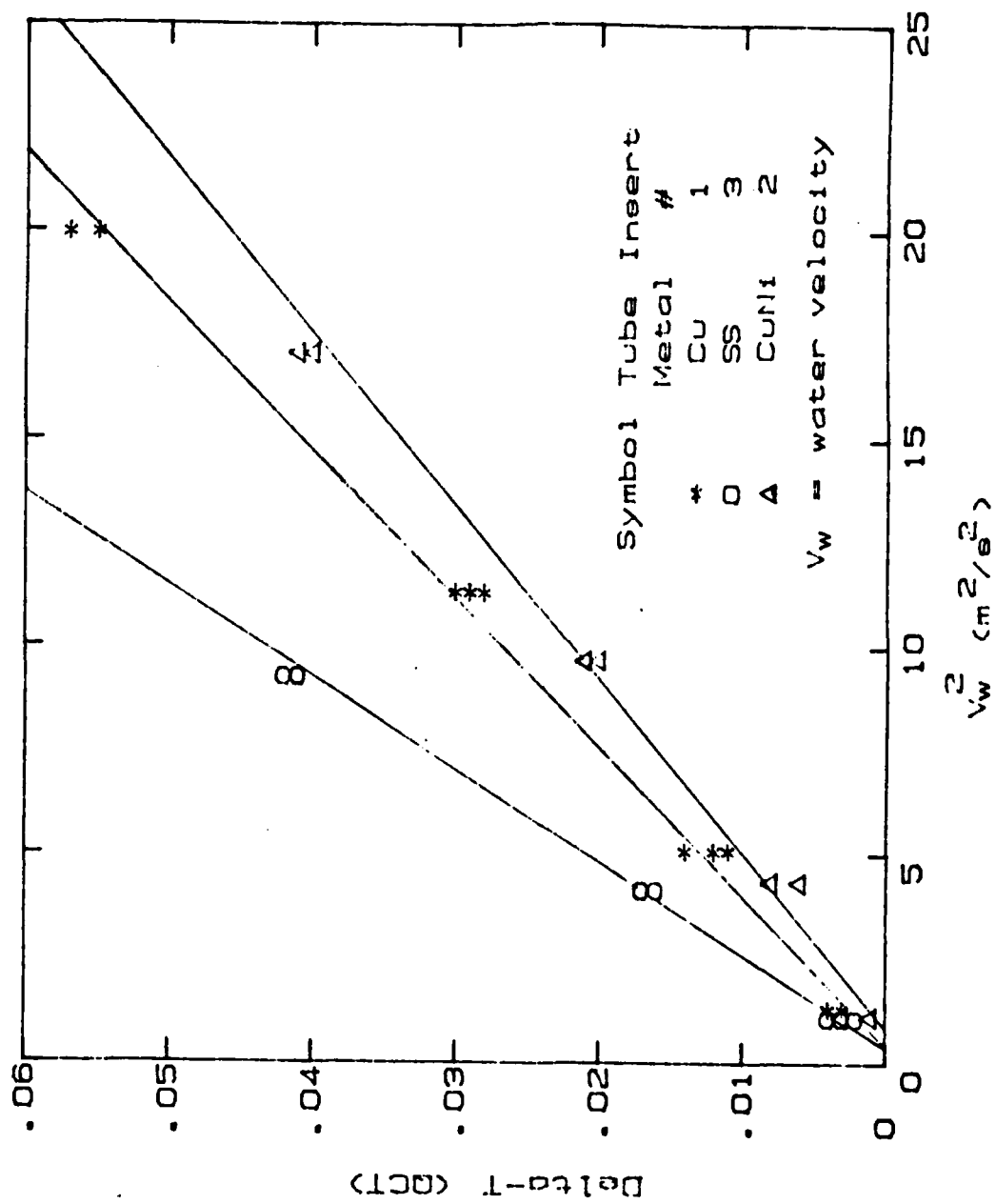


Figure 3.4 Mixing Chamber Calibration.

At least two runs were conducted on different days for each tube. Data runs at atmospheric pressure and 1.0 m/s vapor velocity were taken for thick-walled tubes coated with NRL fluoroacrylic and silver-electroplated thin-walled tubes. The thick-walled copper tube, coated with wash primer and NRL fluoroacrylic, was used to obtain data for different vapor velocities. Dropwise condensation runs were made at a pressure of 85 mmHg for the following vapor velocities: 2.0, 3.0, 4.0, and 6.0 m/s. Vapor velocities were maintained within 3 % of the desired values.

D. DATA REDUCTION

Two data reduction programs were used to process raw data. These were modified versions of the programs used by Poole [Ref. 39]. Listings of these programs are given in Appendices B and C.

1. Modified Wilson Plot Program (WILSON3)

This program calculates the leading constant for the Sieder-Tate equation from the filmwise data. The Sieder-Tate correlation is used to determine the inside heat-transfer coefficient, which is later used in the dropwise data reduction program.

The Modified Wilson Plot method assumes a form of correlation for both the outside heat-transfer coefficient and the inside heat-transfer coefficient, with two coefficients to be found by iteration. In the past, Nusselt's equation for film condensation on horizontal tubes was used for the outside heat-transfer coefficient [Ref. 42]. Equation 3.1 shows the form of the Nusselt equation generally used:

$$h_{Nu} = a_{Nu} \left[\frac{k_f^3 \rho_f^2 g h_{fg}}{\mu_f q D_o} \right]^{1/3} \quad (\text{eqn 3.1})$$

The Nusselt equation results in an value of 0.655 for zero-vapor-shear conditions, and the presence of vapor shear generally results in a higher value, which must be determined iteratively. Since this equation is not valid for high vapor-shear conditions, vapor shear must be held at a low, constant value (corresponding to a velocity less than 1.0 m/s, for example).

To alleviate the deficiency of the Nusselt equation, even with low vapor shear, a correlation developed by Fujii and Honda [Ref. 40] which accounts for the variation of the outside heat-transfer coefficient with vapor velocity was used during this investigation:

$$Nu/Re^{0.5} = 0.96 F^{1/5} \quad (\text{eqn 3.2})$$

This correlation was re-written to express h as a function of heat flux and vapor velocity as shown in equation (3.3):

$$h_o = \alpha_F \left[\frac{q h_{fg}}{q} \right]^{1/4} (\mu_f \eta_o)^{3/8} \rho_f^{3/8} v_v^{1/8} k_f = \alpha_F \Gamma \quad (\text{eqn 3.3})$$

Here α_F is a coefficient to be determined by iteration. Equation 3.4 is the form of the Sieder-Tate equation used to determine the inside heat-transfer coefficient.

$$\frac{h_i \eta_i}{k_f} = C_i Re^{0.8} Pr^{1/3} \left[\frac{\mu}{\mu_w} \right]^{0.14} = C_i \Omega \quad (\text{eqn 3.4})$$

After substitution of equations (3.3) and (3.4) into the equation for the overall heat-transfer resistance (equation (3.5)), a linear equation used to generate the Wilson plot

is obtained (equation (3.6)) :

$$\frac{1}{U_o A_o} = \frac{1}{h_i A_i} + \frac{1}{h_o A_o} + \frac{R_w}{A_o} \quad (\text{eqn 3.5})$$

$$Y = \frac{X}{C_i} + \frac{1}{\alpha_F} \quad (\text{eqn 3.6})$$

where,

$$X = \frac{D_o \Gamma}{\Omega k_F} \quad (\text{eqn 3.7})$$

and

$$Y = \left[\frac{1}{U_o} - R_w \right] \cdot \Gamma \quad (\text{eqn 3.8})$$

The values of X and Y are defined in equations (3.3) and (3.4), respectively.

The parameters X and Y are determined from the fluid property values and the heat flux measured during the film-wise data runs. Iteration between the Sieder-Tate coefficient C_i , and the Fujii coefficient α_F , is continued until convergence within 0.1 % between two successive iterations occurs. The slope of the Wilson plot generated is the inverse of the desired Sieder-Tate coefficient. Sieder-Tate coefficients were determined for each tube-insert configuration used for dropwise data.

2. Dropwise Data Reduction Program

This program was used to determine the outside heat-transfer coefficient from the dropwise data. The outside

heat-transfer resistance was determined by subtracting the inside and wall resistances from the overall heat-transfer resistance as shown in equation (3.5). The overall heat-transfer coefficient was determined from the measured values for the total heat transfer and log-mean-temperature difference (equation (3.9)):

$$U_o = Q/A_o \text{ LMTD} \quad (\text{eqn 3.9})$$

The conduction resistance of the polymer coating was included in the outside heat-transfer resistance. The inside heat-transfer coefficient was determined using the Sieder-Eate equation with the appropriate loading coefficient determined earlier.

Appropriate correlations were used to account for fluid property variations with temperature. The fin effect of the tube ends, outside the condensing section, was included in the analysis [Ref. 39].

IV. RESULTS AND DISCUSSION

A. ENDURANCE TEST RESULTS

The quality of dropwise condensation on the test specimens was classified as excellent, good, fair, or poor based on visual observations. For excellent dropwise condensation, the drops appear spherical in shape with contact angles close to 90 degrees and the drops grow to no more than two to three millimeters in diameter. Drop sweeping action should be swift and vertical while maintaining good contact angles. Drops which appear flat, irregular shaped, and grow to greater than 4 mm in diameter were characteristic of poor dropwise condensation. A summary of the endurance test results is provided in Table III.

During visual observations, it was noticed that the copper condensing block promoted scattered dropwise condensation. This occurred only after the block was cleaned giving a shiny metal appearance. After investigation, it was found that a volatile corrosion inhibitor (di-ethyl amino ethanol) was promoting dropwise condensation on the clean condenser block. This chemical is injected into the house boiler, which provided the steam supply for the endurance test apparatus. After about one month, an oxide layer formed on the condenser block producing filmwise condensation. Based on the short-lived dropwise promotion of the corrosion inhibitor, the lower critical surface tensions of the fluoropolymers tested, and visual observations, it was decided that the chemical promoter had little effect on the quality of dropwise condensation and coating endurance for the coatings evaluated.

1. NRL Fluoroepoxy

Two of the four C-6 fluoroepoxy specimens failed to produce adequate dropwise condensation after about 6,500 hours. The specimen with the CuNi substrate was the first to fail. The quality of dropwise condensation continuously decreased with increased oxidation of the CuNi substrate. Figure 4.1 shows the degradation of the dropwise quality for this specimen. Excellent dropwise condensation on Parylene-D is also shown for comparison. The other specimen which failed had a titanium substrate. In this case, oxidation could not be blamed for coating separation. Observation under an optical microscope revealed tears in the remaining portions of the coating. This was also observed for the CuNi specimen. Since thermosetting polymers tend to be brittle, thermal stresses could be fracturing the coatings, causing eventual failure by erosion.

Substrate oxidation tends to breakdown the mechanical bond between the coating and the substrate. Two types of substrate oxidation were observed to occur on the copper and CuNi substrates. A "green" oxidation layer formed bubbles in the coatings, as shown in Figure 4.1, eventually separating the coatings from the substrate. A "black" oxidation layer formed on some substrates. This layer didn't seem to affect coating durability or the quality of dropwise condensation. No significant pattern was observed to explain why some substrates had a green oxide layer and others a black oxide layer. Whichever oxide layer formed first, prevailed throughout the test for that substrate.

Two C-6 fluoroepoxy coated specimens continued to produce fair to good dropwise condensation. These are shown in Figure 4.2. The titanium specimens showed some wetting, indicating possible fractures existed in the coating which exposed the substrate. It should be noted that the copper specimen shown had a black oxide layer beneath the coating.

The mixed fluoroepoxy coated specimens produced slightly better dropwise condensation than the C-6 fluoroepoxy-coated specimens. At start up, all of the specimens produced good dropwise condensation as shown in Figures 4.3, 4.4, and 4.5. Maximum drop sizes appeared to be larger for the 40-grit and glassbead-roughened surfaces. These roughnesses had larger peak heights, which tend to hold up the drops, allowing them to grow larger before departure. This indicates that the rougher surfaces would tend to reduce the dropwise heat-transfer coefficient. However, this effect is very small as will be seen later. No significant differences were observed between drop contact angle and the different substrate roughnesses as shown in Figures 4.5 and 4.6.

The wash primer used on some specimens significantly reduced substrate oxidation. Figures 4.7 and 4.8 compare CuNi specimens with and without the wash primer. In Figure 4.7, it can be seen that the dropwise quality is poorer for the specimen without the primer, indicating that the coating is starting to fail. This shows definite evidence that the reduction of substrate oxidation can significantly increase coating endurance. It is still unclear as to whether the wash primer improves the adherence of the coating to the substrate.

2. NRI Fluoroacrylic

The two fluoroacrylic coated copper and titanium specimens continued to promote good dropwise condensation in excess of 9,000 hours. Some degradation of the dropwise quality was visible after approximately 7,000 hours. This is shown in Figures 4.9 and 4.10. The copper specimen had an all-black oxide layer until approximately 7,000 hours of continuous dropwise condensation. Then small green oxidation spots appeared, which could explain the degradation in

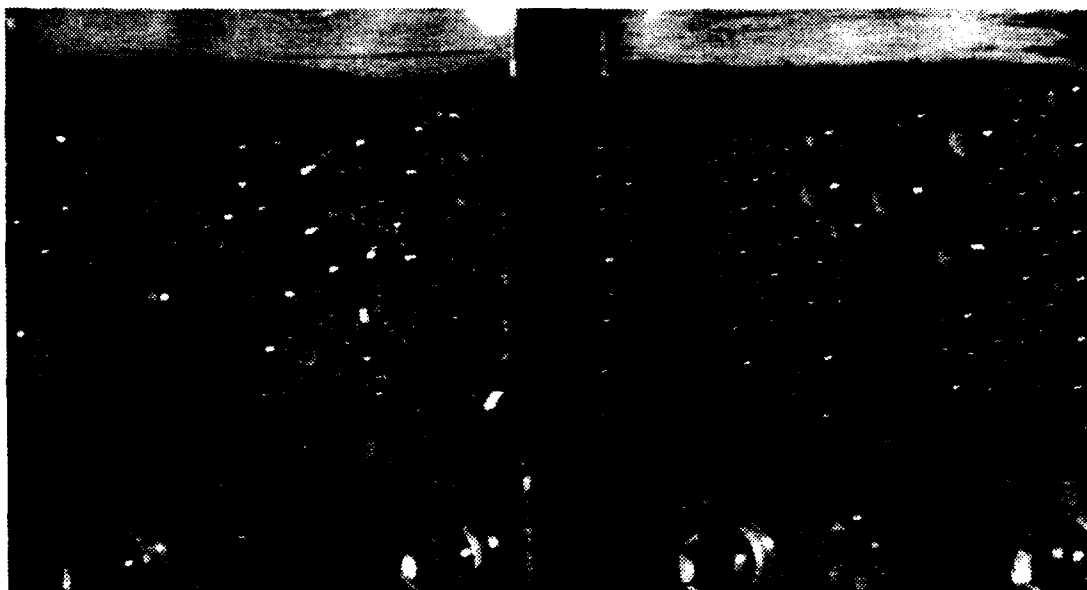


Figure 4.1 NRL C-6 CuNi/R 6,000 hrs. and Parylene-D
on CuNi/R 2,800 hrs..



Figure 4.2 NRL C-6 Ti/R 9,650 hrs. and on Cu/R 7,670 hrs..

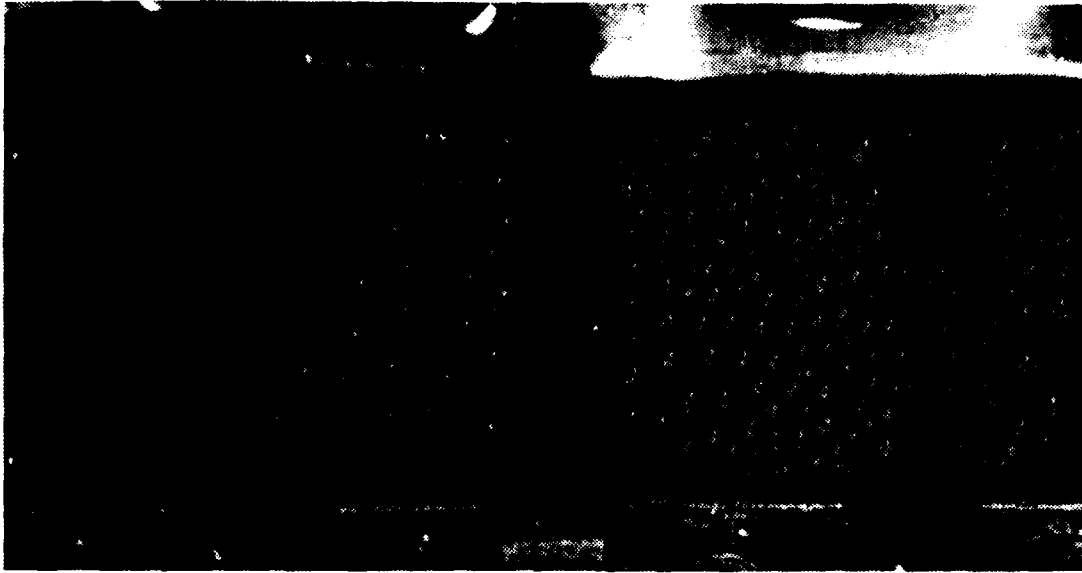


Figure 4.3 NRL Mixed Fluoroepoxy on CuNi/220 grit/wp/0 hrs.
and on CuNi/220 grit/0 hrs..

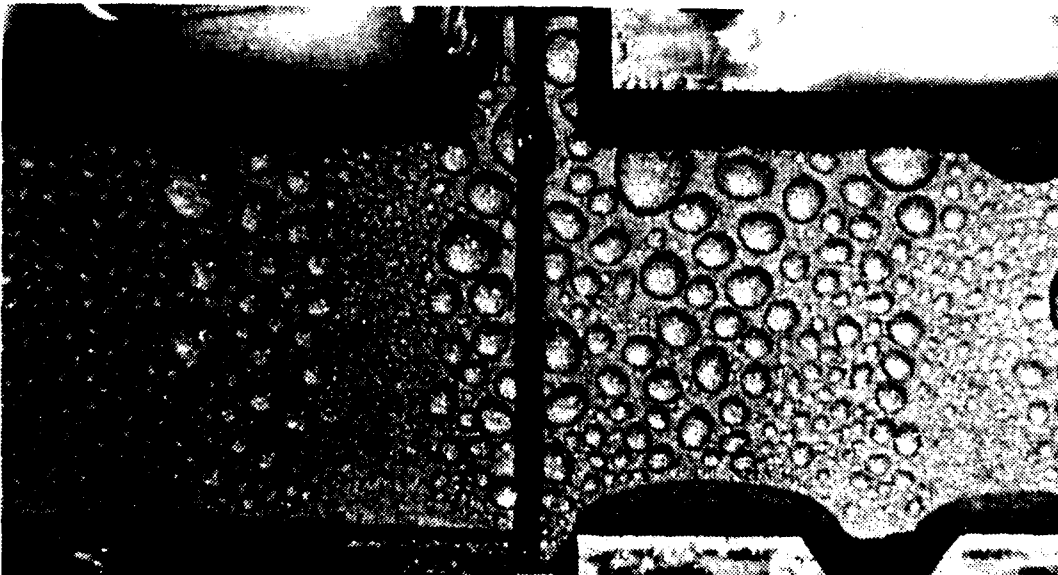


Figure 4.4 NRL Mixed Fluoroepoxy on CuNi/40 grit/wp/0 hrs.
and on CuNi/40 grit/0 hrs..

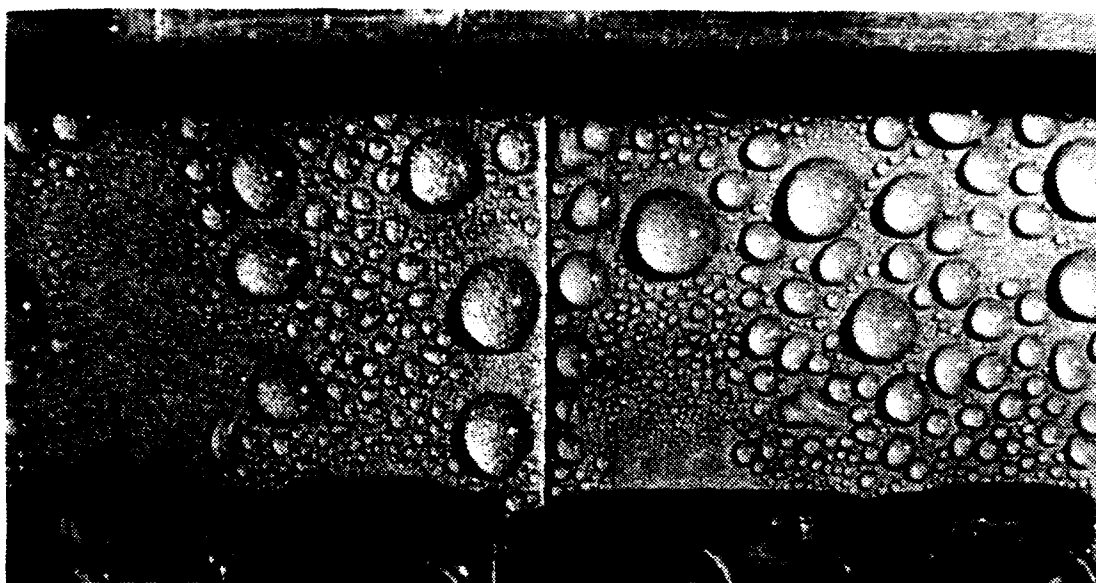


Figure 4.5 NRL Mixed Fluoropolymer on Cu/glassbead/wp/0 hrs.
and on Cu/220 grit/0 hrs..



Figure 4.6 NRL Mixed Fluoropolymer on Ti/40 grit/1,120 hrs.
and on Ti/glassbead/wp/1,120 hrs..

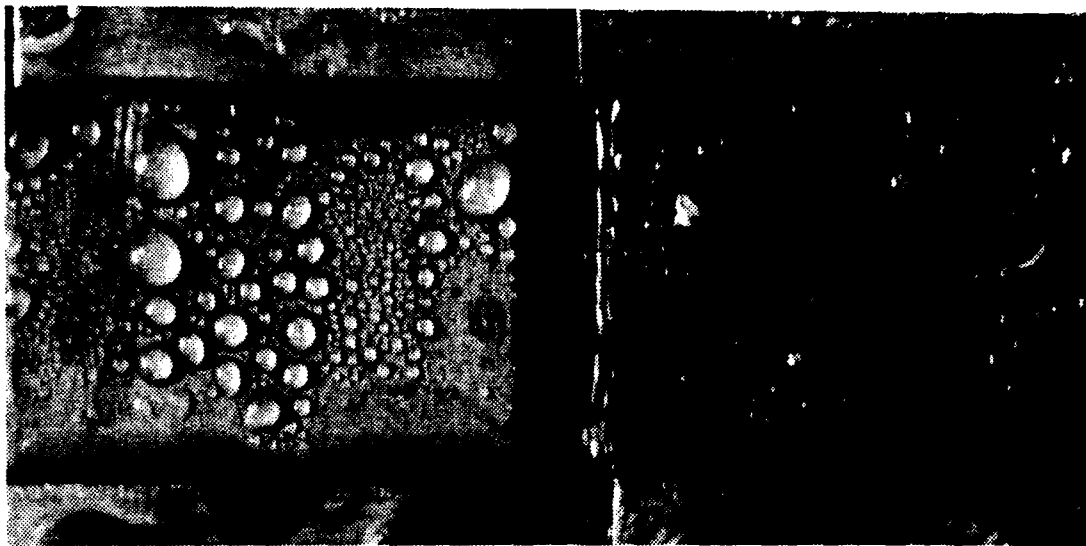


Figure 4.7 NRL Mixed Fluoroepoxy on CuNi/220 grit/wp/1,120 hrs and on CuNi/220 grit/1,120 hrs..

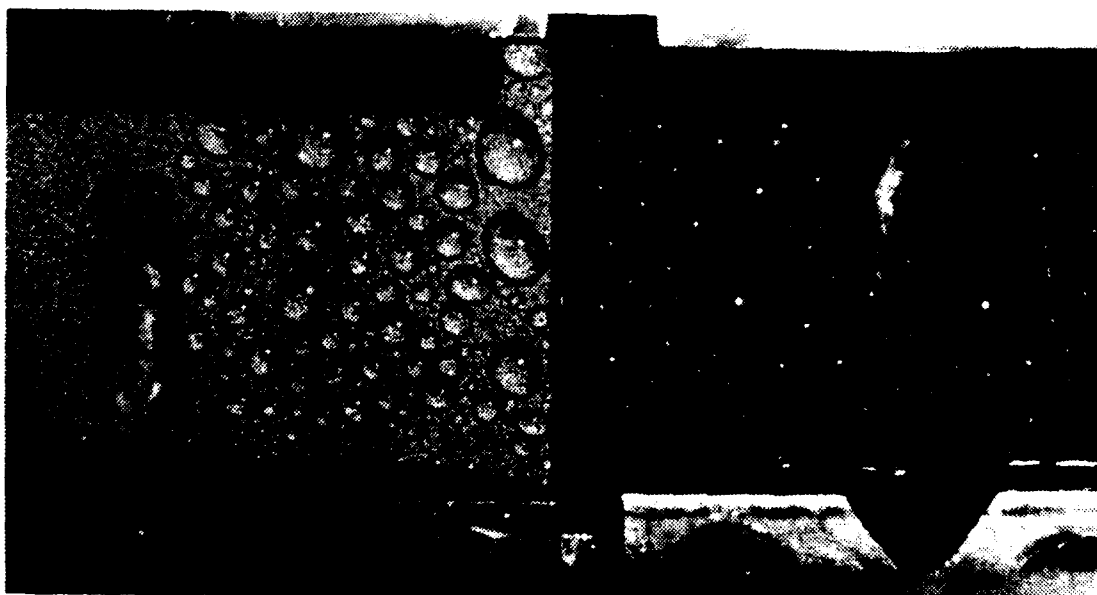


Figure 4.8 NRL Mixed Fluoroepoxy on CuNi/40 grit/wp/350 hrs. and on CuNi/40 grit/350 hrs..

dropwise quality. The fluoroacrylic coated CuNi specimen was removed after 6,500 hours for SEM examination. This specimen had some isolated areas of wetting which were visible prior to removal. SEM observation (Figure 4.11) revealed that cracks were present throughout the coating.

The three fluoroacrylic specimens, which had the vacuum-deposited gold sublayer, continued to produce dropwise condensation in excess of 8,000 hours. As shown in Figures 4.12 and 4.13, the dropwise quality was fair to poor. This was unexpected since the fluoroacrylic coating was applied in the same manner as were the specimens without the gold sublayer. The gold sublayer practically eliminated corrosion.

The results for the crosslinked-fluoroacrylic coated specimens were disappointing. With the exception of the glassbead-roughened specimens, the dropwise quality was good to excellent during the first few hours of testing. Most of the glassbead-roughened specimens produced mixed film and dropwise condensation, which became all film within the first 20 hours of condensing steam. The specimens roughened with a 220-grit blast were the next to fail followed by the 40-grit blasted specimens. Figures 4.14 through 4.17 give a comparison of selected crosslinked-fluoroacrylic specimens during the first hour of testing. Five out of six specimens tested, which had 40-grit roughnesses, gave good dropwise condensation several hundred hours longer than the specimens with the other roughnesses. However, one 40-grit roughened specimen, shown in Figure 4.15, produced filmwise condensation within the first hour.

These results indicate that the 40-grit roughnesses gave the best mechanical interlocking between the coating and the substrate. SEM photos revealed that the specimens with 40-grit roughnesses had relatively deep valleys and sharp peaks compared to the glassbead and 220-grit

roughnesses. In all cases, the coating conformed to the roughness peaks. The glassbead roughness produced rounded peaks and flat valleys with larger spacing between ridges. Figures 4.18 and 4.19 show a comparison of the 40-grit and glassbead roughnesses for crosslinked-fluoroacrylic coated copper specimens.

No significant correlation could be made between specimens with or without the wash primer and failure rate. However, SEM observations showed that the wash primer was exposed for specimens with the glassbead roughness. This can be seen in Figure 4.20.

Dr. J. Griffith pointed out that the coating may have failed because of the increase in the thermal expansion coefficient of the coating from crosslinking. Hardness and adhesion test results shown in Table III support this idea. The crosslinked-fluoroacrylic was much harder and gave better adhesion than the umbrella fluoroacrylic.

Coating thickness was determined by weighing the specimens before and after coating. The coatings proved to be very thin ranging from 2-3 μm . Three of the six specimens evaluated for thickness had wash primer subcoatings. The specimens with the wash primer showed only a 0.1-0.3 μm increase in thickness compared to those without the wash primer.

3. Parylene

All but one of the Parylene-N specimens failed within the first 24 hours of testing. The CuNi specimen gave fair to good dropwise condensation for almost 4,000 hours. SEM observations showed that the CuNi substrates had rough surfaces in the as-received condition, which would have given the greater coating durability. Significantly different values were obtained for the adhesion testing of



Figure 4.9 NRI Fluoroacrylic on Cu/R/6,400 hrs.
and on Ti/R/6,400 hrs..

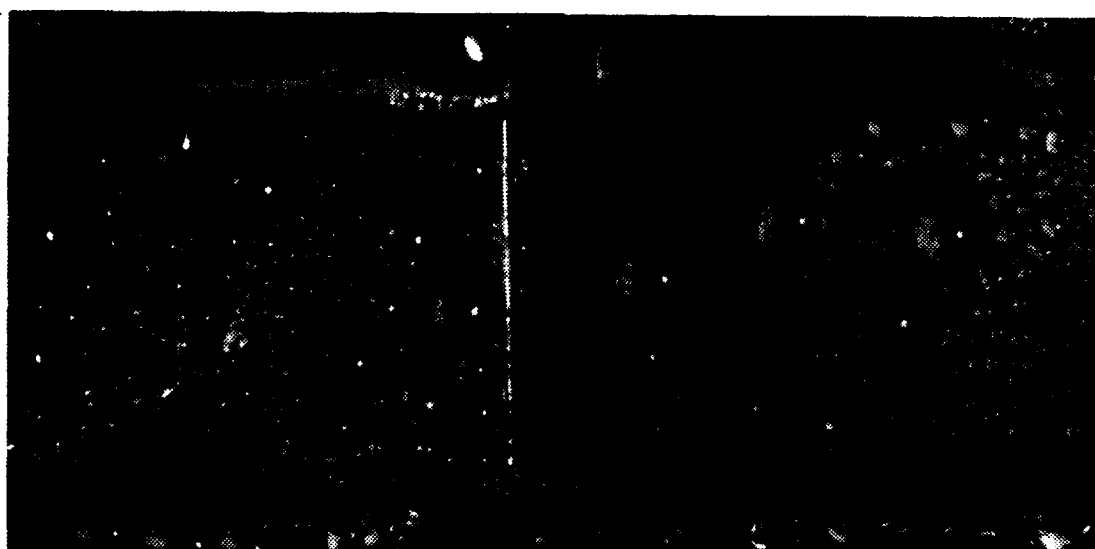


Figure 4.10 NRI Fluoroacrylic on Cu/R/7,690 hrs.
and on Ti/R/7,670 hrs..

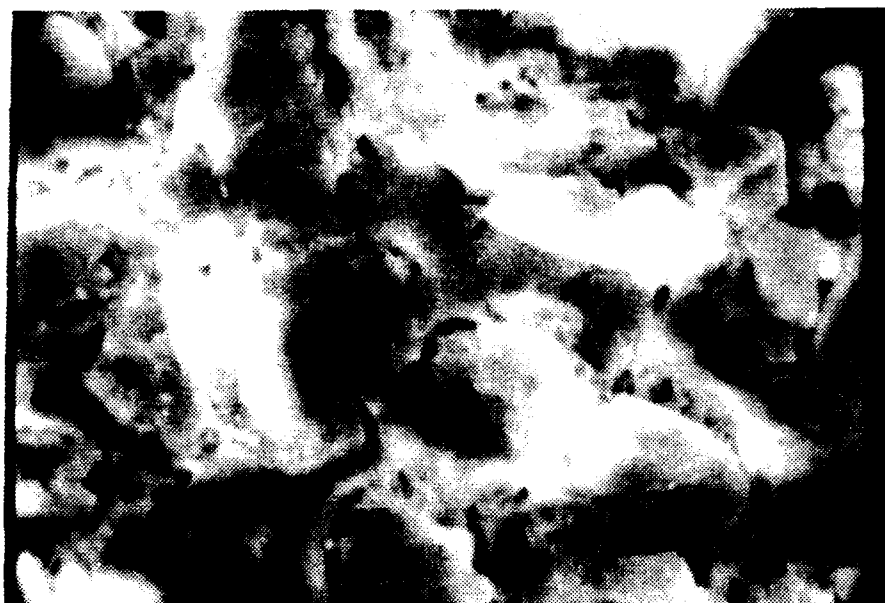


Figure 4.11 NRL Fluoroacrylic on CuNi/R/6,500 hrs. (SEM x1000).

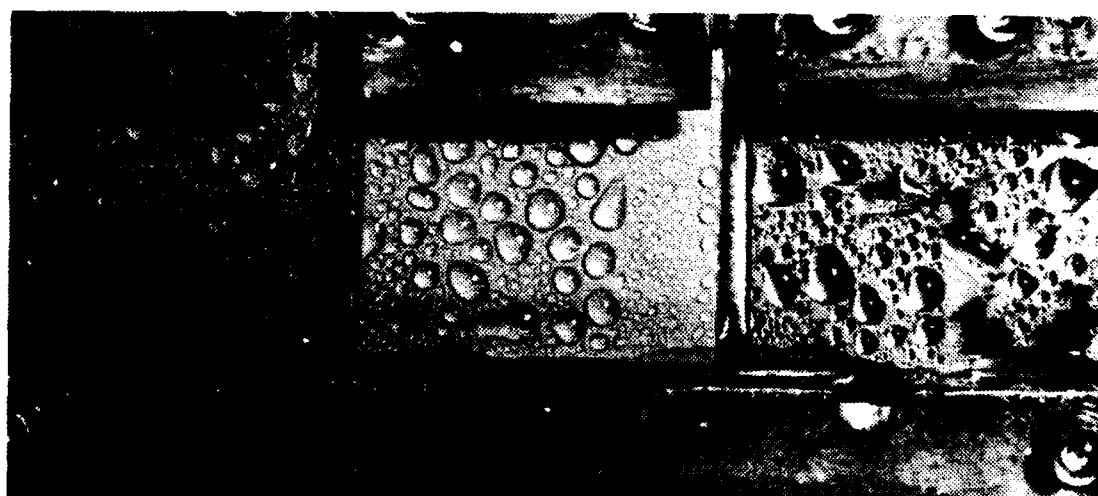


Figure 4.12 NRL Fluoroacrylic on Au-Cu/R, Au-Ti/R,
and Au-Cu/S 2,500 hrs..

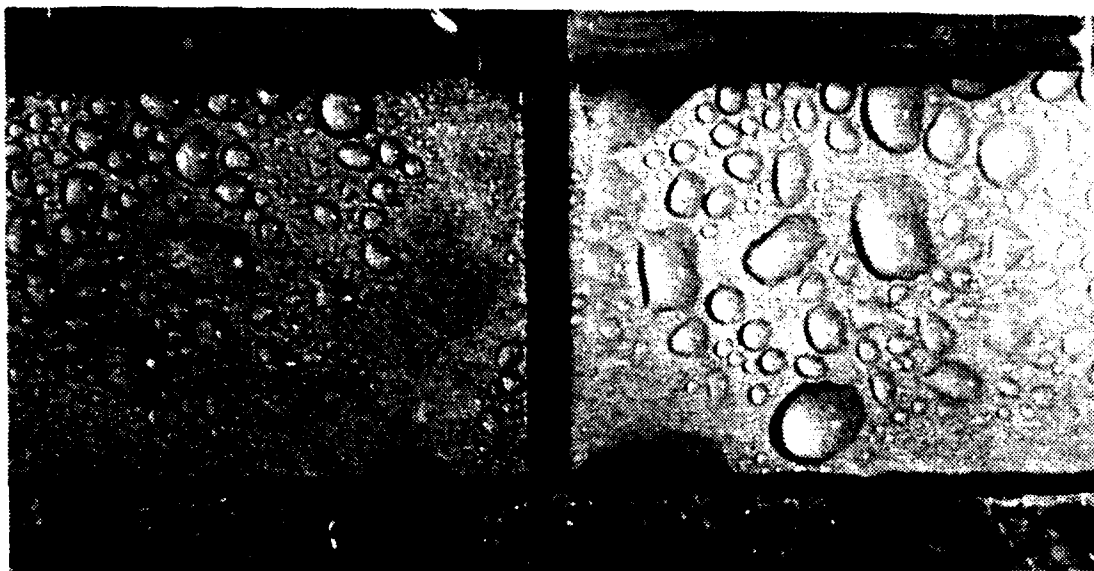


Figure 4.13 NREL Fluoroacrylic on Au-Cu/R and Au-Ti/R 6,540 hrs..

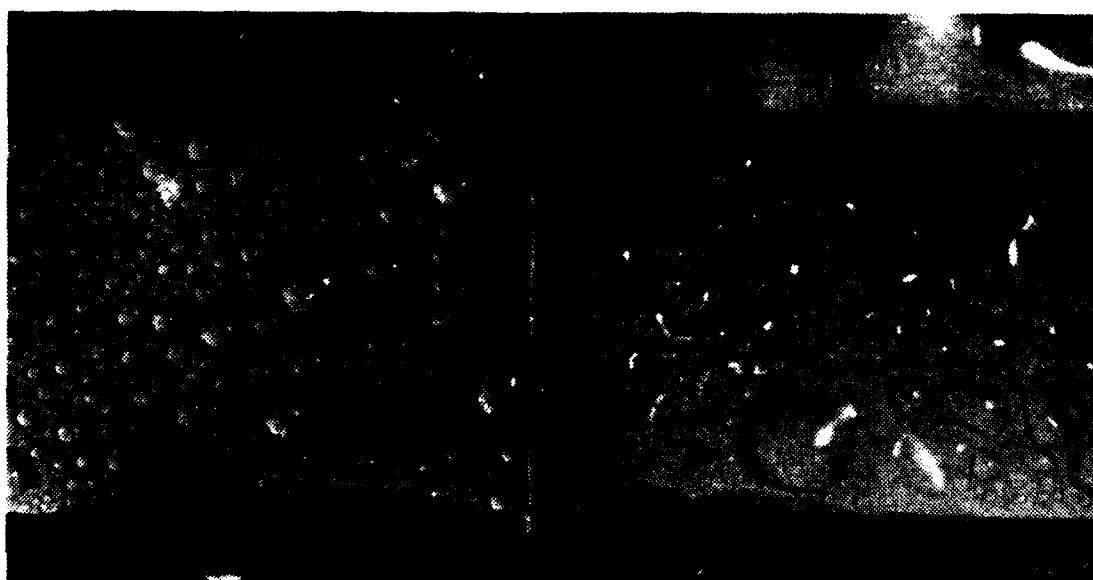


Figure 4.14 NREL Crosslinked Fluoroacrylic on Ti/40 grit
CuNi/220 grit/wp/0 hrs..

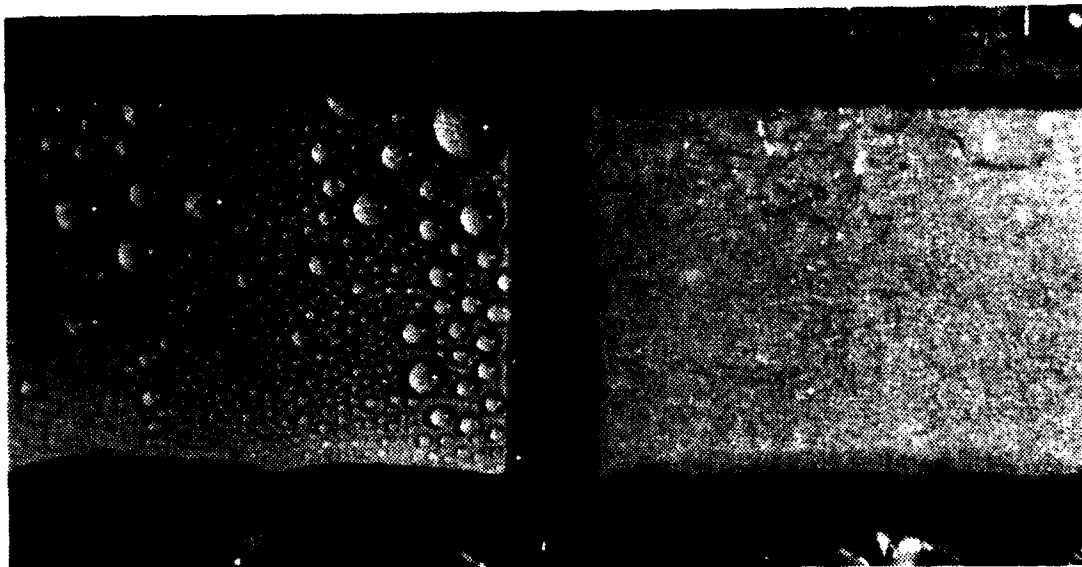


Figure 4.15 NRL Crosslinked Fluoroacrylic on Cu/40 grit and Cu/40 grit/wp/0 hrs..

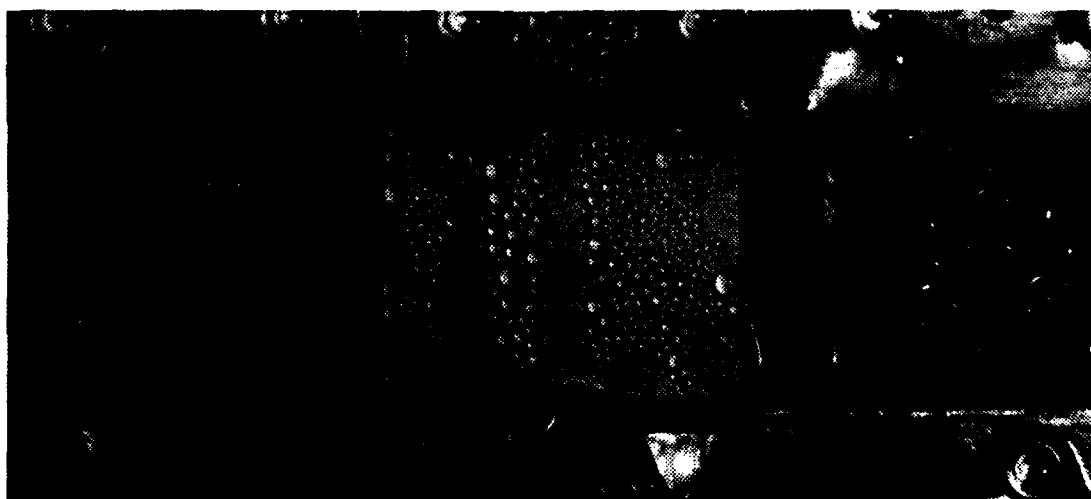


Figure 4.16 NRL Crosslinked Fluoroacrylic on CuNi/40 grit, CuNi/40 grit/wp, and CuNi/glasshead/0 hrs..

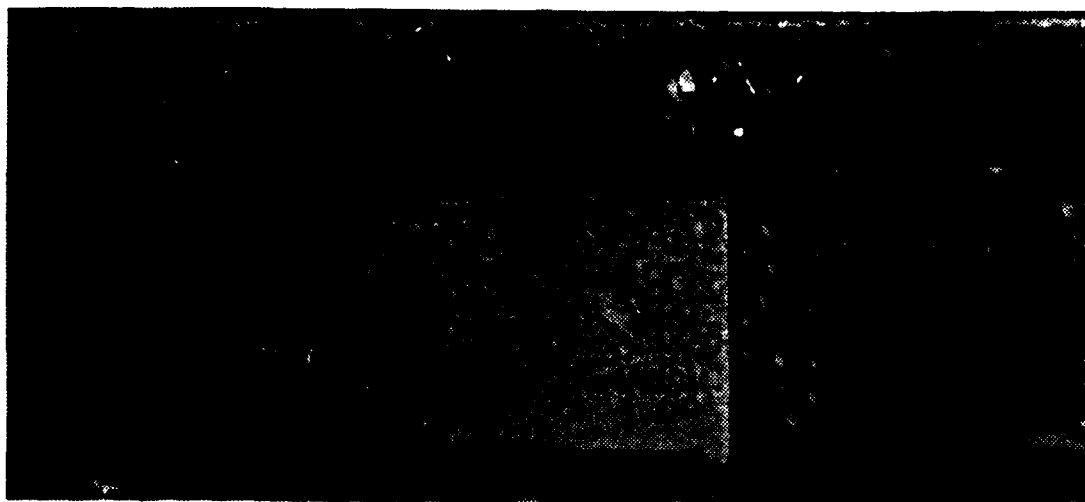


Figure 4.17 NREL Crosslinked Fluoroacrylic on Cu/220 grit/wp, Cu/glassbead/wp, and Ti/40 grit/wp/0 hrs..

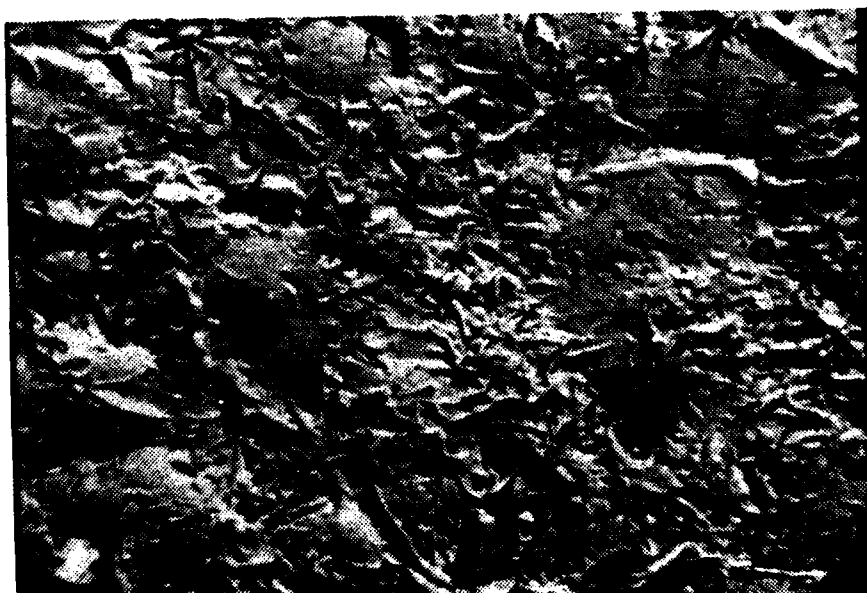


Figure 4.18 NREL Crosslinked Fluoroacrylic on Cu/40 grit SEM (x260).

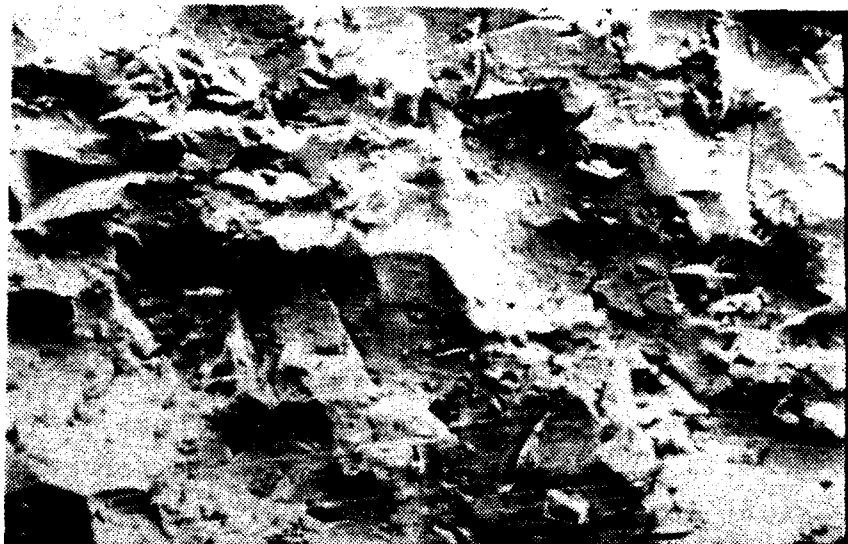


Figure 4.19 NREL Crosslinked Fluoroacrylic on Cu/glb d SEM (x200).



Figure 4.20 NREL Crosslinked Fluoroacrylic on CuNi/glb d/wp SEM (x1000).

Parylene-N than those reported by Holden [Ref. 23]. Adhesion was found to be very poor with 90-100 % of the coating removed during tape testing. This was expected because of the lack of surface preparation prior to coating the specimens.

Parylene-D gave significantly better results. Specimens with smooth substrates generally failed in 100 hours or less. Water-filled bubbles separated the coatings from the substrates as shown in Figure 4.21. Greater than 5,500 hours were obtained on specimens with rough substrates. The quality of dropwise condensation was excellent for all the Parylene-D coated specimens, as shown in Figures 4.21 through 4.24. Figure 4.24 shows similar dropwise quality between Parylene-D coated CuNi and a vacuum-deposited gold specimen.

No significant differences in endurance were observed between the 0.5 and the 1.0 μ m thick coatings. Adhesion tests showed significant improvements for Parylene-D coatings compared to Parylene-N. Only a small increase in the Parylene-D coating hardness was found (see Table III). SEM photos (Figures 4.25 - 4.28) show that the Parylene-D coatings conformed to the surface roughness. These photos also show that increased surface roughness provides the mechanical-interlocking, between the coating and the substrate, necessary for adhesion.

It is important to note that the dropwise quality was better for Parylene-D than for the fluoropolymers tested. Dr. J. Griffith noted that the inclusion of oxygen, nitrogen, or other non-hydrophobic groups in the polymer chains reduces the close-packing of hydrophobic groups, therefore, reducing coating hydrophobicity. Since Parylene-D is free of any inclusions separating carbon atoms, very close-packed hydrophobic surfaces could be obtained.



Figure 4.21 Parylene-D: Cu/R/0.5 μ m/2,800 hrs and Cu/S/1.0 μ m/1,600 hrs.

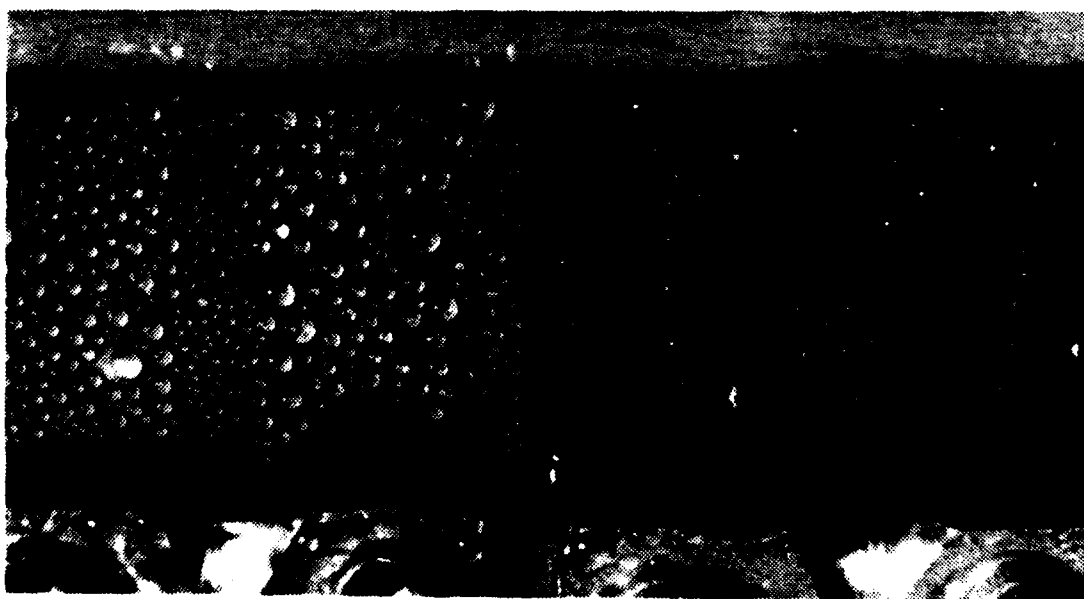


Figure 4.22 Parylene-D: Cu/S/0.5 μ m and Cu/R/0.5 μ m 4080 hrs..

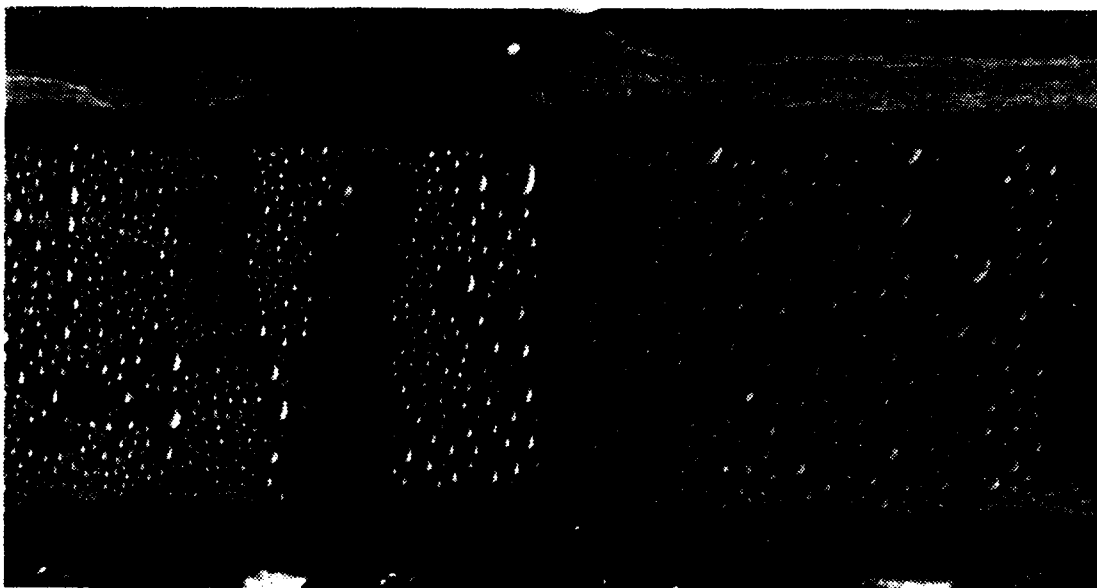


Figure 4.23 Parylene-D: Ti/S/0.5 μ m and Ti/R/0.5 μ m 3275 hrs..

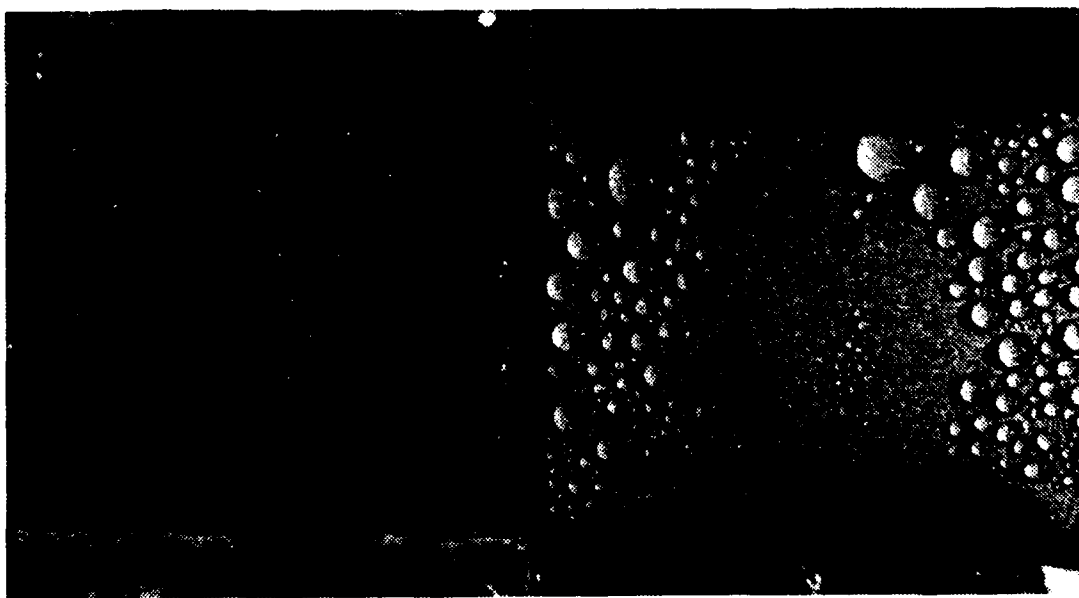


Figure 4.24 Parylene-D CuNi/R/0.5 μ m/4,050 hrs. and Gold on Ti/R/6,540 hrs..

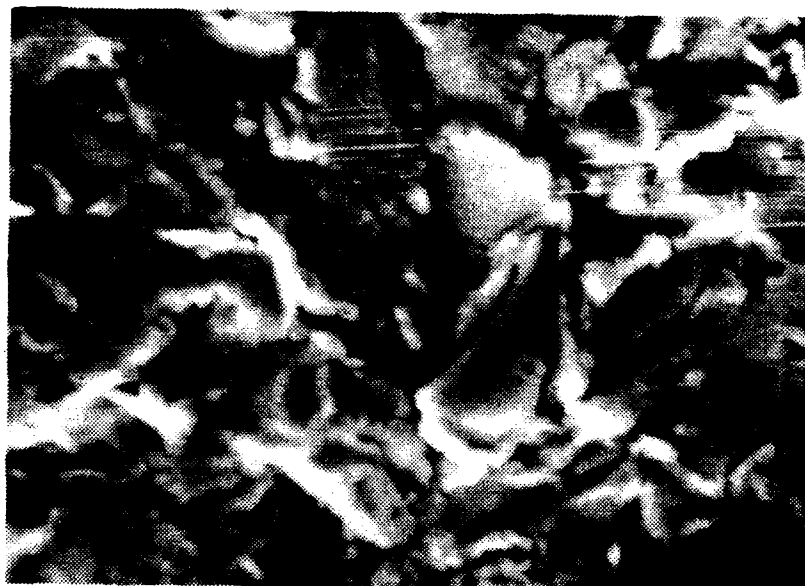


Figure 4.25 Parylene-D on Ti/R/0.5 μm /0 hrs. SEM (x1000).

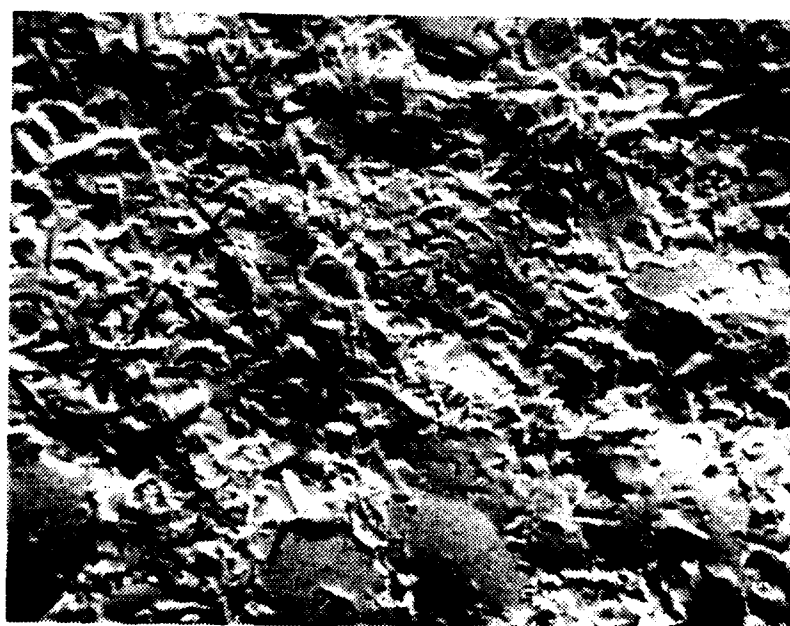


Figure 4.26 Parylene-D on Cu/R/0.5 μm /0 hrs. SEM (x200).

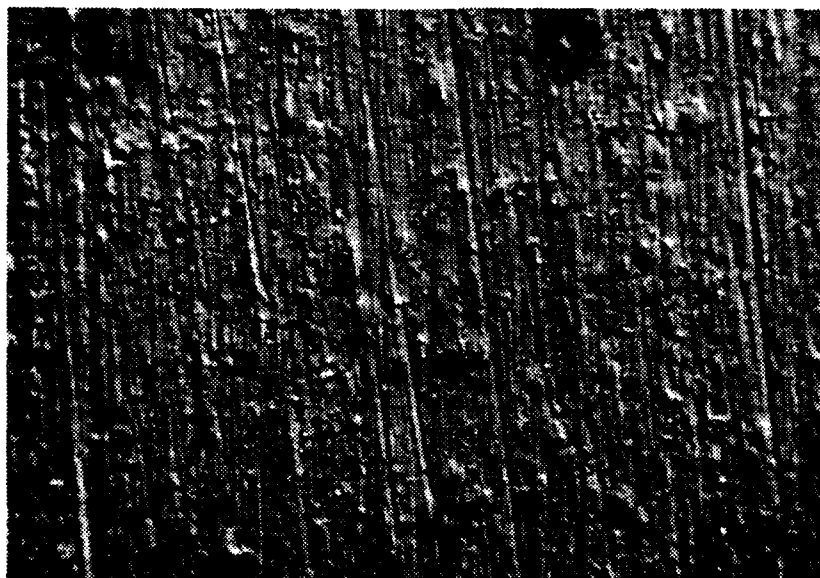


Figure 4.27 Parylene-D on Ti/S/0.5 μm /0 hrs. SEM (x200).



Figure 4.28 Parylene-D on CuNi/S/1.0 μm /0 hrs. SEM (x200).

4. No-Stik

All No-Stik specimens continued to produce excellent dropwise condensation with virtually no coating deterioration (see Figures 4.29 and 4.30). Greater than 11,000 hours were obtained for No-Stik(Cu) specimens. Small green specks were visible indicating that the infused copper base was oxidizing. However, this didn't seem to affect the dropwise quality or coating adhesion.

No-Stik(Al) and No-Stik(NiCr) specimens continued to promote excellent dropwise condensation in excess of 2,000 hours. Coating thicknesses were measured to be about 50 μm . Although these coatings were thinner than the No-Stik(Cu) coating, they were still too thick to obtain significant enhancement from dropwise condensation.

5. Emralon-333

The resin base continued to erode away from the Emralon-333 coating, eventually exposing the substrate. Good to excellent dropwise condensation prevailed until approximately 50 % of the substrate was visible through the coating. Figure 4.31 show a brass specimen with the coating badly eroded. Other specimens shown in Figures 4.31 and 4.32 show Emralon-333 coated specimens with excellent quality dropwise condensation. Endurance lives in excess of 11,000 hours were obtained.

Since polymers are basically non-reactive, very little change in steam-plant chemistry would occur from eroded or washed away polymer coatings, especially since very small quantities (in weight and volume) of the polymers are present when the coatings are thin.



Figure 4.29 No-Stik(Cu) on Ti/7,670 hrs. and Ti/9,650 hrs..

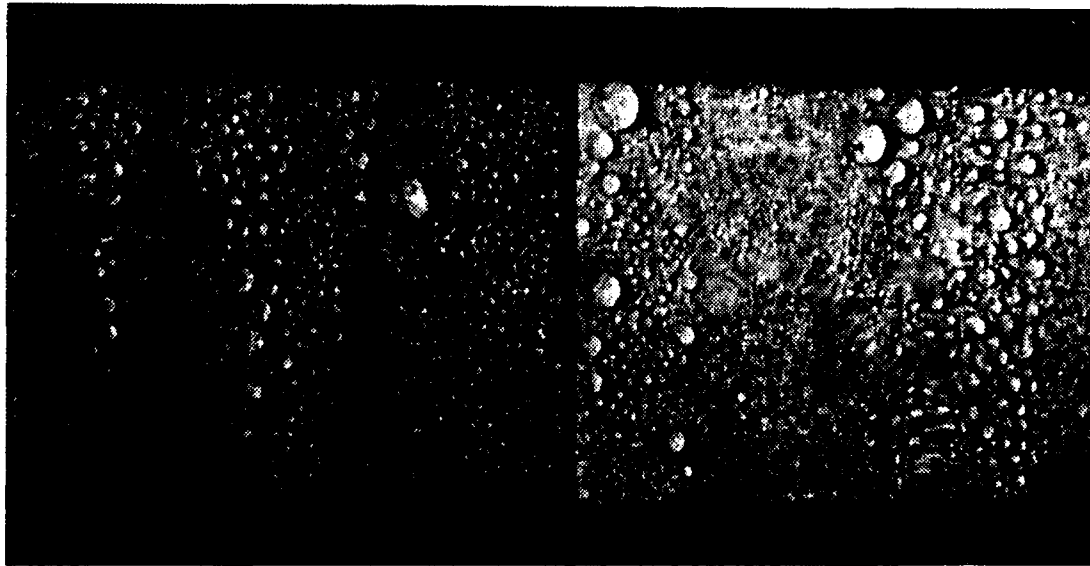


Figure 4.30 No-Stik(NiCr) and No-Stik(Al) on CuNi at 780 hrs..



Figure 4.31 Emralon-333 on Ti/6,400 hrs. and Brass/6,400 hrs..

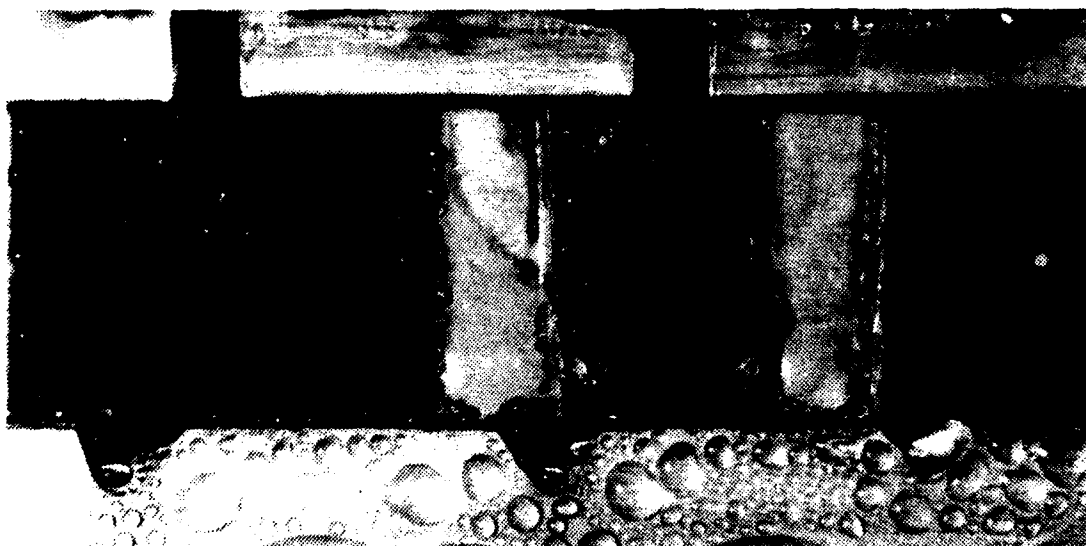


Figure 4.32 Emralon-333 on Ti/7670 hrs, Brass and Ti 9,650 hrs..

B. HEAT-TRANSFER RESULTS FOR PLAIN TUBES

Prior to processing filmwise or dropwise condensation data, appropriate values for the substrate thermal conductivity and the inside heat-transfer coefficient must be determined. A sensitivity analysis demonstrating the importance of selecting an accurate value for substrate thermal conductivity will be discussed first. Then the results obtained from the filmwise condensation data will be discussed, which were used to obtain appropriate values for the Sieder-Tate coefficient.

1. Sensitivity of Data Reduction on Substrate Thermal Conductivity

Proper selection of substrate thermal conductivity was essential in obtaining accurate values for the outside heat-transfer coefficient. A search of several data sources, including the American Society of Metals [Ref. 43] and Touloukian [Ref. 44], showed that differences in reported values of thermal conductivity of metals could be as much as 10 %. A sensitivity analysis showed that a 10 % difference in substrate thermal conductivity made less than 3 % difference in outside heat-transfer coefficients determined from filmwise condensation data. Differences in the Sieder-Tate coefficients, determined from the Modified Wilson Plot method, were also less than 3 %. However, significant errors can result in determining dropwise heat-transfer coefficients for tubes with low thermal conductivities. This was found to be the case for the stainless-steel and 90-10 CuNi tubes. For thick-walled, stainless-steel tubes, as much as a 50 % reduction in the dropwise heat-transfer coefficient was obtained, with a 10 % increase in substrate thermal conductivity (see Figure 4.38). For the thin-walled stainless-steel and 90-10 CuNi tubes, only a 10 % reduction in the dropwise heat-transfer coefficient was obtained.

TABLE III
Endurance Test Results

Coating	Substrate/ Surface	Thickness µm	Hardness	Adhesion	Dropwise Performance	Hours of Operation
C-6 Fluoroepoxy	Ti/D	6-8	2H	5B	Fair	>11,000
	Cu/D	6-8	2H	5B	Fair/Good	>8,950
	CuNi/D	6-8	2H	5B	Fair/Poor	6,500
Mixed Fluoroepoxy	Ti/B,C,D	8-9	6H	5B	Good	>2,500
	Cu/B,C,D	8-9	6H	5B	Good	>2,500
	CuNi/B,C,D	8-9	6H	5B	Good	>2,500
Fluoroacrylic	Ti/D	2-3	F	3B	Good	>9,000
	Cu/D	2-3	F	3B	Good	>9,000
	CuNi/D	2-3	F	3B	Good	6,500
	Cu-Au/D	2-3	F	3B	Fair/Poor	>8,000
	Cu-Au/A	2-3	F	3B	Fair/Poor	>8,000
	Ti-Au/D	2-3	F	3B	Fair/Poor	>8,000
Crosslinked Fluoroacrylic	Ti/B	2-3	4H	5B	Fair	<20
	Ti/C	2-3	4H	5B	Good/Excel	<1,000
	Ti/D	2-3	4H	5B	Fair/Poor	<20
	Cu/B	2-3	4H	5B	Fair/Good	<20
	Cu/C	2-3	4H	5B	Good/Excel	<1,000
	Cu/D	2-3	4H	5B	Fair/Poor	<20
	CuNi/B	2-3	4H	5B	Fair/Good	<20
	CuNi/C	2-3	4H	5B	Good/Excel	<1,000
	CuNi/D	2-3	4H	5B	Fair/Poor	<20
Parylene-N	Cu/A	0.5	B	1B	Good	<20
	Cu/A	1.0	B	1B	Good	<20
	CuNi/D	0.5	B	1B	Good	<20
	CuNi/D	1.0	B	1B	Good	<4,000
Parylene-D	Cu/A	0.5	HB	4B	Excel	>5,500
	Cu/A	1.0	HB	4B	Excel	<100
	Cu/D	0.5,1.0	HB	4B	Excel	>5,500
	CuNi/A	0.5	HB	4B	Excel	>5,500
	CuNi/A	1.0	HB	4B	Excel	<100
	CuNi/D	0.5,1.0	HB	4B	Excel	>5,500
	Ti/A	0.5	HB	4B	Excel	>5,500
	Ti/A	1.0	HB	4B	Excel	<100
	Ti/D	0.5,1.0	HB	4B	Excel	>5,500
	Br/A	0.5,1.0	HB	2B	Excel	<20
	Br/D	0.5,1.0	HB	4B	Excel	>5,500
No-Stik(Cu)	Cu,Ti/U	60	4H	5B	Excel	>9,000
	CuNi,Ti/U	60	4H	5B	Excel	>11,000
No-Stik(Al)	Cu,Ti,CuNi/U	50	5H	5B	Excel	>2,100
No-Stik(NiCr)	Cu,Ti,CuNi/U	50	6H	5B	Excel	>2,100
Emralon-333	Ti,Br/U	13	F	5B	Good/Excel	>11,000
	Br/U	13	F	5B	Good	<6,500
	Ti/U	13	F	5B	Good/Excel	>11,000
	CuNi	13	F	5B	Fair/Good	<6,500
Gold	Ti/D	0.5	-	-	Excel	>8,000

Note: Roughness Hardness Adhesion
A - 600 grit C - 40 grit B - softest 1B - least
B - 220 grit D - glass-bead 6H - hardest 5B - most
U - unknown

The large dependance of the dropwise heat-transfer coefficient on substrate thermal conductivity is a direct result of inferring the outside heat-transfer coefficient from the overall value coefficient. For low thermal conductivity substrates, the wall resistance can become dominating when condensation occurs in the dropwise mode. Therefore, a small error in the wall resistance can give large errors in the outside heat-transfer coefficient. This was the primary reason for selecting thin-walled tubes to evaluate the effect of constriction resistance.

Table IV lists the selected values for substrate thermal conductivities used in the data reduction programs. All of the values in Table IV were taken from [Ref. 44] with the exception of the value for CuNi which was given by the manufacturer. These values were based on an estimated average wall temperature of 310 K, at 85 mmHg condensing pressure.

TABLE IV
Substrate Thermal Conductivity used for Data Reduction

Material	k (W/m°C)
OFHC Copper	385.0
Al 6061-16	167.0
CuNi 90-10	45.0
SS Type 304	16.0

2. Modified Wilson Method Results

Sieder-Tate coefficients were determined for each of the four tube-insert configurations tested. Average values were determined based on the results of the four data runs taken for each tube. Differences between the coefficients, determined for any one tube, were less than 3 %. Table V gives a summary of the average Sieder-Tate coefficients

obtained for each tube configuration. The values are tabulated according to insert number and tube material. The Sieder-Tate coefficients shown were determined using the Fujii-Honda equation (eqn. 3.3) and also using the Nusselt equation (eqn. 3.1) in the Modified Wilson method. A sample Wilson plot is shown in Figure 4.33. The Sieder-Tate coefficients determined using the Fujii-Honda equation predict an inside heat-transfer coefficient 3-4 % higher than the values obtained using the Nusselt equation. Georgiadis [Ref. 41] reported a value of 0.071 for the Sieder-Tate coefficient obtained using the Nusselt equation for a similar tube-insert combination.

TABLE V
Sieder-Tate Coefficients used in Data Reduction

Tube Material	Insert Number	Ci (Fujii-Honda)	Ci (Nusselt)
Cu	1	0.0702	0.0675
Al	1	0.0720	0.0684
CuNi	2	0.0741	0.0716
SS	3	0.0689	0.0666

Differences in the values obtained for the different tube configurations can be attributed to differences in the tube inside diameters, spiral-insert pitch and diameter, and experimental errors. As noted earlier, the copper and aluminum tubes had the same insert and inside diameters. The two Sieder-Tate coefficients obtained for the copper and aluminum tubes are in close agreement with each other (within 2.5 %).

In order to check data reduction procedures and the accuracy of the measurements, the raw data were reprocessed using the Sieder-Tate coefficients determined with the Fujii-Honda correlation (see Table V). Figure 4.34 shows a sample plot for the reprocessed filmwise data obtained for

the copper tube. Good repeatability was demonstrated for all four tubes with less than 3 % scattering of the data points. A theoretical line strictly based on equation (3.1) is also plotted in Figure 4.34 for comparison. This line represents a zero vapor shear condition with α_{Nu} set equal to 0.655.

Figure 4.35 shows a comparison of the filmwise data with the correlation of Fujii and Honda (equation (3.2)). These data show good agreement with the Fujii and Honda correlation. [Ref. 40].

In order to determine the outside heat-transfer coefficient from the dropwise data, the Sieder-Tate coefficients based on the Fujii-Honda equation were used to predict the inside heat-transfer resistance using equation (3.5).

C. HEAT-TRANSFER RESULTS FOR POLYMER-COATED TUBES

A summary plot showing the enhancement obtained from dropwise condensation on the polymer coated tubes is given in Figure 4.36. This plot is shown here because it will be referred to throughout this discussion. The plot gives a comparison of polymer coatings applied to thick-walled copper tubes on which steam is condensing at a pressure of 85 mmHg and a vapor velocity of 2.0 m/s. A plot for filmwise condensation on a copper tube using the same insert and Sieder-Tate coefficient is provided for comparison.

1. Fluoroacrylic Coated Tubes

As shown in Figure 4.36, NRL fluoroacrylic gave the largest enhancement of the outside heat-transfer coefficient of all the polymer coatings tested. An enhancement ratio of 6.5 was obtained. This agrees closely with Holden's

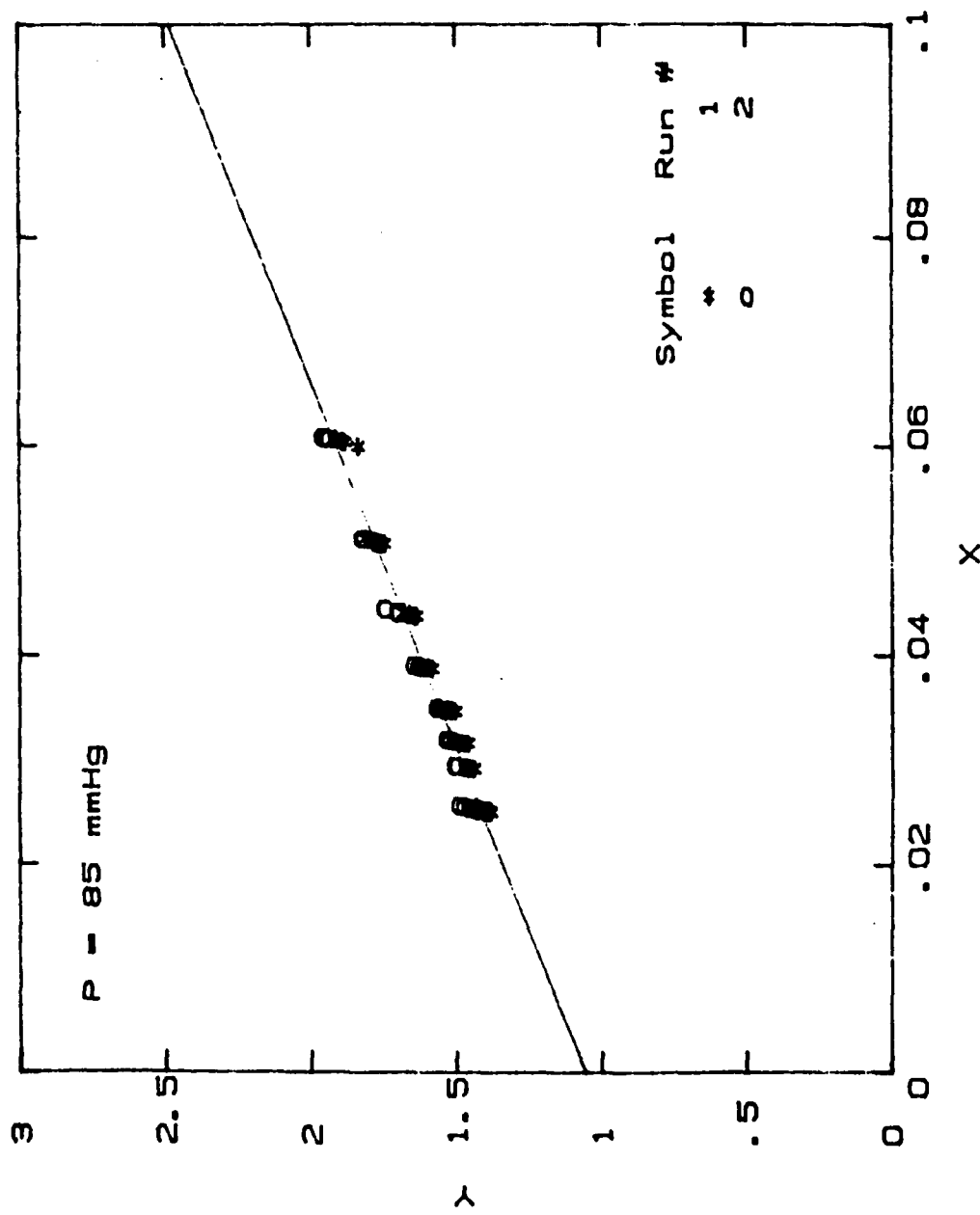


Figure 4.33 Wilson plot Obtained from Data Taken During Filmwise Condensation on a Horizontal Copper Tube.

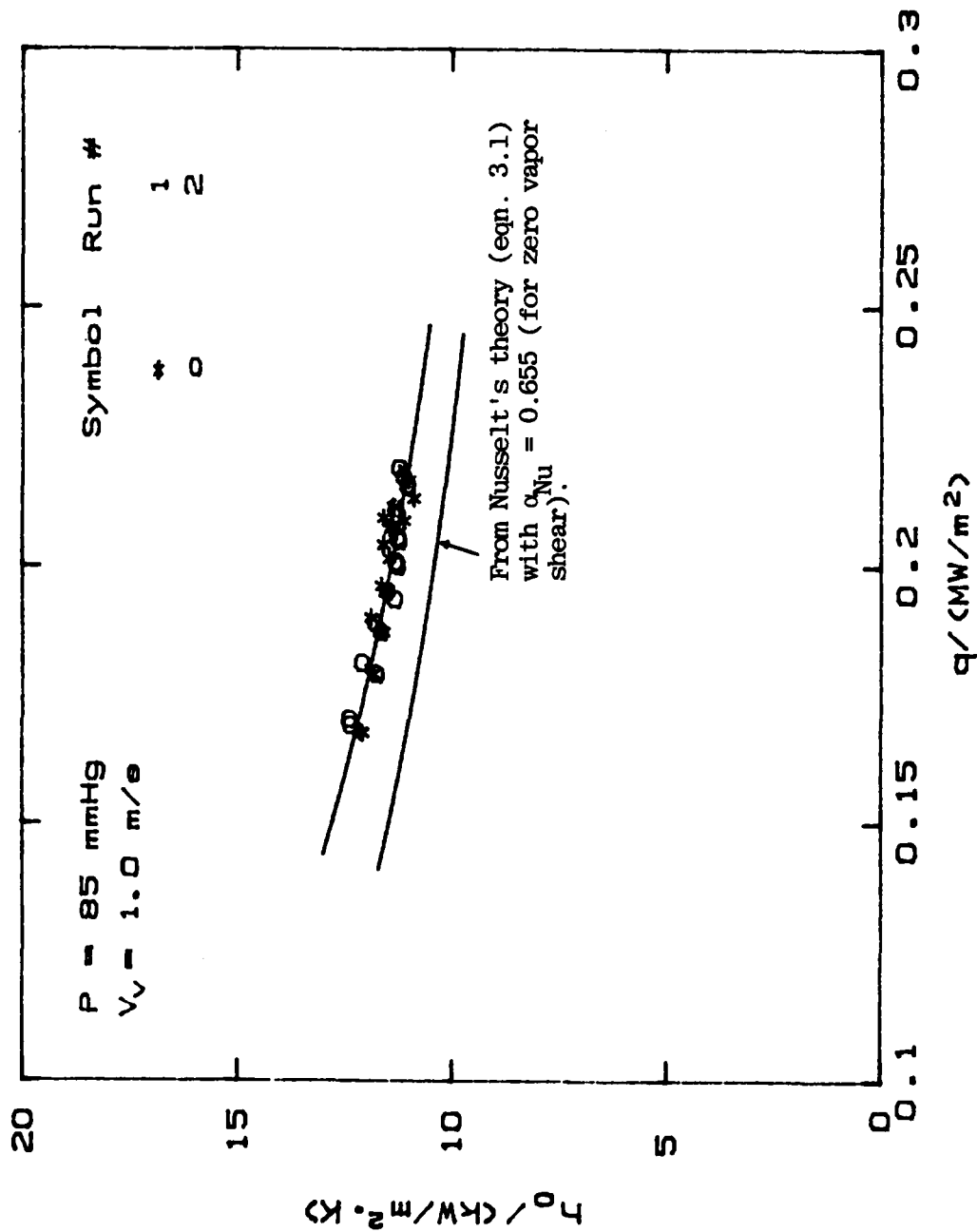


Figure 4.34 Heat-Transfer Results for Filmwise Condensation on a Horizontal Thin-Walled Copper Tube.

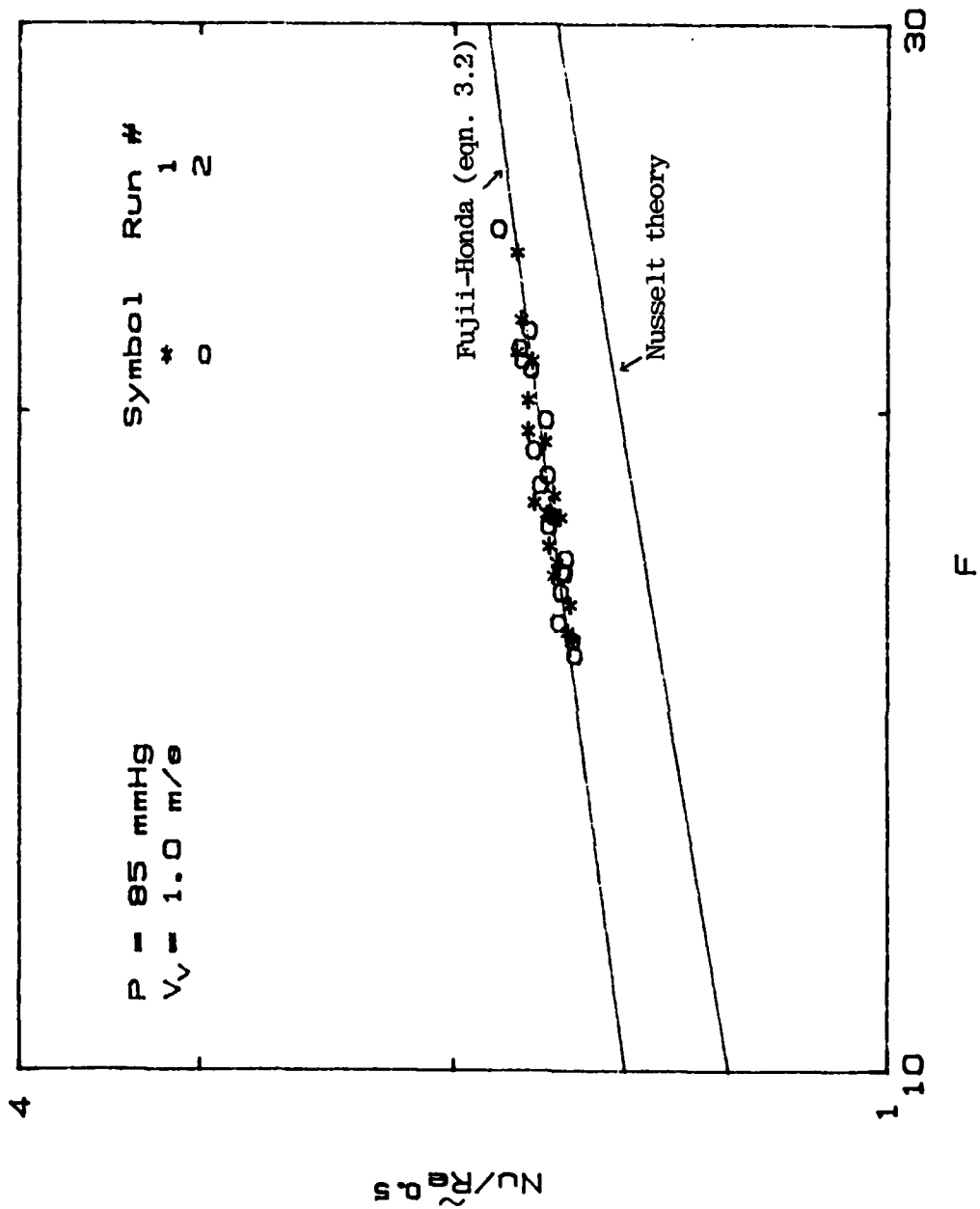


Figure 4.35 Comparison of Filmwise Condensation Data with the Fujii-Honda Correlation and the Nusselt Equation.

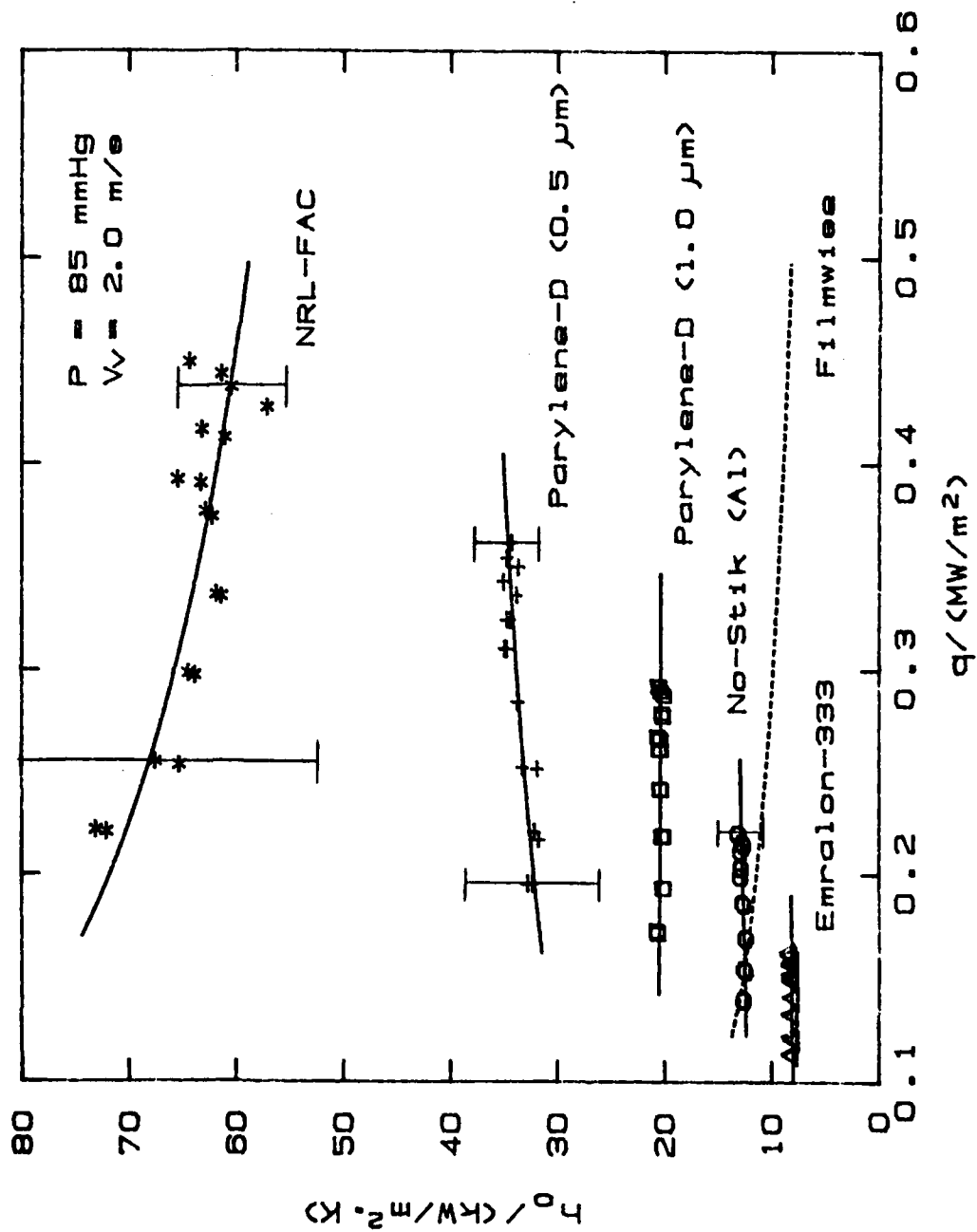


Figure 4.36 Heat-Transfer Results Obtained from Dropwise Condensation on Horizontal, Polymer-Coated, Thick-Walled, Copper Tubes.

results [Ref. 23] for a similar NRL fluoroacrylic coated copper tube. The dropwise quality was good to excellent. Coating thicknesses were estimated to be 2 to 3 micrometers, based on the endurance test results (see Table III).

A comparison of the data obtained for the three thick-walled tubes at vacuum conditions is shown in Figure 4.37. Dropwise quality was visually the same for all three tubes. The tubes with aluminum and copper substrates gave basically the same enhancement. However, the stainless-steel tube gave significantly lower values for the dropwise heat-transfer coefficient. The validity of the data obtained for the stainless-steel tube is questionable, however, based on the sensitivity analysis discussed earlier. For the thick-walled stainless-steel tube, the tube wall resistance is the governing resistance. Therefore, a small error in the wall resistance can cause large errors in the dropwise heat-transfer coefficient.

Data were also taken for thick-walled copper and stainless steel tubes at atmospheric pressure. These results are presented in Figure 4.38. A 15 % increase in the enhancement ratio was obtained for the thick-walled copper tube at atmospheric pressure compared to conditions at vacuum. Although drop sizes appeared to be bigger, sweeping action was increased considerably. This was expected because of the higher condensing rate obtained with the larger LMTD at atmospheric conditions. Graham [Ref. 5] showed a similar pressure effect. The sensitivity of the thick-walled stainless steel tube results to a 10 % change in substrate thermal conductivity is also shown in Figure 4.38. This demonstrates the importance in using thin-walled tubes when considering the effect of substrate thermal conductivity on dropwise heat-transfer coefficients. Atmospheric data were not taken for the thick-walled aluminum tube because coating deterioration was observed on this tube after it had been operated for several runs under vacuum conditions.

The results for the four NRL fluoroacrylic coated, thin-walled tubes are shown in Figure 4.39. These data were taken primarily to evaluate the effect of substrate thermal conductivity on the dropwise heat-transfer coefficient, which will be discussed in more detail later. It should be noted that enhancements were significantly lower than those obtained from the thick-walled NRL fluoroacrylic coated tubes. This was most likely due to the added thermal resistance of the wash primer. Figure 4.40 shows that the dropwise quality was basically the same for each of the tubes. The data runs were repeatable to within 5.0 % for all four tubes. After several runs, some small localized deteriorations were visible in the coatings. This was because the tube surfaces were smooth giving poor coating adhesion. With the exception of the thick-walled aluminum tube, the tubes which had rough surfaces showed no signs of deterioration in the NRL fluoroacrylic coatings after an average of 20 hours of testing.

The effect of the wash primer on the dropwise heat-transfer coefficient can readily be seen in Figure 4.41. The tube without the wash primer gave an enhancement ratio of 6.8, while the tubes with the wash primer gave on the average an enhancement ratio of 3.5. This can only be attributed to the added thermal resistance of the wash primer since both the primer and the coating were included as part of the outside thermal resistance. As also shown in Figure 4.41, substrate roughness has little effect on the dropwise heat-transfer coefficient. The differences shown for the three tubes, which had the wash primer, could easily be attributed to experimental errors or coating thickness variations.

AD-A154 743

ENDURANCE AND HEAT-TRANSFER PERFORMANCE OF POLYMER
COATINGS FOR THE PROMO. (U) NAVAL POSTGRADUATE SCHOOL
MONTEREY CA D J LOONEY DEC 84 NPS-69-84-015

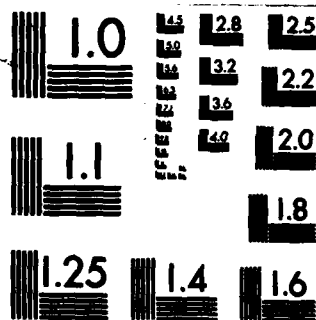
272

UNCLASSIFIED

F/G 11/3

NL

					DE				DE	DE		
					END							
					FILED							
					DTIC							



MICROCOPY RESOLUTION TEST CHART
NATIONAL BUREAU OF STANDARDS-1963-A

2. Parylene-D Coated Tubes

The quality of the dropwise condensation on the two Parylene-D coated tubes was classified as good. Enhancement ratios of 3.3 and 2.0 were obtained for the 0.5 and the 1.0 micrometer thick coatings, respectively (see Figure 4.36). Thicknesses of the coatings were determined by Lawrence Livermore National Laboratory based on the deposition rate used for coating the tubes. This shows the importance of having ultra-thin coatings to obtain suitable enhancements from dropwise condensation. The thermal conductivity of Parylene-D is about one third that of PTFE, which explains why such low enhancements were obtained even though the coatings were thinner than the NRL fluoroacrylic coatings. Although the thermal conductivity of the NRL fluoroacrylic coating has not been adequately measured, it is thought to be close to that of PTFE.

3. No-Stik Coated Tubes

The No-Stik(Al) coated tube gave little enhancement in the outside heat-transfer coefficient (see Figure 4.36) even though good to excellent dropwise conditions were observed (see Figure 4.42). This was expected because of the 50 μ m coating thickness. This was an improvement over the results reported by Holden [Ref. 23] for the No-Stik(Cu) coating. This shows that the insulating resistance of the fluoropolymer used in the coating outweighs any benefits from the thermally conductive base metal. Even though the No-Stik(Al) coating had a lower base metal thermal conductivity than No-Stik(Cu), it gave better heat-transfer results because it was thinner.

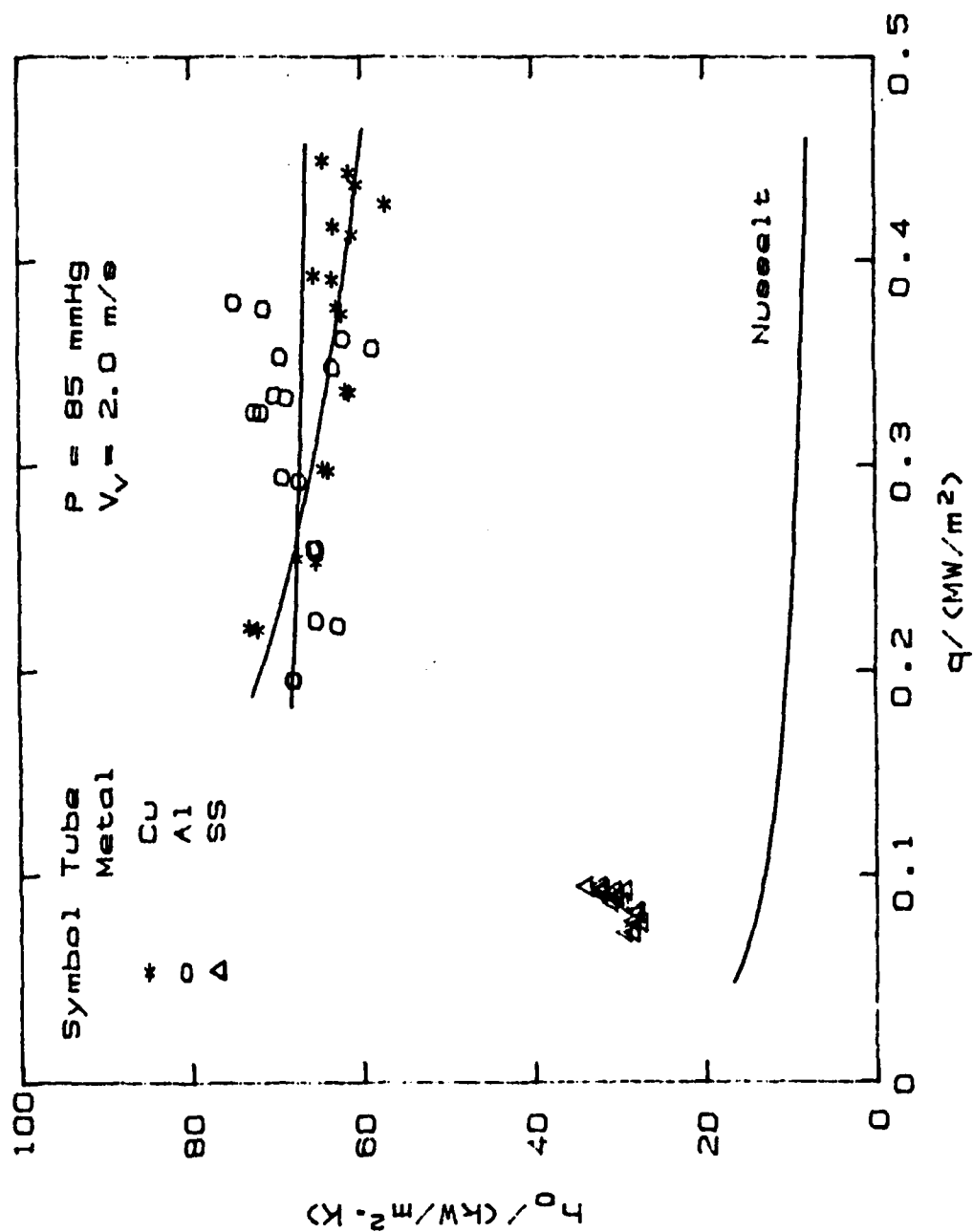


Figure 4.37 Heat-Transfer Results for NRI Fluoroacrylic-Coated, Thick-Walled Copper, Aluminum, and Stainless-Steel Tubes.

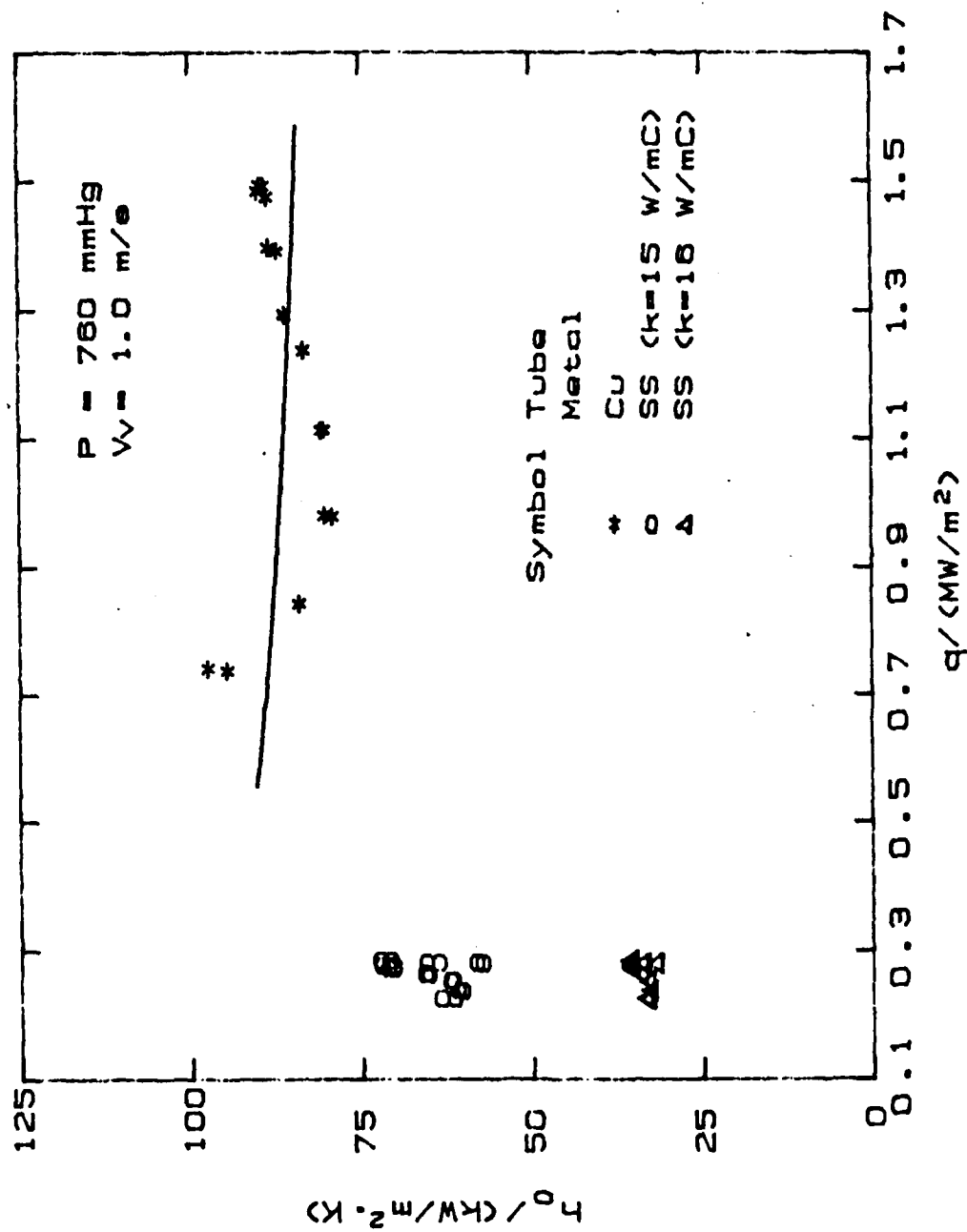


Figure 4.38 Dropwise Heat-Transfer Coefficients for Thick-Walled, MRI Fluoroacrylic-Coated Tubes at Atmospheric Pressure.

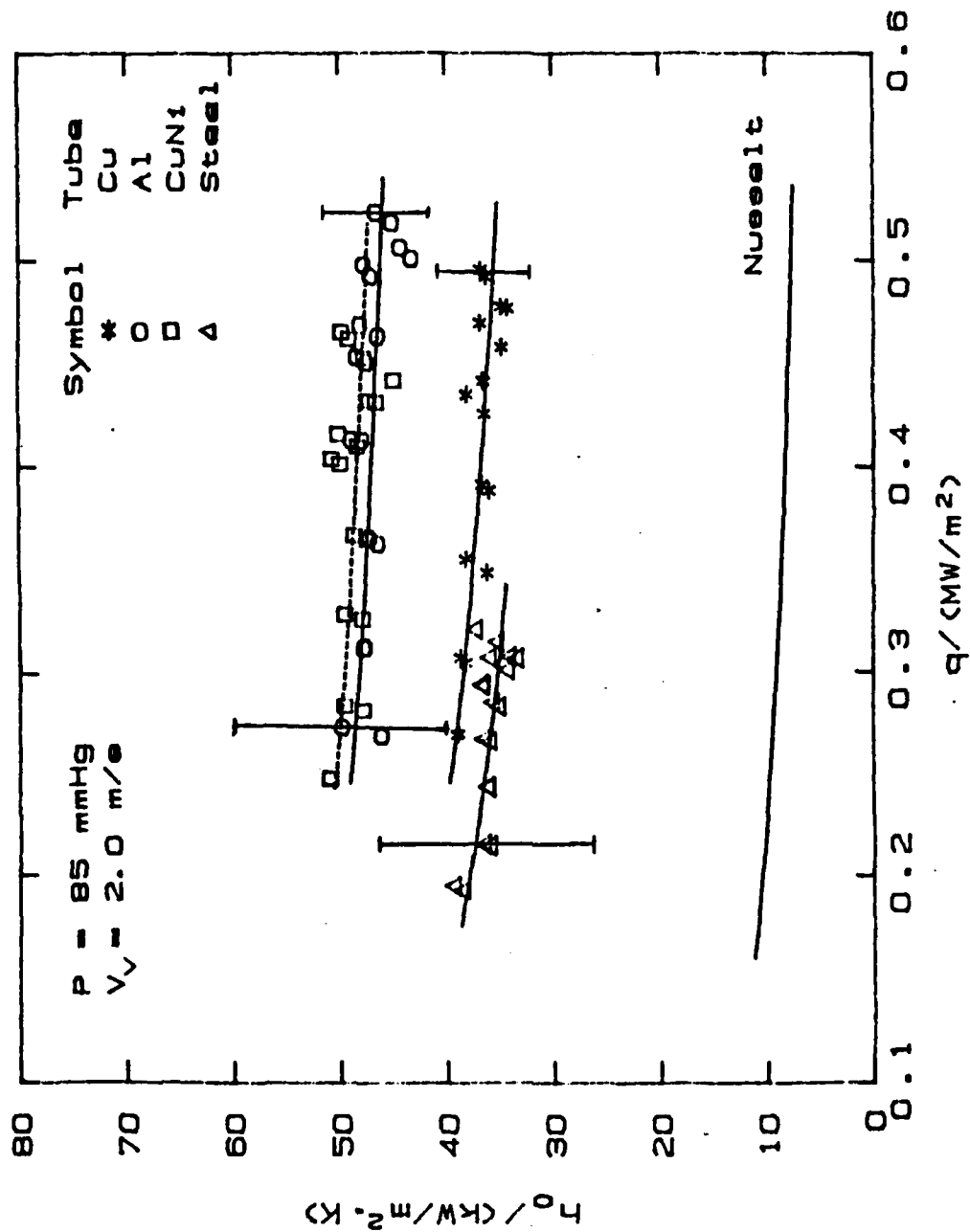


Figure 4.39 Dropwise Condensation Results for NRL Fluoroacrylic-Coated, Thin-Walled Tubes with Wash Primer.

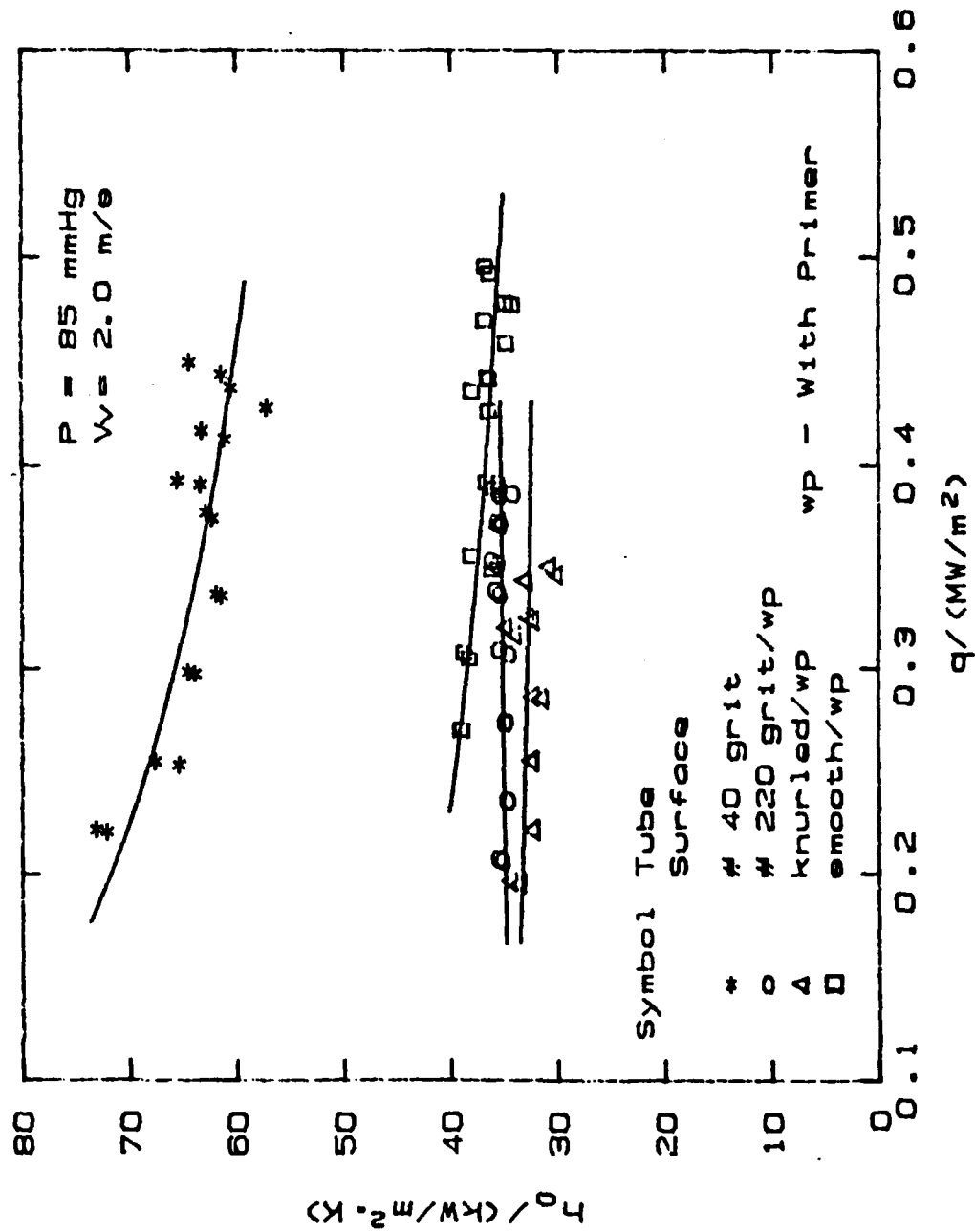


Figure 4.41 Comparison of NRL Fluoroacrylic-Coated Copper Tubes with and without Wash Primer and for Roughness Effects.

The No-Stik (NiCr) coated tube was not evaluated since the coating thickness was also measured to be 50 μm and, therefore, less enhancement would be expected. Since the No-Stik coatings appear to be very durable and corrosion-resistant, an effort to reduce the coating thickness further is warranted.

4. Emralon-333 Coated Tube

The Emralon-333 coating produced good to excellent dropwise condensation as shown in Figure 4.43. The coating thickness was measured to be 13 μm (0.0005 in). The coating was still too thick to obtain any enhancement from dropwise condensation. A 20 % reduction in the outside heat-transfer coefficient was obtained compared to that of filmwise data (see Figure 4.36). The coating showed no signs of deterioration throughout the data run. It should be noted that even though the No-Stik (Al) coating was four times thicker than the Emralon-33, it gave better enhancement in the outside heat-transfer coefficient. This implies that a 5-10 μm thick coating having a dispersion of thermally conductive particles might give good results. On the other hand, the coating must be thick enough since the thicker coatings are usually more durable.

5. Silver-Electroplated Tubes

Coating thicknesses were approximately 10 μm for the two silver-electroplated tubes. The silver-electroplated surfaces were bright and mirror smooth, and were very hydrophobic, promoting excellent dropwise condensation. There was no visible difference in the dropwise quality between the copper and CuNi tubes. This is shown in Figure 4.44 with steam condensing at a pressure of 85 mmHg.

Three complete data runs were conducted at a pressure of 85 mmHg for each tube. The data runs were made on

different days with tube removal between runs. An average enhancement ratio of 10 was obtained for both tubes as shown in Figure 4.45. Three complete data runs are shown for each tube. On one occasion, a data run for the CuNi tube gave dropwise heat-transfer coefficients that were 30 % higher than the previous two runs. Although the tubes remained untouched during installation and handling, it was believed that the increase was due to some unknown source of contamination. The water for the boiler was flushed and replaced with clean distilled water. The tube surface was cleaned with ethanol, rinsed with distilled water, and re-tested. This time the data agreed with the data from the first two runs. It should also be noted that the tubes remained untarnished after a week of testing. The values obtained for the dropwise heat-transfer coefficient are in good agreement with the results O'Neill and Westwater [Ref. 21] for silver-electroplated vertical flat plates.

Data runs were also conducted at atmospheric pressure for both the copper and CuNi tubes. Heat fluxes up to 3.0 MW/m^2 were obtained. The dropwise condensation observed was far superior to that observed for any of the other coatings tested. Drop sweeping rates were extremely fast, preventing drops from growing more than about 2 mm in diameter (based solely on visual observations). The results are plotted in Figure 4.46. Enhancement ratios were found to be between 30-40 times that of filmwise condensation.

A large amount of scatter was evident in the data obtained at atmospheric pressure. This was a result of the large uncertainties that exist when inferring the dropwise heat-transfer coefficient from the overall coefficient, particularly when the outside thermal resistance is very small. Uncertainty trends are discussed in more detail in Appendix A.

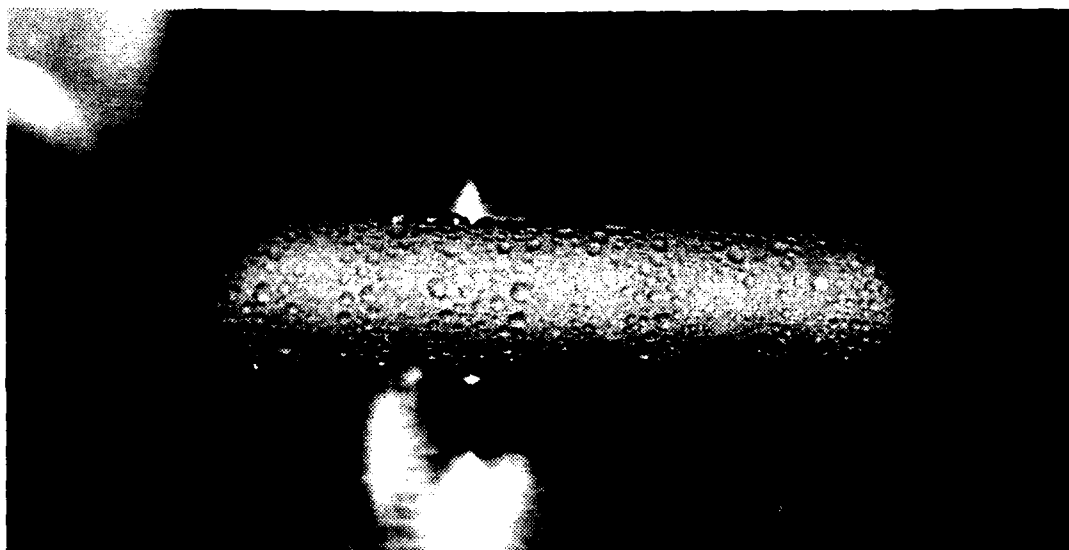


Figure 4.42 Dropwise Condensation on No-Stik(Al) Coated Copper Tube.



Figure 4.43 Dropwise Condensation on Emralon-333 Coated Copper Tube.

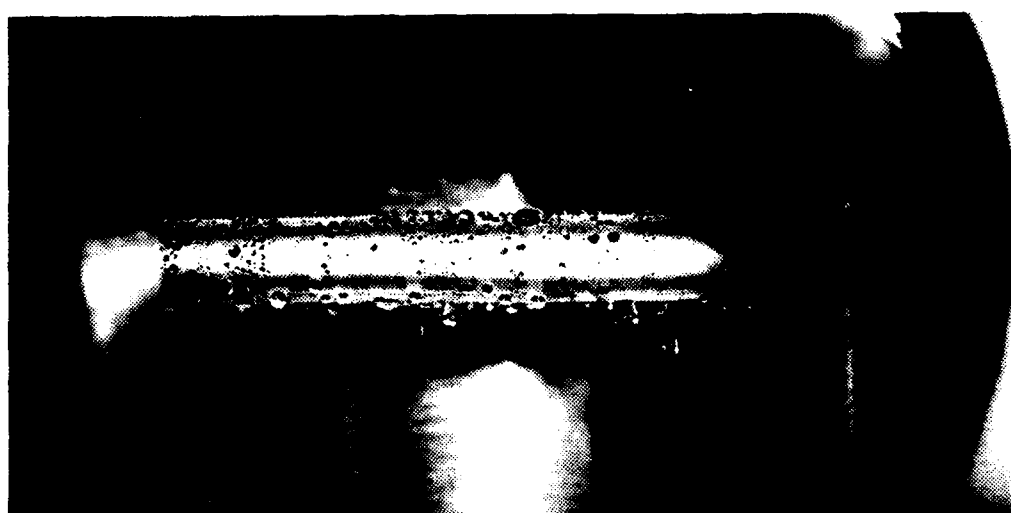
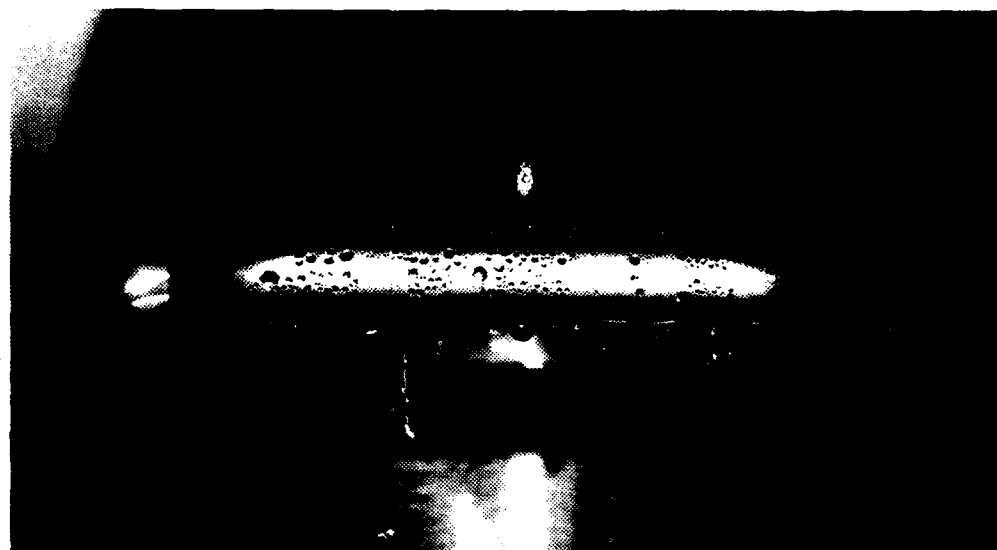


Figure 4.44 Comparison of Dropwise Quality on Silver-Electroplated Cu (top) and CuNi (bottom) Tubes.
 $P = 85 \text{ mmHg}$, $V_v = 2.0 \text{ m/s}$.

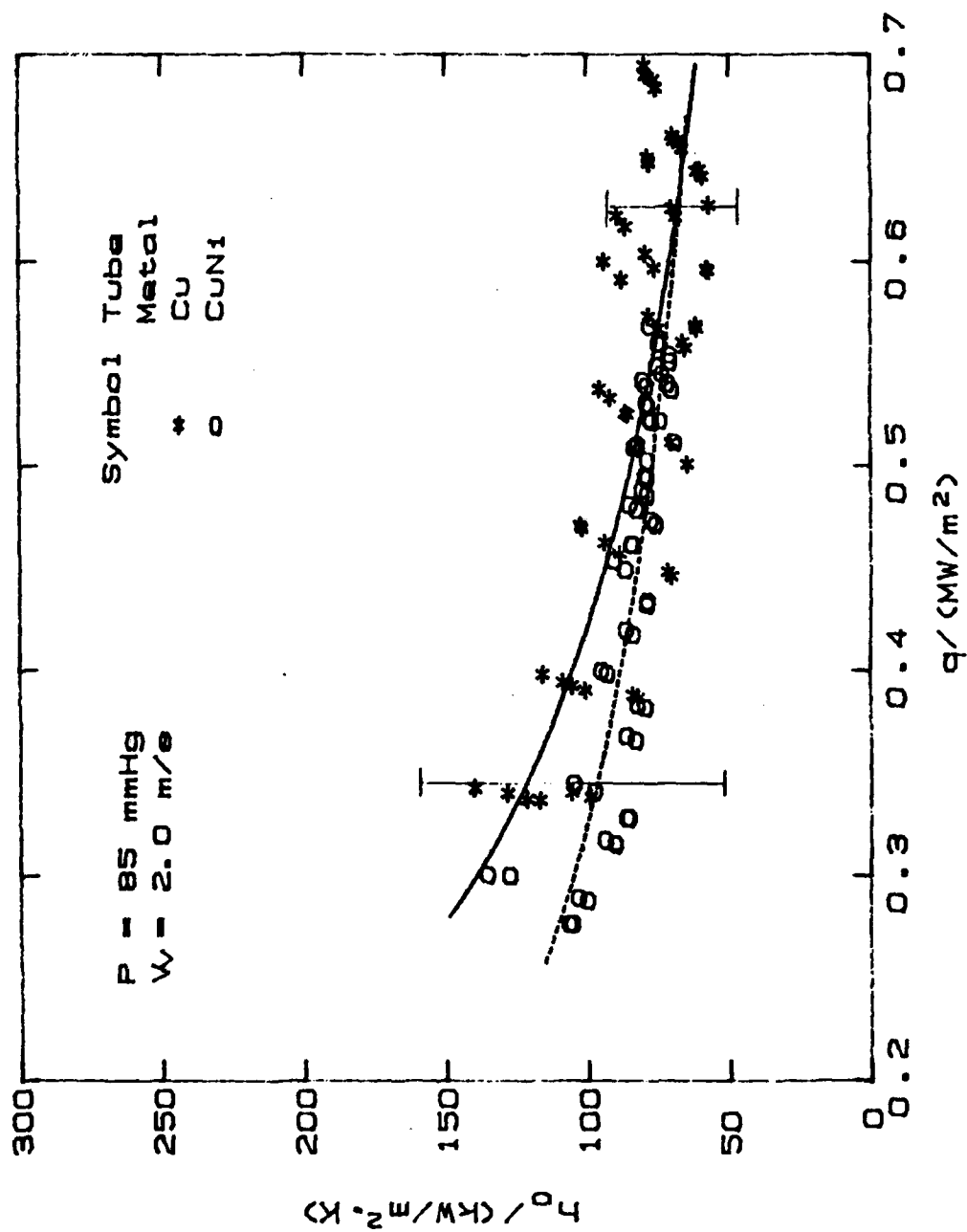


Figure 4.45 Dropwise Heat-Transfer Coefficients for Silver- Electroplated, Thin-Walled Copper and CuNi Tubes.

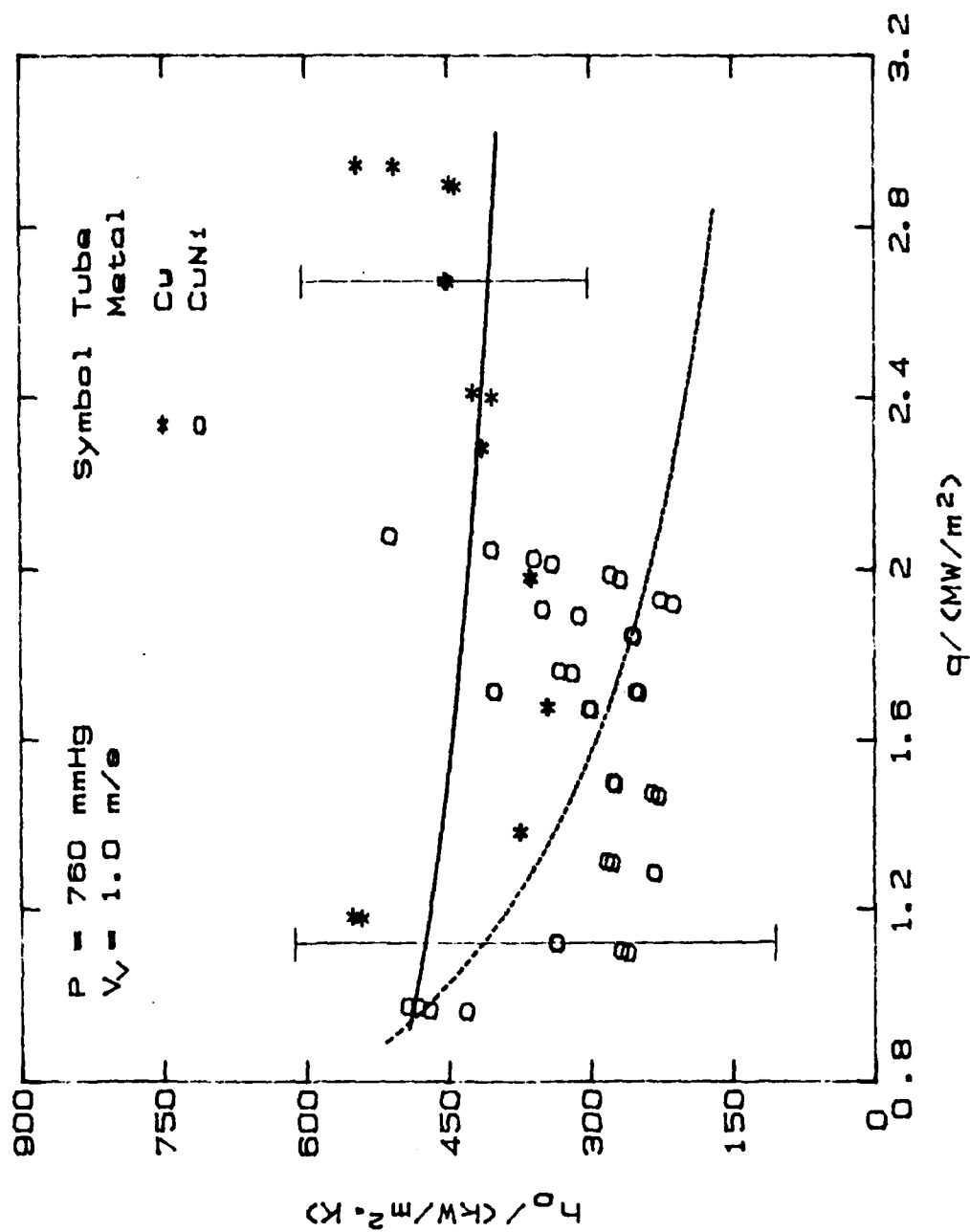


Figure 4.46 Dropwise Heat-Transfer Coefficients for Silver Electroplated Tubes at Atmospheric Pressure.

D. EFFECT OF SUBSTRATE THERMAL CONDUCTIVITY ON THE DROPWISE HEAT-TRANSFER COEFFICIENT

In addition to evaluating the coatings for dropwise promotion, several important conclusions were made concerning the thermal constriction resistance. In particular, the data obtained from the silver-electroplated copper and CuNi tubes (Figure 4.45) support the view of Rose [Ref. 12] that substrate thermal conductivity has little effect on the dropwise results. The data shown in Figure 4.46 also support Rose's view if the uncertainty of the data is considered.

The data obtained from the four thin-walled fluoroacrylic coated tubes (Figure 4.39) also support the view that the thermal constriction resistance effect is small, particularly when polymer coatings are concerned. The data for the aluminum and the CuNi tubes were 20 % higher than the data for the copper tube. The stainless-steel data agreed within 3 % of the copper data. Since the dropwise qualities were essentially the same for the four tubes, the differences are believed to be primarily due to variations in the coating thickness. From a simple heat-transfer resistance analysis, assuming a coating with a $0.35 \text{ W/m}\cdot\text{K}$ thermal conductivity (PTFE), it can be shown that a $0.5 \mu\text{m}$ difference in coating thickness can cause a 20 % difference in the dropwise heat-transfer coefficient.

The data obtained from the thick-walled NRL fluoroacrylic coated tubes must be excluded because of the sensitivity of the stainless-steel data on substrate thermal conductivity, which was discussed earlier. In addition, variations in the coating thickness must be considered. Because of the thinness of the NRL fluoroacrylic coatings, accurate measurements of their thicknesses could not be made with the facilities on hand.

Another important note is that the tubes tested had very thin walls (0.762 mm or 0.03 in). This would tend to show the largest effect of the thermal constriction resistance as noted by Hanneman [Ref. 14].

E. EFFECT OF VAPOR VELOCITY ON THE DROPWISE HEAT-TRANSFER COEFFICIENT

The thick-walled copper tube, coated with wash primer and NRL fluoroacrylic, was used to evaluate the vapor velocity effect on the dropwise heat-transfer coefficient. The results are shown in Figure 4.47 for four different vapor velocities at the same condensing pressure. The data show that the dropwise heat-transfer coefficient continuously increases with increasing vapor velocity. However, the increase in dropwise heat-transfer coefficient becomes less with increasing vapor velocity. This can readily be seen in Figure 4.48, which is a crossplot of the dropwise heat-transfer coefficient versus vapor velocity, for a 0.35 MW/m^2 heat flux. This trend agrees with the results presented by Graham [Ref. 5].

F. AN ALTERNATIVE APPROACH TO THE MODIFIED WILSON METHOD

The accuracy in determining the dropwise heat-transfer coefficient, from an overall heat-transfer resistance analysis, can be strongly dependent on the value of the Sieder-Tate coefficient used to predict the inside heat-transfer resistance. During dropwise condensation, the outside heat-transfer resistance is small and the inside heat-transfer resistance can become the dominating resistance. Therefore, a small error in determining the Sieder-Tate coefficient can cause large errors in the dropwise heat-transfer coefficient.

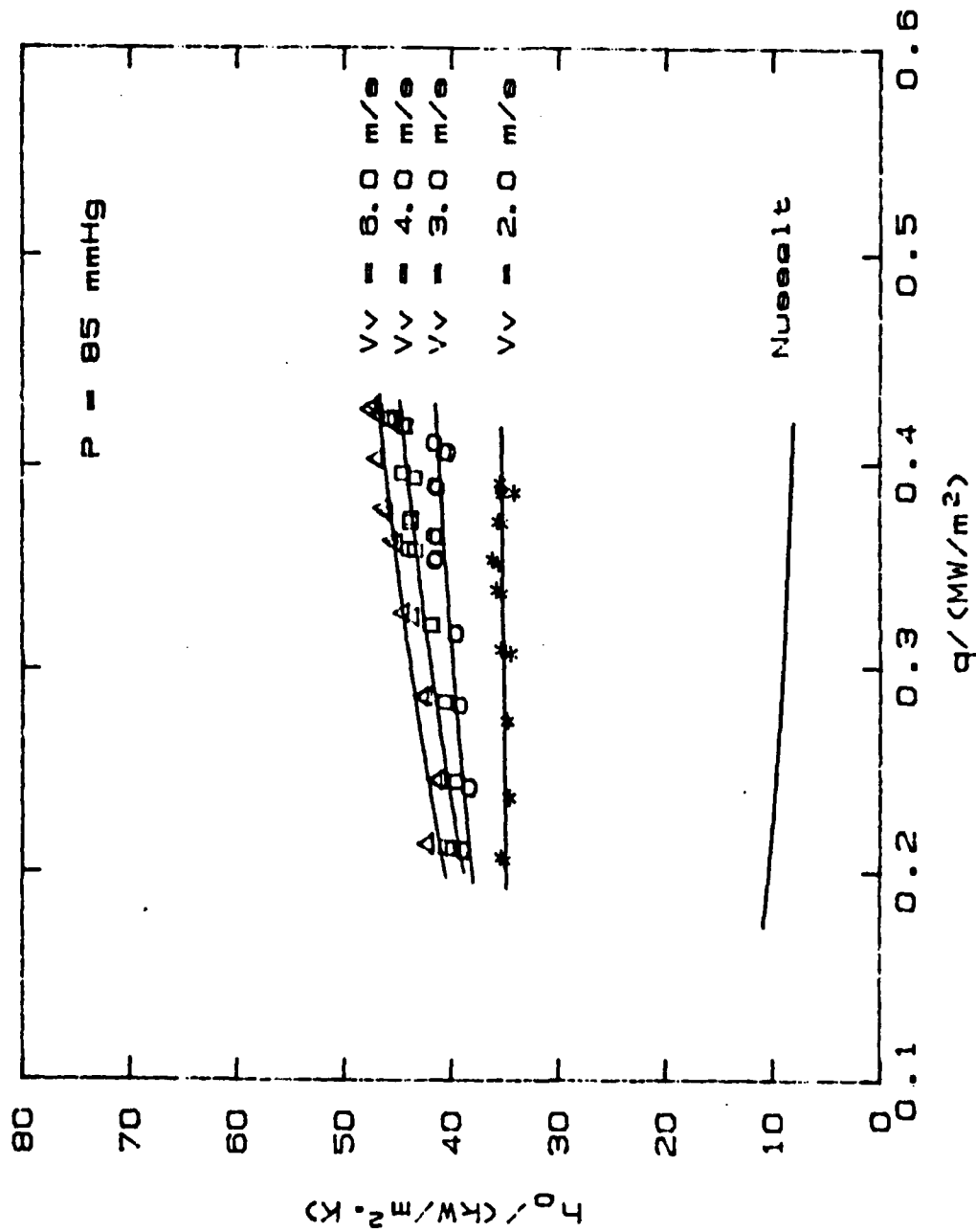


Figure 4.47 Effect of Vapor Velocity on the Dropwise Heat-Transfer Coefficient (NRL Fluoroacrylic with Wash Primer).

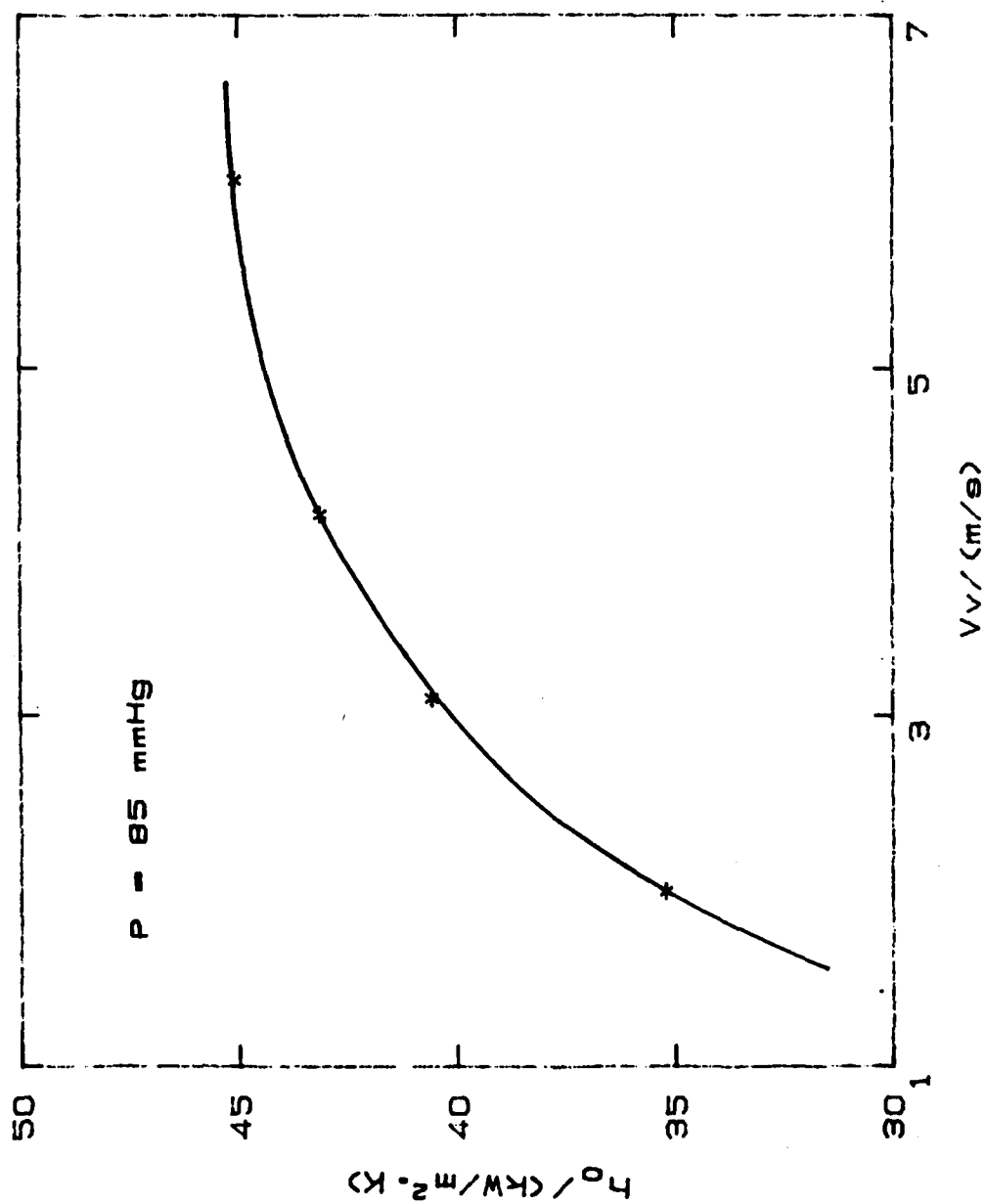


Figure 4.48 Dropwise Heat-Transfer Coefficient Versus Vapor Velocity.
NBL Fluoroacrylic with Primer on Copper Tube.

For this thesis, data obtained during filmwise condensation was used in the Modified Wilson method to determine the Sieder-Tate coefficient. The primary reason for using filmwise data was that known correlations for predicting the filmwise heat-transfer coefficient were available (i. e. Nusselt or Fujii-Honda). These could be easily used for the Modified Wilson Plot method.

During filmwise condensation, a relatively large temperature variation exists around the circumference of the horizontal tube [Ref. 45]. Since this is the case, the Sieder-Tate coefficient determined using filmwise data would underpredict the inside heat-transfer coefficient. This in turn would result in larger errors for the dropwise heat-transfer coefficient.

In order to get an understanding of the difference in the inside heat-transfer coefficient resulting from the circumferential temperature distribution, an alternate approach to the Modified Wilson method was attempted. In this case, the dropwise heat-transfer coefficient was assumed to be equal to a constant, independent of heat flux, in the Modified Wilson method. In addition, dropwise condensation data obtained from the silver-electroplated copper tube, condensing at a pressure of 85 mmHg, were used in the WILSON3 data reduction program. Iteration between the constant value for the dropwise heat-transfer coefficient and the Sieder-Tate coefficient was continued until convergence occurred. A value of 0.0861 was obtained for the Sieder-Tate coefficient. This shows an 18 % increase in the inside heat-transfer coefficient compared to the value obtained using the Fujii-Honda correlation for the Modified Wilson method ($C = 0.0702$). The value obtained for the constant dropwise heat-transfer coefficient was approximately 46,000 W/m²K. This value is about 18 % lower than the value obtained using the Sieder-Tate coefficient based on

the Fujii-Honda correlation at the highest heat flux (see Figure 4.45) and, as can be seen from the Figure, a larger difference in the dropwise heat-transfer coefficient occurs at the lower heat fluxes. Thus, there is a significant difference between the results obtained from these two Modified Wilson methods, and a thorough investigation is warranted to determine which method is more accurate.

V. CONCLUSIONS AND RECOMMENDATIONS

A. CONCLUSIONS

1. Using No-Stik, Emralon-333, and NRL fluoroepoxy coatings, dropwise condensation was promoted in excess of 11,000 hours. However, for these coatings, enhancement of the outside heat-transfer coefficient is limited (0-2 times filmwise) by coating thicknesses which were greater than 5.0 μm .
2. Using NRL fluoroacrylic coatings, dropwise condensation was promoted in excess of 9,000 hours on rough substrate surfaces. Outside heat-transfer coefficients were enhanced by a factor of 4 to 8.
3. Using Parylene-D coatings, dropwise condensation was promoted in excess of 5,500 hours. Outside heat-transfer coefficients can be enhanced by a factor of 2 to 4, depending on the coating thickness.
4. Using vacuum-deposited gold coatings, dropwise condensation was promoted in excess of 8,000 hours.
5. Excellent dropwise condensation was obtained with the silver-electroplated tubes. Outside heat-transfer coefficient enhancements of 8-12 were obtained under vacuum conditions, and enhancements of 30-40 were obtained at atmospheric conditions. However, the uncertainty in the results must be considered when large dropwise heat-transfer coefficients are obtained.
6. Dropwise data obtained from silver-electroplated copper and 90-10 CuNi tubes provide further evidence that the effect of thermal constriction resistance on the dropwise heat-transfer coefficient is small.

7. A uniform grit-blasted roughness provides the mechanical interlocking required between the coating and the substrate for good adhesion. A coarse grit (number 40) gave the best results.
8. A wash primer or gold subcoating greatly reduces substrate corrosion, which significantly improves coating endurance. However, when a wash primer is used, a trade off in heat-transfer enhancement must be made.
9. Variations in coating thickness have the largest effect on outside heat-transfer coefficient enhancement when polymer coatings are used to promote dropwise condensation.
10. Thermal stresses can cause failure of crosslinked polymer coatings by causing cracks to form, leading to further deterioration.
11. Surface roughness has little effect on the dropwise heat-transfer coefficient.
12. The dropwise heat-transfer coefficient can be improved with increased vapor velocity. Above a velocity of 6 m/s, further improvement is minimal.

B. RECOMMENDATIONS

1. Evaluate the change in the dropwise heat-transfer coefficient after prolonged exposure of polymer coatings to steam condensation. This could give some measure of the added thermal resistance from water absorption and substrate corrosion.
2. Re-evaluate Parylene-N coatings using proper surface preparation (roughness, primer, gold flash, etc.).
3. Investigate the plasma (glow-discharge) polymerization coating technique as a possibility of applying durable PTFE coatings.

4. Evaluate durability and heat-transfer performance of polymer coatings which are 5.0-10.0 μm thick and which have a silver or copper matrix mixed throughout the coatings. NRL fluoroepoxies might be suitable.
5. In order to improve coating adhesion, evaluate effects of different chemical cleaning compounds and acid etching of substrates.
6. Re-evaluate thin-walled tubes, with different thermal conductivities, coated with NRL fluoroacrylic excluding the wash primer for thermal constriction resistance effects.
7. Continue research into the use of the Modified Wilson method to obtain a suitable procedure for determining the Sieder-Tate coefficient for dropwise condensation. Use a dropwise-promoted, instrumented tube to obtain data for calculation of the Sieder-Tate coefficient directly. Compare this result to those obtained from filmwise condensation and by using different correlations in the Modified Wilson method.

APPENDIX A

UNCERTAINTY ANALYSIS

An uncertainty analysis was conducted using the Kline and McClintock method. The details of this analysis was given by Georgiadis [Ref. 41]. The same "ERROR" program was used with some minor changes. A listing of this program was also given by Georgiadis [Ref. 41].

The primary change in the program was to include the discrepancies found in the values used for substrate thermal conductivity. A ten percent uncertainty was assumed for substrate thermal conductivity. Other changes included the mixing chamber calibration and the Sieder-Tate coefficients. Values obtained during this thesis were used in the program. Error bars shown in Figures 4.36, 4.39, 4.45, and 4.46 are based on the results obtained from the ERROR program output.

When determining the outside heat-transfer coefficient, from the overall heat-transfer coefficient the controlling (largest) thermal resistance contributes the largest errors. As discussed earlier, for thick-walled low thermal conductivity substrates, the wall resistance can control the process and small errors in substrate thermal conductivity can cause large errors in the outside heat-transfer coefficient. As also discussed earlier, the inside heat-transfer resistance can become the controlling resistance when the condensing mode is dropwise. This is why the importance of obtaining an accurate value for the Sieder-Tate coefficient was stressed. The cooling water temperature rise measurement is also a significant source of error since this is used to determine the overall heat-transfer coefficient. As shown in Figure 4.36, the largest errors exist at the low heat fluxes and increase with increasing outside heat-transfer coefficient.

APPENDIX B

COMPUTER PROGRAM USED FOR WILSON PLOT DATA REDUCTION

The following pages contain a listing of the computer program (WILSON3) used to determine the Seider-Tate coefficients with the Modified Wilson method.

```

1000: FILE NAME: WILSON3
1010: REVISED: October 16, 1984
1020:
1030 CGM /Cg/ C(7)
1040 DATA 0.10086091,25727.94369,-767345.3295,79025595.31
1050 DATA -9247486589.6,97688E11,-2.66192E13,3.94078E14
1060 READ C(*)
1070 DIM Emf(4)
1080 L=.13335
1090 L1=.060325
1100 L2=.034925
1101 BEEP
1102 PRINTER IS 1
1103 PRINT USING "4X." "Select tube-wall type:"
1104 PRINT USING "4X." " 0 Thickwall 1 Thinwall"
1105 INPUT Itt
1106 IF Itt=0 THEN Do=.01905
1107 IF Itt=1 THEN Do=.01422
1120 D1=.0127
1121 D1=.01905
1130 D2=.015785
1160 PRINTER IS 701
1170 BEEP
1180 CLEAR 709
1190 INPUT "ENTER MONTH, DATE, AND TIME (MM:DD:HH:MM:SS).BS
1200 OUTPUT 709:"TD":BS
1210 Jp=0
1220 OUTPUT 709:"TD"
1230 ENTER 709:AS
1240 PRINT USING "10X." "Month, date and time : ""."14A":AS
1250 BEEP
1260 INPUT "ENTER DISK NUMBER".Dn
1270 PRINT
1280 PRINT USING "10X." "NOTE: Program name : WILSON3"
1290 PRINT USING "16X." "Disk number : ""."DD":Dn
1300 BEEP
1310 INPUT "ENTER INPUT MODE (1=3054A,2=FILE)".Im
1320 BEEP
1330 PRINTER IS 1
1340 PRINT USING "4X." "Select material code:"
1350 PRINT USING "4X." "0 Copper 1 Stainless steel"
1360 PRINT USING "4X." "2 Aluminum 3 90:10 CuNi"
1370 INPUT Imc
1371 BEEP
1372 PRINT USING "4X." "Select Ho correlation:"
1373 PRINT USING "4X." " 0 Nusselt 1 Fujii"
1374 INPUT Ioc
1375 PRINTER IS 701
1377 IF Ioc=0 THEN PRINT USING "16X." "Nusselt correlation is used for Ho"
1378 IF Ioc=1 THEN PRINT USING "16X." "Fujii correlation is used for Ho"
1379 BEEP
1380 PRINTER IS 1
1381 PRINT USING "4X." "Enter the value for vapor velocity,m/s"
1382 INPUT Uv
1383 PRINTER IS 701
1384 PRINT USING "16X." "Vapor Velocity : ""."D.DD":Uv
1390 IF Imc=0 THEN Kcu=385
1400 IF Imc=1 THEN Kcu=16

```

```

1410 IF Imc=2 THEN Kcu=167
1420 IF Imc=3 THEN Kcu=45
1421 IF Imc=1 THEN D1=.01335
1422 IF Imc=3 THEN D1=.01321
1423 Rm=D0-LOG(D0/D1)/(2-Kcu)
1430 IF Im=1 THEN
1440 BEEP
1450 INPUT "GIVE A NAME FOR THE DATA FILE".D_files
1460 BEEP
1470 INPUT "ENTER INSERT NUMBER".Inn
1480 CREATE BDAT D_files.10
1490 ELSE
1500 BEEP
1510 INPUT "GIVE THE NAME OF THE DATA FILE".D_files
1520 PRINT USING "16X.";"This analysis is for data in file """,14A":D_files
1530 BEEP
1540 INPUT "ENTER THE NUMBER OF RUNS STORED".Nrun
1550 END IF
1560 BEEP
1570 INPUT "GIVE A NAME FOR PLOT-DATA FILE".Plots
1580 BEEP
1590 INPUT "ENTER OPTION (1-QCT,2-T-PILE,3-AVE)".Itm
1600 BEEP
1620 IF Itm=1 THEN PRINT USING "16X.";"This analysis uses QCT readings""
1630 IF Itm=2 THEN PRINT USING "16X.";"This analysis uses T-PILE readings""
1640 IF Itm=3 THEN PRINT USING "16X.";"This analysis uses average of QCT and T-PILE readings""
1650 PRINT USING "16X.";"This analysis includes end-fin effect""
1670 CREATE BDAT Plots.10
1680 ASSIGN @File TO Plots
1690 J1=0
1700 ASSIGN @File TO D_files
1710 IF Im=2 THEN ENTER @File:Inn
1720 IF Inn=0 THEN C1=.03
1730 IF Inn>0 THEN C1=.07
1740 J=0
1750 Sx=0
1760 Sy=0
1770 Sxs=0
1780 Sxy=0
1790 PRINT
1791 BEEP
1800 PRINT USING "16X.";"Iteration number" = """,DD":J1+1
1810 IF J1=0 OR J=1 THEN
1820 PRINT
1830 PRINT USING "16X.";"T1      T2      Tact      Lmtd      Vu      X      y""
1840 END IF
1850 IF J1>0 THEN ASSIGN @File TO D_files
1860 IF J1>0 THEN ENTER @File:Inn
1870 IF Im=1 AND J1=0 THEN
1880 READ DATA THROUGH THE DATA ACQUISITION SYSTEM
1890 IF THE INPUT MODE (Im) = 1
1900 BEEP
1910 INPUT "ENTER FLOWMETER READING".Fm
1920 OUTPUT 709:"AR AF50 AL53"
1930 OUTPUT 709:"AS SA"
1940 Etp=0
1950 FOR I=1 TO 20
1960 ENTER 709:Et
1970 Etp=Etp+Et

```

```

1980 NEXT I
1990 Etp=Etp/20
2000 OUTPUT 709:"AS SA"
2010 Ptran=0
2020 FOR I=1 TO 50
2030 ENTER 709:Pt
2040 Ptran=Ptran+Pt
2050 NEXT I
2060 Ptran=Ptran/50
2070 OUTPUT 709:"AS SA"
2080 ENTER 709:Bvol
2090 OUTPUT 709:"AS SA"
2100 ENTER 709:Bamp
2110 OUTPUT 709:"AR AF20 AL24"
2120 FOR I=0 TO 4
2130 OUTPUT 709:"AS SA"
2140 ENTER 709:Emf(I)
2150 Emf(I)=ABS(Emf(I))
2160 NEXT I
2170 OUTPUT 713:"T1R2E"
2180 WAIT 2
2190 ENTER 713:T11
2200 OUTPUT 713:"T2R2E"
2210 WAIT 2
2220 ENTER 713:T2
2230 OUTPUT 713:"T1R2E"
2240 WAIT 2
2250 ENTER 713:T12
2260 T1=(T11+T12)*.5
2270 CLEAR 713
2280 ELSE
2290 READ DATA FROM A USER-SPECIFIED FILE IF INPUT MODE (Im) = 2
2300 ENTER #File:Bvol,Bamp,Ptran,Etp,Emf(-),Fm,T1,T2
2310 END IF
2320 Tsat=FNTvsv(Emf(0))
2330 T1=FNTvsv(Emf(2))
2340 Grad=FNGrad((T1+T2)*.5)
2350 To=T1+ABS(Etp)/(10*Grad)*1.E-5
2360 IF Jj=0 THEN
2370 Er1=ABS(T1-T1)
2380 PRINTER IS 1
2390 PRINT USING "####T1" = "###.00.00":T1
2400 PRINT USING "####T1" = "###.00.00":T1
2410 IF Er1>.5 THEN
2420 BEEP
2430 PRINT "OCT AND T1 DIFFER MORE THAN 0.5 C"
2440 BEEP
2450 INPUT "OK TO GO AHEAD (Y=0=N)?" :Ok1
2460 END IF
2470 PRINT USING "####T (OCT)" = "###.2.00":T2-T1
2480 PRINT USING "####T (T-PILE)" = "###.2.00":To-T1
2490 IF Ok1=0 AND Er1>.5 THEN 3770
2500 Er2=ABS((T2-T1)-(To-T1))/(T2-T1)
2510 IF Er2>.05 THEN
2520 BEEP
2530 PRINT "OCT AND T-PILE DIFFER MORE THAN 5%"
2540 BEEP
2550 INPUT "OK TO GO AHEAD (Y=0=N)?" :Ok2
2560 IF Ok2=0 AND Er2>.05 THEN 3770
2570 END IF
2580 PRINTER IS 701

```

```

2590 END IF
2600! CALCULATE THE LOG-MEAN-TEMPERATURE DIFFERENCE
2610 IF Itm=1 THEN
2620 Tf=Tf
2630 Tl=T2
2640 END IF
2650 IF Itm=2 THEN
2660 Tf=Tf
2670 Tl=To
2680 END IF
2690 IF Itm=3 THEN
2700 Tf=(Tf+Tl)*.5
2710 Tl=(T2+To)*.5
2720 END IF
2730 Tavg=(Tf+Tl)*.5
2740 Trise=Tl-Tf
2750 Lmtc=Trise/LOG((Tsat-Tf)/(Tsat-Tl))
2760 Cpw=FNCpw(Tavg)
2770 Rhow=FNRRhow(Tavg)
2780 Kw=FNKw(Tavg)
2790 Muwa=FNMuw(Tavg)
2800 Prw=FNPrw(Tavg)
2820 Mdt=1.04805E-2+6.80932E-3*Fn
2830 Md=Mdt*(1.0365-Tf*(1.96644E-3-Tf*5.252E-6))/.995434
2840 Vf=Md/Rhow
2850 Vw=Vf/(PI*D1^2/4)
2860 IF Inn=0 THEN Trise=Trise-(.00138+.001*Vw^2)
2870 IF Inn=1 THEN Trise=Trise-.004*Vw^2
2880 IF Inn=2 THEN Trise=Trise-(.0012+.0023*Vw^2)
2881 IF Inn=3 THEN Trise=Trise-(.0017+.0045*Vw^2)
2882 IF Inn=4 THEN Trise=Trise-(.0021+.0024*Vw^2)
2890 Q=Md*Cpw*Trise
2900 Qp=Q/(PI*Do*L)
2910 Uo=Qp/Lmtc
2920 Re=Rhow*Vw*Do/Muwa
2930 Fe1=0
2940 Fe2=0
2950 Cf=1
2960 Two=Tsats-5
2970 Tfilm=Tsats/3+Two*2/3
2980 Kf=FNKw(Tfilm)
2990 RhoF=FNRRhow(Tfilm)
3000 MuF=FNMuw(Tfilm)
3010 Hfgp=FNHfg(Tsats)+.58*FNCpw(Tfilm)*(Tsats-Two)
3020 New=Kf*(RhoF^2+9.799*Hfgp/(MuF*Do*Qp))^.3333
3021 IF Loc=1 THEN
3022 New=Kf*((9.799*Hfgp/Qp)^.25)*((MuF*Do)^(-.375))*(RhoF^.625)*(Vw^.125)
3023 END IF
3030 Ho=.74*New
3040 Twoc=Tsats-Qp/Ho
3050 IF ABS((Twoc-Two)/Twoc)>.001 THEN
3060 Two=Twoc
3070 GOTO 2970
3080 END IF
3090 Cf=1.0
3100 Omega=Re*.9+Prw*.3333-Cf
3110 H1=Kw/Do-C1*Omega
3130 P1=P1-(D1+D1)
3140 P2=P1-(D1-D2)
3150 A1=(D1-D1)*P1-(D1+D1)*.5

```

```

3160 A2=(D2-D1)/PI*(D1+D2)*.5
3170 M1=(H1-P1/(Kcu*A1))*.5
3180 M2=(H1-P2/(Kcu*A2))*.5
3190 Fe1=FNtanh(M1-L1)/(M1-L1)
3200 Fe2=FNtanh(M2-L2)/(M2-L2)
3210 Dt=0/(PI*D1*(L+L1+Fe1+L2+Fe2)*H1)
3220 Cfc=(Muwa/FNMuw(Tavg+Dt))*.14
3230 IF ABS((Cfc-Cf)/Cfc)>.01 THEN
3240 Cf=(Cf+Cfc)*.5
3250 GOTO 3100
3260 END IF
3270 X=Do*New*L/(Omega*Ku*(L+L1+Fe1+L2+Fe2))
3280 Y=New*(1/Uo-Rm)
3290! COMPUTE COEFFICIENTS FOR THE LEAST-SQUARES-FIT STRAIGHT LINE
3300 IF Jp=1 THEN OUTPUT #File:X,Y
3310 Sx=Sx+X
3320 Sy=Sy+Y
3330 Sxs=Sxs+X*X
3340 Sxy=Sxy+X*Y
3350! STORE RAW DATA IN A USER-SPECIFIED FILE IF INPUT MODE (Im) = 1
3360 IF Im=1 AND Jj=0 THEN OUTPUT #File:Bvol.Bamp.Ptran.Etp.Emf(*).Fm.T1.T2
3370 IF Jj=0 OR Jp=1 THEN PRINT USING "8X.5(2X.3D.0D).2(2X.0.5D)":Tf.T1.Tsat.Lm
td.Vw.X,Y
3380! BEEP
3390 J=J+1
3400 IF Im=1 AND Jj=0 THEN
3410 INPUT "DO YOU HAVE MORE DATA (1-Y,0-N)?":Go_on
3420 Nrun=J
3430 IF Go_on=1 THEN 1870
3440 ELSE
3450 IF J<Nrun THEN 1870
3460 END IF
3470 S1=(Nrun*Sxy-Sy*Sx)/(Nrun*Sxs-Sx^2)
3480 Ac=(Sy-S1*Sx)/Nrun
3490 C1c=1/S1
3500 Jj=Jj+1
3510 IF Jp=1 THEN Jp=2
3520 IF ABS((C1c-C1)/C1c)>.001 THEN
3530 C1=(C1c+C1)*.5
3540 PRINT USING "10X. ""Intermediate Sieder-Tate coefft = ""Z.4D":C1
3550 GOTO 1740
3560 ELSE
3570 IF Jp=0 THEN Jp=1
3580 END IF
3590 IF Jp=1 THEN 1740
3600 C1=(C1+C1c)*.5
3610 PRINT
3620 PRINT USING "10X. ""Sieder-Tate coefficient = ""Z.4D":C1
3630 PRINT
3640 PRINT USING "10X. ""Least-Squares Line: ""
3650 PRINT USING "10X. "" Slope = ""Z.5DE.":S1
3660 PRINT USING "10X. "" Intercept = ""Z.5DE.":Ac
3670 PRINT
3680 IF Im=1 THEN
3690 BEEP
3700 PRINT USING "10X. ""NOTE: ""Z.Z. "" data runs are stored in file ""Z.9A":J.D_
file$
3710 ELSE
3720 PRINT USING "10X. ""NOTE: Above analysis was performed for data in file ""
10A":D_file$
3730 END IF

```



```

3740 PRINT USING "15X." "Plot data are stored in file "".'0A":Plots
3750 ASSIGN #File TO -
3760 ASSIGN #Filep TO -
3770 END
3780 DEF FNRhow(T)
3790 Ro=1006.35724-T*(.774489-T*(2.262459E-2-T*3.03304E-4))
3800 RETURN Ro
3810 FNEND
3820 DEF FNPru(T)
3830 Pru=FNCow(T)+FNMuw(T)/FNKw(T)
3840 RETURN Pru
3850 FNEND
3860 DEF FNMuw(T)
3870 A=247.3/(T+133.15)
3880 Mu=2.4E-5+10^-A
3890 RETURN Mu
3900 FNEND
3910 DEF FNKw(T)
3920 X=(T+273.15)/273.15
3930 Kw=-.92247+X*(2.3395-X*(1.3007-X*(.52577-.07344*X)))
3940 RETURN Kw
3950 FNEND
3960 DEF FNTvsv(Emf)
3970 COM /Cc/ C(7)
3980 T=C(0)
3990 FOR I=1 TO 7
4000 T=T+C(I)*Emf^I
4010 NEXT I
4020 T=T+4.733862E-3+T*(7.592934E-3-3.077927E-5*T)
4030 RETURN T
4040 FNEND
4050 DEF FNCow(T)
4060 Cow=(4.21120858-T*(2.26326E-3-T*(4.42361E-5+2.71429E-7)))*1000
4070 RETURN Cow
4080 FNEND
4090 DEF FNTann(X)
4100 P=EXP(X)
4110 Q=EXP(-X)
4120 Tann=(P+Q)/(P-Q)
4130 RETURN Tann
4140 FNEND
4150 DEF FNGrad(T)
4160 COM /Cc/ C(7)
4170 Grad=37.9853+.104388*T
4180 RETURN Grad
4190 FNEND
4200 DEF FNFvst(T)
4210 F=466.444+T*(7.09451-T*1.55808E-2)
4220 RETURN F
4230 FNEND
4240 DEF FNHfg(T)
4250 Hfg=2477200-2450*(T-10)
4260 RETURN Hfg
4270 FNEND

```

APPENDIX C

COMPUTER PROGRAM USED FOR HEAT-TRANSFER DATA REDUCTION

The following pages contain a listing of the computer program (DRP5) used for data acquisition and data reduction.

```

1000! FILE NAME: DRPS
1005! REVISED: October 26, 1984
1010!
1015 COM /C(7)
1020 DIM Emf(10)
1025 DATA 0.10086091,25727.94369,-767345.3295,78025595.81
1030 DATA -9247486589.6,97688E+11,-2.66192E+13,3.94078E+14
1035 READ C(7)
1040 D1=.0127 ! Inside diameter of test tube
1045 D2=.01905 ! Outside diameter of test tube
1050 D1=.01905 ! Outside diameter of the inlet end
1055 D2=.015875 ! Outside diameter of the outlet end
1060 Dssp=.1524 ! Inside diameter of stainless steel test section
1065 L=.13335 ! Condensing length
1070 Ax=PI*Dssp 2/4
1075 L=.13335 ! Condensing length
1080 L1=.060325 ! Inlet and "fin length"
1085 L2=.034925 ! Outlet and "fin length"
1090 Kcu=385 ! Thermal conductivity of Copper
1095 PRINTER IS :
1100 BEEP
1105 PRINT USING "4X." "Select option:"
1110 PRINT USING "5X." "0 Taking data or re-processing previous data"
1115 PRINT USING "6X." "1 Plotting previous data"
1120 PRINT USING "6X." "2 Labelling"
1125 PRINT USING "6X." "3 Plotting on log-log"
1130 INPUT Iso
1135 Iso=Iso+1
1140 IF Iso>1 THEN 3355
1145 PRINTER IS 701
1150 CLEAR 709
1155 BEEP
1160 INPUT "ENTER MONTH, DATE AND TIME (MM:DD:HH:MM:SS)".Dates
1165 OUTPUT 709:"D":Dates
1170 OUTPUT 709:"D"
1175 ENTER 709:Dates
1180 PRINT " Month, date and time :":Dates
1185 PRINT
1190 PRINT USING "10X." "NOTE: Program name : DRPS"
1195 BEEP
1200 INPUT "ENTER DISK NUMBER".Dn
1205 PRINT USING "16X." "Disk number = ".Dn
1210 BEEP
1215 INPUT "ENTER INPUT MODE (0=3054A.1=FILE)".Im
1220 BEEP
1225 PRINTER IS :
1230 PRINT USING "4X." "Select tube wall type"
1235 PRINT USING "4X." "0 Thickwall 1 Thinwall"
1240 INPUT Itt
1245 BEEP
1250 PRINT
1255 PRINT USING "4X." "Select option:"
1260 PRINT USING "4X." "0=Dropwise 1=Plain"
1265 INPUT Ito
1270 IF Itt=0 THEN D2=.01905
1275 IF Itt=1 THEN D2=.01422
1280 BEEP
1285 PRINT USING "4X." "Select material code:"
1290 PRINT USING "4X." "0 Copper 1 Stainless steel"

```

```

1295 PRINT USING "4X,""2 Aluminum 3 30:10 Cwll""
1300 INPUT Imc
1305 IF Imc=0 THEN Kcu=385
1310 IF Imc=1 THEN Kcu=16
1315 IF Imc=2 THEN Kcu=167
1320 IF Imc=3 THEN Kcu=45
1325 IF Imc=1 THEN Di=.01336
1330 IF Imc=3 THEN Di=.01321
1335 Rm=Do*LOG(Do/Di)/(2*Kcu) ! WALL RESISTANCE BASED ON OUTSIDE AREA
1340 PRINTER IS 701
1345 Im=Im+1
1350 IF Im=1 THEN
1355 BEEP
1360 INPUT "GIVE A NAME FOR THE RAW DATA FILE".D_files
1365 PRINT USING "16X,""File name : """,14A":D_files
1370 CREATE BDAT D_files.15
1375 ASSIGN @File TO D_files
1380 Ifg=0 ! Smooth tube
1385 BEEP
1390 INPUT "ENTER INSERT NUMBER (0=NO INSERT)".Inn
1395 OUTPUT @File:Ifg,Inn,Iut
1400 BEEP
1405 INPUT "ENTER PRESSURE CONDITION (0=V,1=A)".Ipc
1410 ELSE
1415 BEEP
1420 INPUT "GIVE THE NAME OF THE EXISTING DATA FILE".D_files
1425 PRINT USING "16X,""This analysis was performed for data in file """,10A":D_
files
1430 BEEP
1435 INPUT "ENTER THE NUMBER OF RUNS STORED".Nrun
1440 BEEP
1445 INPUT "ENTER PRESSURE CONDITION (0=V,1=A)".Ipc
1450 ASSIGN @File TO D_files
1455 ENTER @File:Ifg,Inn,Iut
1460 END IF
1465 IF Ito=1 THEN
1470 BEEP
1475 INPUT "WANT TO CREATE A FILE FOR Nr vs F (1=Y,0=N)".Inf
1480 ELSE
1485 Inf=0
1490 END IF
1495 IF Inf=1 THEN
1500 BEEP
1505 INPUT "GIVE A NAME FOR Nr vs F FILE".Nrfs
1510 CREATE BDAT Nrfs.2
1515 ASSIGN @Nrfs TO Nrfs
1520 END IF
1525 BEEP
1530 INPUT "ENTER OPTION (0=OCT,1=T-PILE,2=AVE)".Itm
1535 Itm=Itm+1
1540 IF Itm=1 THEN PRINT USING "16X,""This analysis uses OCT readings""
1545 IF Itm=2 THEN PRINT USING "16X,""This analysis uses T-PILE readings""
1550 IF Itm=3 THEN PRINT USING "16X,""This analysis uses average of OCT and T-P
ILE readings""
1555 PRINT USING "16X,""This analysis includes end-fin effect""
1560 IF Inn=2 AND Imc=0 THEN C1=.0702
1565 IF Inn=2 AND Imc=2 THEN C1=.0720
1570 IF Inn=3 THEN C1=.0689
1575 IF Inn=4 THEN C1=.0741
1580 PRINT USING "16X,""Slider-Fate coefficient = """,2.4D":C1
1585 PRINT USING "16X,""Insert number = """,1.0":Inn

```

```

1590 BEEP
1595 INPUT "GIVE A NAME FOR PLOT DATA FILE".P_files
1600 CREATE BDATA P_files.S
1605 ASSIGN %Filep TO P_files
1610 BEEP
1615 INPUT "ENTER OUTPUT VERSION (0=SHORT,1=LONG)".Iov
1620 Iov=Iov+1
1625 J=0
1630 IF Iov=1 THEN
1635 PRINT
1640 IF Inf=1 THEN
1645 PRINT USING "10X." "Data Vu Uo Ho Gp Vv F Nr
.....
1550 PRINT USING "10X." " (m/s) (W/m^2-K) (W/m^2-K) (W/m^2) (m/s)""
1555 ELSE
1660 PRINT USING "10X." "Data Vu Uo Ho Gp Vv""
1665 PRINT USING "10X." " (m/s) (W/m^2-K) (W/m^2-K) (W/m^2) (m/s)""

1670 END IF
1675 END IF
1680 Zx=0
1685 Zx2=0
1690 Zxy=0
1695 Zv=0
1700 Sx=0
1705 Sy=0
1710 Sxs=0
1715 Sxy=0
1720 Go_on=1
1725 Repeat:
1730 Ok3=1
1735 J=J+1
1740 IF Im=1 THEN
1745 BEEP
1750 INPUT "LIKE TO CHECK NG CONCENTRATION (1=Y,0=N)?" .Ng
1755 BEEP
1760 INPUT "ENTER FLOWMETER READING".Fn
1765 OUTPUT 709:"AR AF50 AL63 VR5"
1770 OUTPUT 709:"AS SA"
1775 ENTER 709:Ecp
1780 BEEP
1795 INPUT "CONNECT VOLTAGE LINE".Ok
1795 OUTPUT 709:"AS SA"
1797 ENTER 709:Bvol
1810 BEEP
1815 INPUT "DISCONNECT VOLTAGE LINE".Ok
1816 OUTPUT 709:"AS SA"
1817 ENTER 709:Vtran
1820 OUTPUT 709:"AS SA"
1825 ENTER 709:Bano
1830 OUTPUT 709:"AR AF20 AL24 VR1"
1835 FOR I=0 TO 4
1840 OUTPUT 709:"AS SA"
1845 IF I<2 THEN
1850 Se=0
1855 FOR K=1 TO 10
1860 ENTER 709:E
1865 Se=Se+E
1870 NEXT K
1875 Enf(I)=ABS(Se/10)

```

```

1880 ELSE
1885 ENTER 709:E
1890 Emf(1)=ABS(E)
1895 END IF
1900 NEXT I
1905 OUTPUT 709:"AS SA"
1910 OUTPUT 713:"T1R2E"
1915 WAIT 2
1920 ENTER 713:T11
1925 OUTPUT 713:"T2R2E"
1930 WAIT 2
1935 ENTER 713:T2
1940 OUTPUT 713:"T1R2E"
1945 WAIT 2
1950 ENTER 713:T12
1955 T1=(T11+T12)*.5
1960 OUTPUT 713:"T3R2E"
1965 IF Ng=0 THEN 2030
1970 BEEP
1975 INPUT "ENTER MANOMETER READING (HL,HR,Hrw)".H1.Hr.Hrw
1980 BEEP
1985 INPUT "OK TO ACCEPT THIS RUN (1=Y-DEFAULT,0=N)".Ok3
1990 IF Ok3=0 THEN
1995 J=J-1
2000 GOTO 1730
2005 END IF
2010 Phg=H1+Hr
2015 Pwater=Hr-Hrw
2020 ELSE
2025 ENTER #File:9vol.8amp.Vtran.Etp,Emf(0),Emf(1),Emf(2),Emf(3),Emf(4),Fa,T1,T
2.Phg,Pwater
2030 IF J=1 OR J=20 OR J=Hrun THEN
2035 Ng=1
2040 ELSE
2045 Ng=0
2050 END IF
2055 END IF
2060 Tsteam=FNTvsu((Emf(0)+Emf(1))*0.5) ! COMPUTE STEAM TEMPERATURE
2065 Troom=FNTvsu(Emf(3))
2070 Tcon=FNTvsu(Emf(4))
2075 Psat=FNPvst(Tsteam)
2080 Rong=13529-122*(Troom-26.85)/50
2085 Rowater=FNRhou(Troom)
2090 Ptest=(Phg-Rong-Pwater-Rowater)*9.799/1000
2095 Pmm=Ptest/133.322
2100 Pkm=Ptest*1.E-3
2105 Pks=Psat*1.E-3
2110 Pkt=Pks
2115 Tst=FNTvsp(Ptest)
2120 Vst=FNVvst(Tsteam)
2125 Pong=(Ptest-Psat)/Ptest
2130 Post=1-Pong
2135 Mfng=1/(1+18.015/29.97*Psat/(Ptest-Psat))
2140 Vfng=Mfng/(1.608-.608*Mfng)
2145 Mfng=Mfng*100
2150 Vfng=Vfng*100
2155 BEEP
2160 IF Iov=2 THEN
2165 PRINT
2170 PRINT USING "10X." "Data set number" - "" .DD":J
2175 OUTPUT 709:"AR AF20 AL20 VRS"

```

```

2180 OUTPUT 709:"AS SA"
2185 END IF
2190 IF Iov=2 AND Ng=1 THEN
2195 PRINT USING "10X. "" P Psat Ptran Tneas Tsat N
G 7 ""
2200 PRINT USING "10X. "" (mm) (kPa) (kPa) (kPa) (C) (C) Molal
Mass ""
2205 PRINT USING "10X.5(3D.DD.2X).2(3D.DD.2X).2(M3D.D.2X)":Pmm.Pkm.Pks.Pkt.Tste
am.Tsat.Vfng.Mfng
2210 PRINT
2215 END IF
2220 IF Mfng>.5 THEN
2225 BEEP
2230 IF Im=1 AND Ng=1 THEN
2235 BEEP
2240 PRINT
2245 PRINT USING "10X. ""Energize the vacuum system ""
2250 BEEP
2255 INPUT "OK TO ACCEPT THIS RUN (1=Y,0=N)?" Ok
2260 IF Ok=0 THEN
2265 BEEP
2270 DISP "NOTE: THIS DATA SET WILL BE DISCARDED!! "
2275 WAIT 5
2280 GOTO 1740
2285 END IF
2290 END IF
2295 END IF
2300 IF Im=1 THEN
2305 IF Fm<10 OR Fm>100 THEN
2310 Ifm=0
2315 BEEP
2320 INPUT "INCORRECT FM (1=ACCEPT,0=DELETE)".Ifm
2325 IF Ifm=0 THEN 1730
2330 END IF
2335 END IF
2340 ANALYSIS BEGINS
2345 T1=FNTvsv(Emf(2))
2350 Grad=FNGrad((T1+T2)*.5)
2355 To=T1+ABS(Etp)/(10*Grad)*1.E+6
2360 Er1=ABS(T1-T1)
2365 PRINTER IS 1
2370 PRINT USING ""T1 (QCT) = "" DD.3D":T1
2375 PRINT USING ""T1 (TC) = "" DD.3D":T1
2380 IF Er1>.5 THEN
2385 BEEP
2390 PRINT "QCT AND TC DIFFER BY MORE THAN 0.5 C"
2395 BEEP
2400 INPUT "OK TO GO AHEAD (1=Y,0=N)?" Ok1
2405 END IF
2410 PRINT USING ""DT (QCT) = "" DD.3D":T2-T1
2415 PRINT USING ""DT (T-PILE) = "" DD.3D":To-T1
2420 IF Ok1=0 AND Er1>.5 THEN 3370
2425 Er2=ABS((T2-T1)-(To-T1))/(T2-T1)
2430 IF Er2>.05 THEN
2435 BEEP
2440 PRINT "QCT AND T-PILE DIFFER BY MORE THAN 5%"
2445 BEEP
2450 INPUT "OK TO GO AHEAD (1=Y,0=N)?" Ok2
2455 IF Ok2=0 AND Er2>.05 THEN 3370
2460 END IF

```

```

2465 PRINTER IS 701
2470 IF Itm=1 THEN
2475 T11=T1
2480 T2o=T2
2485 END IF
2490 IF Itm=2 THEN
2495 T11=T1
2500 T2o=T2
2505 END IF
2510 IF Itm=3 THEN
2515 T11=(T1+T11)*.5
2520 T2o=(T2+T2o)*.5
2525 END IF
2530 Tavg=(T11+T2o)*.5
2535 Cpw=FNCpw(Tavg)
2540 Rhow=FNRhow(Tavg)
2545 Md=1.04805E-2+6.80932E-3*Fm
2550 Md=Md*(1.0365-1.96644E-3*T11+5.252E-6*T11^2)/.995434
2555 Mf=Md/Rhow
2560 Vu=Mf/(PI*D1^2/4)
2565 IF Inn=0 THEN T2o=T2o-(.0138+.001*Vu^2)
2570 IF Inn=1 THEN T2o=T2o-.004*Vu^2
2575 IF Inn=2 THEN T2o=T2o-(-.0012+.0028*Vu^2)
2580 IF Inn=3 THEN T2o=T2o-(-.0017+.0045*Vu^2)
2585 IF Inn=4 THEN T2o=T2o-(-.0021+.0024*Vu^2)
2590 Q=Md*Cpw*(T2o-T11)
2595 Qp=Q/(PI*Do*L)
2600 Ku=FNKu(Tavg)
2605 Muw=FNMuw(Tavg)
2610 Re1=Rhow*Vu*Di/Muw
2615 Pru=FNPru(Tavg)
2620 Fe1=0.
2625 Fe2=0.
2630 Cf=1.
2635 Qme=Re1*.8*Pru*.3333
2640 H1=Ku/Di*(C1-Jme*Cf+Ac)
2645 Dt=Q/(PI*Di*(L+L1*Fe1+L2*Fe2)*H1)
2650 Cfc=(Muw/FNMuw(Tavg+Dt))*.14
2655 IF ABS((Cfc-Cf)/Cfc)>.01 THEN
2660 Cf=(Cf+Cfc)*.5
2665 GOTO 2640
2670 END IF
2675 P1=PI*(D1+D1)
2680 A1=(D1-D1)*PI*(D1+D1)*.5
2685 M1=(H1*P1/(Kcu*A1))*.5
2690 P2=PI*(D1+D2)
2695 A2=(D2-D1)*PI*(D1+D2)*.5
2700 M2=(H1*P2/(Kcu*A2))*.5
2705 Fe1=FNtanh(M1*L1)/(M1*L1)
2710 Fe2=FNtanh(M2*L2)/(M2*L2)
2715 Dtc=Q/(PI*Di*(L+L1*Fe1+L2*Fe2)*H1)
2720 IF ABS((Dtc-Dt)/Dtc)>.01 THEN 2640
2725 Lmtd=(T2o-T11)/LOG((Tsteam-T11)/(Tsteam-T2o))
2730 Uo=Q/(Lmtd*PI*Do*L)
2735 Ho=1/((1/Uo-Do*L)/(D1*(L+L1*Fe1+L2*Fe2)*H1)-Rm)
2740 Hfg=FNHfg(Tsteam)
2745 Two=Tsteam-Qp/Ho
2750 Tfil=Tsteam/2+Two/2
2755 Kf=FNKu(Tfil)
2760 Rhof=FNRhow(Tfil)
2765 Muf=FNMuw(Tfil)

```



```

2770 Hpq=.651*Kf*(Rho2*9.31*Hfg/(Muf-Do-Qp)).3333
2775 Y=Hq=Hp.3333
2780 X=Up
2785 Sx=Sx+X
2790 Sy=Sy+Y
2795 Sxs=Sxs+X2
2800 Sxy=Sxy+X*Y
2805 Q1=500
2810 Qloss=Q1/(100-25)*(Tsteam-Troom)
2815 Hfc=FNHF(Tcon)
2820 Hf=FNHF(Tsteam)
2825 Mdv=0
2830 Bp=(Bvol*100)2/5.76
2835 Mdv=((Bp-Qloss)-Mdv*(Hf-Hfc))/Hfg
2840 IF ABS((Mdv-Mdv)/Mdv)>.01 THEN
2845 Mdv=(Mdv+Mdv)*.5
2850 GOTO 2835
2855 END IF
2860 Mdv=(Mdv+Mdv)*.5
2865 Vg=FNHf(Tsteam)
2870 Vv=Mdv*Vg/Ax
2875 IF Inf=1 THEN
2880 F=(9.799*Do*Muf*Hfg)/(Vv2*Kf*(Tsteam-Two))
2885 Nu=Ho*Do/Kf
2890 Ret=Vv*Rho*Do/Muf
2895 Nr=Nu/Ret*.5
2900 END IF
2905 IF Iov=2 THEN
2910 PRINT USING "10X.*** T (Inlet)      Delta-T***"
2915 PRINT USING "10X.*** QCT      TC      QCT T-PILE***"
2920 PRINT USING "10X.2(DD.DD.2X).2(DD.3D.2X)":T1.T1.T2-T1.To-T1
2925 PRINT USING "10X.*** Vv      Rel      H1      Uo      Ho      q"
      Vv***
2930 PRINT USING "10X.Z.DD.IX.5(MZ.3DE.IX).MZ.DD":Vv.Rel.H1.Uo.Ho.Qp.Vv
2935 END IF
2940 IF Iov=1 THEN
2945 IF Inf=1 THEN
2950 PRINT USING "11X.DD.2X.Z.DD.2X.2(5D.D.2X).Z.3DE.IX.Z.DD.2(1X.3D.DD)":J,Vv,
      Uo.Ho.Qp.Vv.F.Nr
2955 ELSE
2960 PRINT USING "11X.DD.2X.Z.DD.2X.2(MD.4DE.2X).Z.3DE.3X.Z.DD":J,Vv.Uo.Ho.Qp.V
      V
2965 END IF
2970 END IF
2975 IF Im=2 THEN
2980 IF Inf=1 THEN OUTPUT @Nrf:F.Nr
2985 OUTPUT @Filep:Qp.Ho
2990 END IF
2995 IF Im=1 THEN
3000 BEEP
3005 INPUT "OK TO STORE THIS DATA SET (1=Y,0=N)?".Qks
3010 IF Qks=1 THEN
3015 OUTPUT @File:Bvol.Bamp.Vtran.Etp.Emf(0).Emf(1).Emf(2).Emf(3).Emf(4).Fm.T1.
      T2.Phg.Pwater
3020 IF Inf=1 THEN OUTPUT @Nrf:F.Nr
3025 OUTPUT @Filep:Qp.Ho
3030 ELSE
3035 J=J-1
3040 GOTO 1725
3045 END IF
3050 BEEP

```

```

3055 INPUT "WILL THERE BE ANOTHER RUN (I=Y.O=N)?",Go_on
3060 Nrun=J
3065 IF Go_on<>0 THEN Repeat
3070 ELSE
3075 IF J<Nrun THEN Repeat
3080 END IF
3085 PRINT
3090 S1=(Nrun*Sxy-Sy*Sx)/(Nrun*Sxs-Sx^2)
3095 Ac=(Sy-S1*Sx)/Nrun
3100 IF Ito=1 THEN
3105 PRINT USING "10X." "Least-Squares Line for Hnu vs q curve:"
3110 PRINT USING "10X." "Slope = ".MD.4DE":S1
3115 PRINT USING "10X." "Intercept = ".MD.4DE":Ac
3120 END IF
3125 BEEP
3130 INPUT "ENTER PLOT FILE NAME".Fplots
3135 ASSIGN @File4 TO Fplots
3140 FOR I=1 TO Nrun
3145 ENTER @File4:Qp,Ho
3150 Xc=LOG(Qp/Ho)
3155 Yc=LOG(Qp)
3160 Zx=Zx+Xc
3165 Zx2=Zx2+Xc^2
3170 Zxy=Zxy+Xc*Yc
3175 Zy=Zy+Yc
3180 NEXT I
3185 Bb=(Nrun*Zxy-Zy*Zx)/(Nrun*Zx2-Zx^2)
3190 Aa=EXP((Zy-Bb*Zx)/Nrun)
3195 PRINT
3200 PRINT USING "10X." "Least-squares line for q = a*delta-T^b"
3205 PRINT USING "12X." "a = ".Z.4DE":Aa
3210 PRINT USING "12X." "b = ".Z.4DE":Bb
3215 IF Ipc=0 THEN
3220 Qps=3.5E+5
3225 Hop=8919
3230 END IF
3235 IF Ipc=1 THEN
3240 Qps=1.E+6
3245 Hop=7007
3250 END IF
3255 Hos=Aa*(1/Bb)*Qps*((Bb-1)/Bb)
3260 Enr=Hos/Hop
3265 PRINT
3270 PRINT USING "10X." "Values computed at q = ".Z.DD." (MW/m^2):":Qps/1.E+
5
3275 PRINT USING "12X." "Heat-transfer coefficient = ".DDD.DDD." (kW/m^2.K)"
:Hos/1000
3280 PRINT USING "12X." "Enhancement ratio = ".3D.3D":Enr
3285 IF Im=1 THEN
3290 BEEP
3295 PRINT
3300 PRINT USING "10X." "NOTE: ".ZZ." data runs were stored in file ".10A":J.
D files
3305 END IF
3310 BEEP
3315 PRINT
3320 PRINT USING "10X." "NOTE: ".ZZ." X-Y pairs were stored in plot data file
".10A":J.P files
3325 IF Inf=1 THEN
3330 PRINT USING "16X.ZZ." "pairs of Nr-F are stored in file ".14A":J.NrfS
3335 END IF

```

```

3340 ASSIGN #File TO *
3345 ASSIGN #File1 TO *
3350 ASSIGN #File2 TO *
3355 IF Iso=2 THEN CALL Plot
3360 IF Iso=3 THEN CALL Label
3365 IF Iso=4 THEN CALL Lplot
3370 END
3375 DEF FNPvst(Tsteam)
3380 DIM K(8)
3385 DATA -7.691234564,-26.08023696,-168.1706546.64.23285504,-118.9646225
3390 DATA 4.16711732,20.9750676.1.E9.6
3395 READ K(*)
3400 T=(Tsteam+273.15)/647.3
3405 Sum=0
3410 FOR N=0 TO 4
3415 Sum=Sum+K(N)*((1-T)^(N+1))
3420 NEXT N
3425 Br=Sum/(T*(1+K(5)*((1-T)+K(6)*((1-T)^2))-(1-T)/(K(7)*((1-T)^2+K(8))))
3430 Pr=EXP(Br)
3435 P=22120000*Pr
3440 RETURN P
3445 FNEND
3450 DEF FNHfg(T)
3455 Hfg=2477200-2450*(T-10)
3460 RETURN Hfg
3465 FNEND
3470 DEF FNMuw(T)
3475 A=247.8/(T+133.15)
3480 Mu=2.4E-5*10^A
3485 RETURN Mu
3490 FNEND
3495 DEF FNVvst(Tt)
3500 P=FNPvst(Tt)
3505 T=Tt+273.15
3510 X=1500/T
3515 F1=1/(1+T*1.E-4)
3520 F2=((1-EXP(-X))^2.5*EXP(X)/X^1.5)
3525 B=.0015*F1-.000942*F2-.0004882*X
3530 K=2*P/(461.52*T)
3535 V=(1+(1+2*B*K)^.5)/K
3540 RETURN V
3545 FNEND
3550 DEF FNCpw(T)
3555 Cpw=4.21120858-T*(2.26826E-3-T*(4.42361E-5+2.71428E-7*T))
3560 RETURN Cpw*1000
3565 FNEND
3570 DEF FNRhow(T)
3575 Ro=999.52946+T*(.01269-T*(5.482513E-3-T*1.234147E-5))
3580 RETURN Ro
3585 FNEND
3590 DEF FNPtw(T)
3595 Ptw=FNCpw(T)*FNMuw(T)/FNKu(T)
3600 RETURN Ptw
3605 FNEND
3610 DEF FNKu(T)
3615 X=(T+273.15)/273.15
3620 Ku=-.92247+X*(2.8395-X*(1.8007-X*(.52577-.07344*X)))
3625 RETURN Ku
3630 FNEND
3635 DEF FNTanh(X)
3640 P=EXP(X)

```

```

3645 Q=EXP(-X)
3650 Tanh=(P-Q)/(P+Q)
3655 RETURN Tanh
3660 FNEND
3665 DEF FNTvsv(V)
3670 COM /Cc/ C(7)
3675 T=C(0)
3680 FOR I=1 TO 7
3685 T=T+C(I)*V-I
3690 NEXT I
3695 RETURN T
3700 FNEND
3705 DEF FNHF(T)
3710 HF=T*(4.203849-T*(5.88132E-4-T*4.55160317E-5))
3715 RETURN HF*1000
3720 FNEND
3725 DEF FNGrad(T)
3730 Grad=37.9853+.104388*T
3735 RETURN Grad
3740 FNEND
3745 DEF FNTvsp(P)
3750 Tu=110
3755 Tl=10
3760 Ta=(Tu+Tl)*.5
3765 Pc=FNpvst(Ta)
3770 IF ABS((P-Pc)/P)>.0001 THEN
3775 IF Pc<P THEN Tl=Ta
3780 IF Pc>P THEN Tu=Ta
3785 GOTO 3760
3790 END IF
3795 RETURN Ta
3800 FNEND
3805 DEF FNPvsv(V)
3810 P=8133.5133+2.236051E+4*V
3815 RETURN P
3820 FNEND

```

LIST OF REFERENCES

1. Search, H. T., A Feasibility Study of Heat Transfer Improvement in Marine Steam Condensers, M. S. Thesis, Naval Post Graduate School, Monterey, Ca., December, 1977.
2. ASME Paper No. 64-WA/HT-3, Mechanism of Dropwise Condensation, by Umur, A., and Griffith, P., June 1964.
3. McCormick, J. I., and Westwater, J. W., "Nucleation Sites for Dropwise condensation," Chem. Eng. Science, v20, 1965.
4. Reisbig, R.I., "Microscopic Growth Mechanisms in Dropwise Condensation," 5th Int. Heat Transfer Conference, v.3., 1974.
5. Graham, C., The Limiting Heat Transfer Mechanisms of Dropwise Condensation, Ph.D. Thesis, M.I.T., 1969.
6. Graham, C., and Griffith, P., "Drop Size Distributions and Heat Transfer in Dropwise Condensation," Int. Journal of Heat and Mass Transfer, v.16, 1973.
7. Tanasawa, I., and Ochiai, J., "Experimental Study on Dropwise Condensation," Bulletin of Japan Society of Mechanical Engineers, v.16, 1973.
8. ASME Paper No. 75-ht-BBE, Measurements of Dropwise Distributions During Transient Dropwise condensation, by Tanaka, H., September 1975.
9. Zisman, W.A., "Relation of Equilibrium Contact Angle to Liquid and Solid Constitution," Advances In Chemistry Series, v.43, 1964.
10. Hannemann, R.J., and Mikic, B.B., "An Experimental Investigation Into The Effect of Surface Thermal Conductivity on The Rate of Heat Transfer in Dropwise Condensation," Int. J. of Heat Mass Transfer, v.19, 1976.
11. Askan, S.N., and Rose, J.W., "Dropwise Condensation the Effect of Thermal Properties of the Condenser Material," Int. J. of Heat Mass Transfer, v.16, No.2, Feb. 1973.

12. Rose, J.W., "Effect of Condenser Tube Material on Heat Transfer During Dropwise Condensation of Steam," Int. J. of Heat Mass Transfer, v.21, No.7, July, 1978.
13. Stylianou, S.A., and Rose, J.W., "Dropwise Condensation on Surfaces Having Different Thermal Conductivities," Journal of Heat Transfer, v.102, August, 1980.
14. Hannemann, R.J., "Condensing Surface Thickness Effects in Dropwise Condensation," Int. J. Heat Mass Transfer, v.21, No.1, January, 1978.
15. Waas, P., Straub, J., and Grigull, U., "The Influence of The Thermal Diffusivity of the Condenser Material on The Heat Transfer Coefficient in Dropwise Condensation," Heat Transfer 1982, 7th Int. Heat Transfer Conf., Munich, v.5, 1982.
16. Brown, A., and Thomas, M., "Filmwise and Dropwise Condensation of Steam at Low Pressures," Proceedings of 3rd Int. Heat Transfer Conference, v.2, 1966.
17. Blackman, L., Dewar, M., and Hampson, H., "An Investigation of Compounds Promoting the Dropwise Condensation of Steam," Journal of Applied Chemistry, v.7, 1957.
18. Bennett, M., and Zisman, W., "Confirmation of Spontaneous Spreading By Water on Pure Gold," The Journal of Physical Chemistry, v.74, No.11, 1970.
19. Erb, R., and Thelen, E., "Dropwise Condensation," First International Symposium on Water Desalination, Washington, D.C., 1965.
20. Woodruff, D., and Westwater, J.W., "Steam Condensation on Electroplated Gold: Effect of Plating Thickness," Int. J. of Heat and Mass Transfer, v.22, 1979.
21. O'Neill, G., Westwater, J.W., "Dropwise Condensation of Steam on Electroplated Silver Surfaces," Int. J. Heat and Mass Transfer, v.27, 1984.
22. Brenner, A., Electro-deposition of Alloys, Principles and Practice, Academic Press Inc., 1963, pg.53.
23. Holden, K.M., An Evaluation of Polymer Coatings for the Promotion of Dropwise Condensation of Steam, M.S.Thesis, Naval Post Graduate School, Monterey, Ca., March, 1984.
24. Brydson, J.A., Plastics Materials, 4th ed., Butterworth Scientific, pg.760, 1982.

25. Fish, J.G., "Organic Polymer Coatings," Disposition Technologies for Films and Coatings, Bunshah, R.F., ed., Noyes Publications, 1982.
26. Schuessler, P., "Hydrophobic Resins and Surface Modifiers," Proceedings of 3rd Annual International Electronics Packaging Conference, October, 1983.
27. Gaynes, N.I., Testing of Organic Coatings, Noyes Data Corp., pg. 42, 1977.
28. Holden, K.M., Wanniarachchi, A.S., Marto, P.J., Boone, D.H., Rose, J.W., "Evaluation of Organic Coatings for the Promotion of Dropwise Condensation of Steam," ASME Paper, ASME Winter Annual Meeting, New Orleans, December, 1984.
29. Nasa Lewis Research Center Case No. 13,122-1, Ion Beam Sputter Deposition of Fluoropolymers, by Banks, B.A., and Sovey, J.S., May, 1979.
30. Sharma, A.K., and Yasuda, H., "Effect of Glow Discharge Treatment of Substrates on Parylene-Substrate Adhesion," Journal of Vacuum Science Technology, 21(4), Nov., 1982.
31. Sadhir, R.K., and Saunders, H.E., "Protective Thin Film Coatings by Plasma Polymerization," Proceedings of 4th Annual Int. Electronics Packaging Conference, pg. 789, October, 1984.
32. U.S. Navy Marine Engineering Laboratory Report 71-106, A Review of Literature on the Promotion of Dropwise Condensation, by Fox, R.N., July, 1964.
33. Manvel, J.T., An Experimental Study of Dropwise Condensation on Horizontal Condenser Tubes, M.S. Thesis, Naval Post Graduate School, Monterey, Ca., June, 1979.
34. Perkins, P.K., An Experimental Study of Dropwise Condensation on Vertical Discs, M.S. Thesis, Naval Post Graduate School, Monterey, Ca., December, 1979.
35. Griffith, J.R., O'Rear, J.G., and Reines, S.A., "Fluorinated Epoxy Resins," CHEMTECH, May 1972.
36. Hunston, D.L., Griffith, J.R., and Bowers, R.C., "Fluoroepoxies: Surface Properties and Applications," Ind. Eng. Chem. Prod. Res. Dev., v.17, No.1, 1978.
37. ASTM Specification D 3359-83, Measuring Adhesion By Tape Test, March, 1983.

38. ASTM Specification D 3363-74 (Reapproved 1980), Film Hardness By Pencil Test, November, 1974.
39. Poole, M.W., Filmwise Condensation of Steam on Externally-Finned Horizontal Tubes, MS Thesis, Naval Postgraduate School, Monterey, California, December, 1983.
40. Fujii, T., Honda, H., "Condensation of Steam on a Horizontal Tube," Condensation Heat Transfer, ASME, New York, 1979.
41. Georgiadis, I. V., Filmwise Condensation of Steam on Low Integral-Finned Tubes, M.S. Thesis, Naval Post Graduate School, Monterey, Ca., September, 1984.
42. Nobbs, D. W., The Effect of Downward Vapor Velocity and Inundation on The Condensation Rates on Horizontal Tubes and Tube Banks, PhD Thesis, University of Bristol, England, April 1975.
43. ASM Metals Reference Book, 2nd ed., American Society for Metals, 1983.
44. Touloukian, Y. S. and others, Thermophysical properties of Matter, vol. 1, IFI Plenum Data Corporation, 1970.
45. Wanniarachchi, A. S., Marto, P. J., and Rose, J. W., "Filmwise Condensation of Steam on Externally-Finned Horizontal Tubes," ASME Publication HTD-Vol. 38, pp. 133-141, December 1984.

INITIAL DISTRIBUTION LIST

	No.	Copies
1. Defense Technical Information Center Cameron Station Alexandria, VA 22314		2
2. Library, Code 0142 Naval Postgraduate School Monterey, CA 93943		2
3. Department Chairman, Code 6S Department of Mechanical Engineering Naval Postgraduate School Monterey, CA 93943		1
4. Professor Paul J. Marto Code 69Mx Department of Mechanical Engineering Naval Postgraduate School Monterey, CA 93943		5
5. Dr. John W. Rose Department of Mechanical Engineering University of London London E1 4NS England		1
6. Dr. Win Aung Program Director for Heat Transfer Division of Engineering National Science Foundation Washington, D.C. 20550		1
7. Dr. A. S. Wanniarachchi, Code 69Wa Department of Mechanical Engineering Naval Postgraduate School Monterey, CA 93943		2
8. Dr. James R. Griffith Code 6120 Naval Research Laboratory Monterey, D. C. 20375		1
9. Dr. D. H. Boone Code 69Bi Department of Mechanical Engineering Naval Postgraduate School Monterey, CA 93943		1
10. Lt. Daniel J. Looney 19 Lafayette Ave. Sea Cliff, N.Y. 11579		2

END

FILMED

7-85

DTIC